The functional relevance of MKK4 and MKK7 splice variants in neural cells

Dissertation
zur Erlangung des Doktorgrades
der Mathematisch-Naturwissenschaftlichen Fakultät
der Christian-Albrechts-Universität zu Kiel

vorgelegt von

Dipl.-Biol. Wiebke Häusgen

Kiel
2010

Referent:	Prof. Dr. Thomas Herdegen
Korreferent:	Prof. Dr. Manuela Dittmar
Tag der mündlichen Prüfung:	30. November 2010
Zum Druck genehmigt:	30. November 2010

gez. Prof. Dr. Lutz Kipp, Dekan

Meinen Eltern

Table of contents

1 Introduction 1

1.1 Mitogen-activated protein kinase kinase 4 2

1.2 Mitogen-activated protein kinase kinase 7 4

1.3 The c-Jun N-terminal kinases 6

1.4 Regulation of JNKs by MKK4 and MKK7 8

1.5 PC12 cells- a versatile model for peripheral mammalian neurons 9

1.6 Aims of the study 10

2 Materials and methods 12

2.1 Materials 12

2.2 Centrifuges, cell culture equipment and sterilization 16

2.3 Culture, staining, stimulation and transfection of cells 17

2.3.1 PC12 cells 17

2.3.2 Electronic cell counting 19

2.3.3 Trypan blue viability staining 19

2.3.4 Flow cytometric analysis 20

2.3.5 5-bromo-2-deoxyuridine (BrdU) incorporation assay 20

2.3.6 Differentiation 20

2.3.7 Neurite outgrowth 21

2.3.8 Coomassie blue staining 21

2.3.9 Incubation with inhibitors and stressors 21

2.3.10 Transfection 22

2.4 Processing of PC12 cells for RNA extraction 23

2.4.1 Experimental precautions to minimize RNA degradation 23

2.4.2 Harvesting cells 23

2.5 Isolation of RNA 23

2.5.1 RNA extraction 23

2.5.2 RNA quantification and quality control 24

2.5.3 RNA agarose gel 24

2.6 Reverse transcription polymerase chain reaction (RT-PCR) 25

2.6.1 Reverse transcription of mRNA 25

2.6.2 PCR 26

2.7 TaqMan Real-Time-quantitative PCR (QRT-PCR) 28

2.8 Cloning of cDNA fragments 29

2.8.1 General principles and procedure 29
2.8.2 Production of competent *E. coli* DH5α cells 29
2.8.3 Generation of cloning primers and selection of restriction enzymes 30
2.8.4 Amplification and purification of a PCR product 31
2.8.5 Restriction digestion 32
2.8.6 Purification of a digestion reaction 33
2.8.7 Ligation of DNA fragments into the pEGFP-C3 vector 33
2.8.8 Heat-shock transformation of *E. coli* DH5α cells 34
2.8.9 Preparation of plasmid DNA 34
2.8.9.1 Mini preparation of plasmid DNA 34
2.8.9.2 Midi preparation of plasmid DNA 35
2.8.9.3 Endotoxin-free maxi preparation of plasmid DNA 35
2.8.9.4 Plasmid purification 36
2.8.10 Sequence verification 36
2.9 Denaturing protein extraction and protein quantification 36
2.9.1 Harvesting cells 36
2.9.2 Denaturing extraction of whole cell proteins 37
2.9.3 Denaturing extraction of nuclear proteins 37
2.9.4 Non-denaturating extraction of whole cell proteins 37
2.9.5 Non-denaturating extraction of whole cell proteins for immunoprecipitations 38
2.9.6 Determination of protein concentrations 38
2.9.7 Immunoprecipitation (IP) and immunodepletion (ID) 39
2.9.8 Chromatin immunoprecipitation (ChIP) 39
2.10 Sodium dodecyl sulfate polyacrylamide gel electrophoresis (SDS-PAGE) and Western blot 40
2.10.1 SDS-PAGE 40
2.10.2 Western blot 42
2.10.3 Stripping of Western blot membranes 45
2.10.4 Ponceau S staining of Western blot membranes 45
2.11 Statistical analysis and replication of the experiments 45
3 Results 47
3.1 Stable transfection of PC12 cell lines 47
3.1.1 Cloning of MKK4 and MKK7 expression vectors 47
3.1.2 Stable transfection of PC12 cells with MKK4 and MKK7 constructs 52
3.2 Functional analysis of MKK7γ1 in naïve PC12 cells 53
3.2.1 MKK7γ1 under normal cell growth conditions 53

3.2.1.1 Characterisation of MKK7γ1-transfected PC12 cells ... 53
3.2.1.2 Cell proliferation ... 56
3.2.1.3 Apoptotic proteins ... 58
3.2.1.4 mRNA levels of targets ... 59
3.2.1.5 Summary I ... 61
3.2.2 MKK7γ1 under stress conditions ... 62
3.2.2.1 Cell death ... 62
3.2.2.2 JNK signalling pathway ... 63
3.2.2.3 Apoptotic proteins ... 66
3.2.2.4 Cell proliferation ... 68
3.2.2.5 Cell cycle regulators ... 69
3.2.2.6 Inhibition of JNKs by SP600125 ... 71
3.2.2.7 Cell cycle distribution patterns ... 72
3.2.2.8 JNK protein levels, activation and localization ... 75
3.2.2.9 JNK signalosomes ... 77
3.2.2.10 Summary II ... 80
3.3 Functional analysis of MKK7γ1 in differentiated PC12 cells ... 81
3.3.1 Characterisation of NGF-treated MKK7γ1-transfected PC12 cells ... 81
3.3.2 Cell numbers ... 82
3.3.3 Sprouting ... 83
3.3.4 Activation of AKT, ERK1/2 and JNK pathways ... 85
3.3.4.1 JNK protein levels, activation and localization ... 87
3.3.4.2 JNK targets ... 89
3.3.4.3 Inhibition of JNKs ... 90
3.3.4.4 p53 actions ... 91
3.3.5 MKK7γ1 under stress conditions in NGF-treated PC12 cells ... 92
3.3.5.1 Cell death ... 93
3.3.5.2 JNKs and their targets ... 97
3.3.5.3 Summary III ... 99
3.4 Characterisation of MKK4 and MKK4Δ in naïve PC12 cells ... 100
3.4.1.1 Summary IV ... 104
4 Discussion ... 105
4.1 The cellular system ... 105
4.2 Methodology ... 106
4.3 MKK7γ1 as a regulator of cell proliferation in PC12 cells ... 107
4.3.1 Naïve PC12 cells ... 107

4.3.2 NGF-treated PC12 cells 108
4.4 MKK7γ1 is a negative regulator of neuritogenesis in PC12 cells 109
4.5 MKK7γ1 as regulator of PC12 cell stress response 110
4.5.1 Naïve PC12 cells 110
4.5.2 NGF-treated PC12 cells 111
4.6 MKK7γ1 activates a distinct JNK signalling pathway in PC12 cells 111
4.6.1 Naïve PC12 cells 111
4.6.2 NGF-treated PC12 cells 113
4.7 Conditional changes in MKK7-JNK complex formation in naïve PC12 cells 115
4.8 MKK4 and MKK4Δ differently affect naïve PC12 cells 116
4.9 Perspectives 117
5 Summary 119
6 Zusammenfassung 121
7 References 123
8 Appendix 137
8.1 Abbreviations and symbols 137
8.2 Index of figures and tables 142
8.2.1 Figures 142
8.2.2 Tables 144
9 Curriculum vitae 145
10 Declaration (Erklärung) 146
11 Publications 147

1 Introduction

The mitogen-activated protein kinase (MAPK) pathways are ubiquitous and highly conserved in all eukaryotic cells. They consist of a large enzyme network that contributes to the amplification and specificity of a signal by sequential activation of cytoplasmic and nuclear proteins and finally initiates cellular processes like gene transcription, protein synthesis, proliferation, differentiation or apoptosis (145, 157, 199).

MAPKs are activated by different stimuli acting through diverse receptor families, including cytokines, hormones, growth factors and environmental stress. After ligand binding, activated receptors recruit adaptor proteins and activate small GTP-binding proteins. Subsequently, a three-tiered signalling module is turned on, consisting of MAP3Ks (MKKKs), MAP2Ks (MKKs) and MAPKs. So far, there are 20 defined MKKKs that activate 7 MKKs which in turn activate 11 MAPKs (89). They represent the three major MAPK pathways: the extracellular signal-regulated kinase (ERK) pathway, the p38 kinase pathway and the c-Jun N-terminal kinase (JNK) pathway (Fig. 1).

Fourteen of the 20 defined MKKKs activate the c-Jun N-terminal kinase (JNK) pathway (like apoptosis signal-regulating kinase 1 (ASK-1), dual leucine zipper kinase (DLK), mitogen-activated protein/extracellular signal-regulated kinase kinase (MEKK-1) and mixed lineage kinases 1-4 (MLK-1-4)), demonstrating the importance and versatility of JNK signalling in the cellular response to stimuli (72). Some of them phosphorylate both JNK activators, MKK4 and MKK7, and some of them are specific for a single MKK only. In turn, activated MKK4 and MKK7 phosphorylate JNKs (JNK1-3). Thus, a diversity of stimuli turns on a variety of MKKKs, which activate three JNK isoforms with only two MKKs as intermediates. How can MKK4 and MKK7 transfer, as well as multiply and ensure signal specificity? This problem is underestimated and often simplified as linear sequential bimolecular signalling. The number of published studies about MKK4, MKK7 and their upstream kinases is much less addressed (~ 1,400) compared to publications on JNKs (~ 15,000). The introduction of this thesis focuses on the present knowledge of molecular and functional characteristics of MKK4 and MKK7. In addition, different ways of JNK regulation via MKK4 and MKK7 are presented and as yet unknown aspects are revealed.

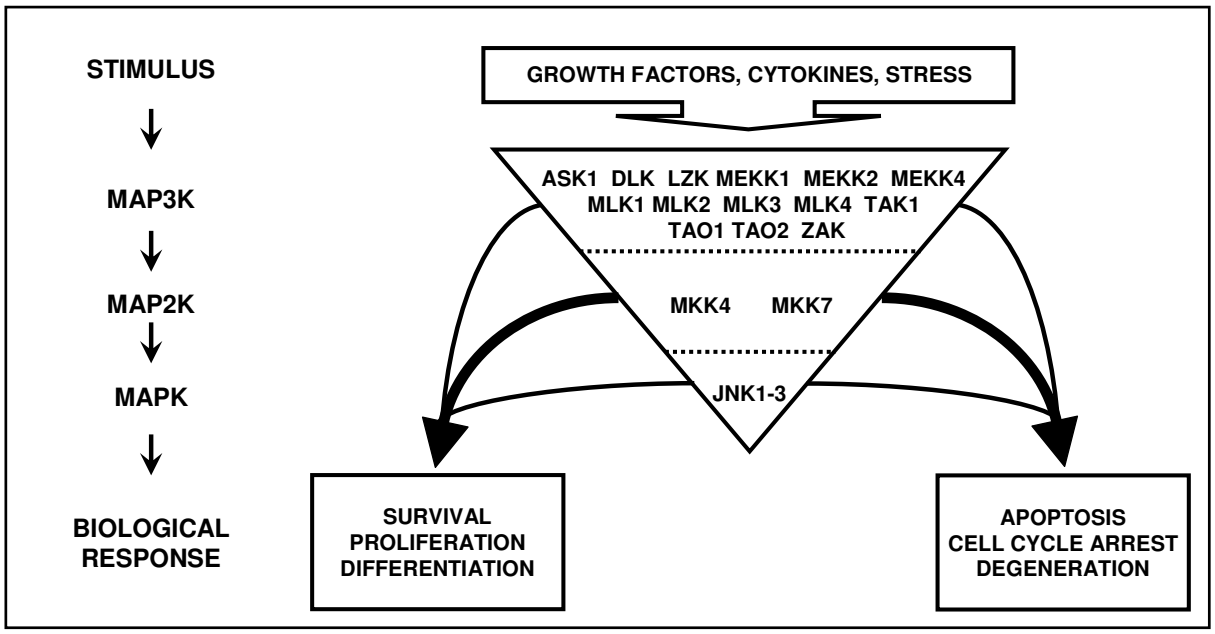

Fig. 1: Simplified model of the JNK signalling cascade.
The three-tiered core module of MKKKs, MKKs and MAPKs induces a multiplicity of cellular processes.

1.1 Mitogen-activated protein kinase kinase 4

The mitogen-activated protein kinase kinase 4 (MKK4) was first identified in a cDNA library from *Xenopus laevis* embryos by a PCR-based screen and called XMEK2 (211). Thereafter, *Drosophila*, mouse, rat and human homologs were cloned and named stress-activated protein kinase/extracellular signal-related protein kinase kinase 1 (SEK1), MKK4 and c-Jun N-terminal kinase kinase 1 (JNKK1), respectively (46, 73, 115, 128, 154).

Molecular characteristics- The *mkk4* gene is located on human chromosome 17 (mouse chromosome 11; rat chromosome 10; *Drosophila* chromosome 3R) and encodes a protein of 399 amino acids. So far, only one *mkk4* gene product has been described. The human MKK4 shares 94% homology with the mouse and rat MKK4 protein (79% with *Drosophila*; mouse and rat share 100% homology).

The kinase domain of the serine/threonine kinase MKK4 contains two phosphorylation sites in the **S**-I-A-K-**T** (Ser-Ile-Ala-Lys-Thr) motif (209). MKK4 is activated by the majority of MKKKs, such as ASK-1, MEKK, MLK, and transforming growth factor-β activated kinase (TAK) (145). Additionally, MKK4 contains a domain of versatile docking (DVD) located at the C-terminus (Fig. 2), where upstream MKKKs and other MKKs can bind (173, 204). Association with upstream kinases affects the activity of MKK4 and leads to conformational changes (27, 173). Furthermore, MKK4 binds via its DVD to scaffold proteins such as JIP-3.

Similar to other MAPKs, MKK4 contains motifs for binding of upstream and downstream signalling components. The D-domain type docking site in the N-terminal region of MKK4 binds to its MAPK substrates JNKs and p38 (78). In the ability to phosphorylate both MAPKs, MKK4 is unique among all known MKKs. In particular the JNK activation is well examined. *In vitro* studies revealed that MKK4 preferentially phosphorylates the tyrosine residue of JNKs (115, 154). Moreover, some stressors were found, where MKK4 is the main JNK activator such as anisomycin and arsenite (188). Other stimuli only require MKK4 for complete/optimal JNK activation, whereas MKK7 is essential for triggering JNK activity (178).

Functions- MKK4 is involved in a variety of physiological and pathophysiological processes. Until embryonic day 10 (E10) in mice, *mkk4* mRNA is exclusively expressed in the central nervous system (CNS) (110). By E12 the *mkk4* transcript can be detected in several tissues of the developing embryo, with high *mkk4* mRNA levels in the liver. Mice with a targeted deletion of the *mkk4* gene die between E11.5 and E13.5 of anemia and abnormal hepatogenesis (62). Thus, MKK4 fulfils essential functions that cannot be compensated by other MKKs. Similarly, MKK4 is relevant in the heart, immune system and the development of cancer. In a mice model of hypertrophy, gene transfer of a kinase-inactive MKK4 inhibited JNK signalling and blocked cardiac hypertrophy (28). Studies on the function of MKK4 in the immune system were mostly carried out on chimeric $sek1^{-/-}/rag2^{-/-}$ mice and brought up conflicting data. On the one hand, these mice developed smaller thymi with decreased proliferation of peripheral T cells (133). On the other hand, mice had no impaired B and T cell development but generated massive lymphadenopathy (169). This discrepancy could be ascribed to the missing constancy of different $mkk4^{-/-}$ embryonic stem cell clones. The human *mkk4* gene is located proximal to the *p53* tumour suppressor gene on chromosome 17, suggesting that MKK4 is involved in the inhibition of tumour formation. Indeed, studies on a wide spectrum of primary cancers demonstrated a loss-of-function mutation in *mkk4* in 5% of especially lung and pancreatic tumours (99, 130, 167, 175, 205). Additionally, endogenous expression of MKK4 could reduce metastasis of pancreatic and ovarian tumours in mice (206, 214). However, an equal number of studies revealed a pro-oncogenic role for MKK4. Knockdown of MKK4 by siRNA increased apoptosis of breast cancer cells after serum deprivation and suppressed tumour growth in a mouse model (194). Furthermore, injection of $mkk4^{-/-}$ pancreatic cell line into mice reduced lung metastases of the primary pancreatic tumour and caused a longer tumour volume-doubling rate compared to $mkk4^{+/-}$ cell injection (38).

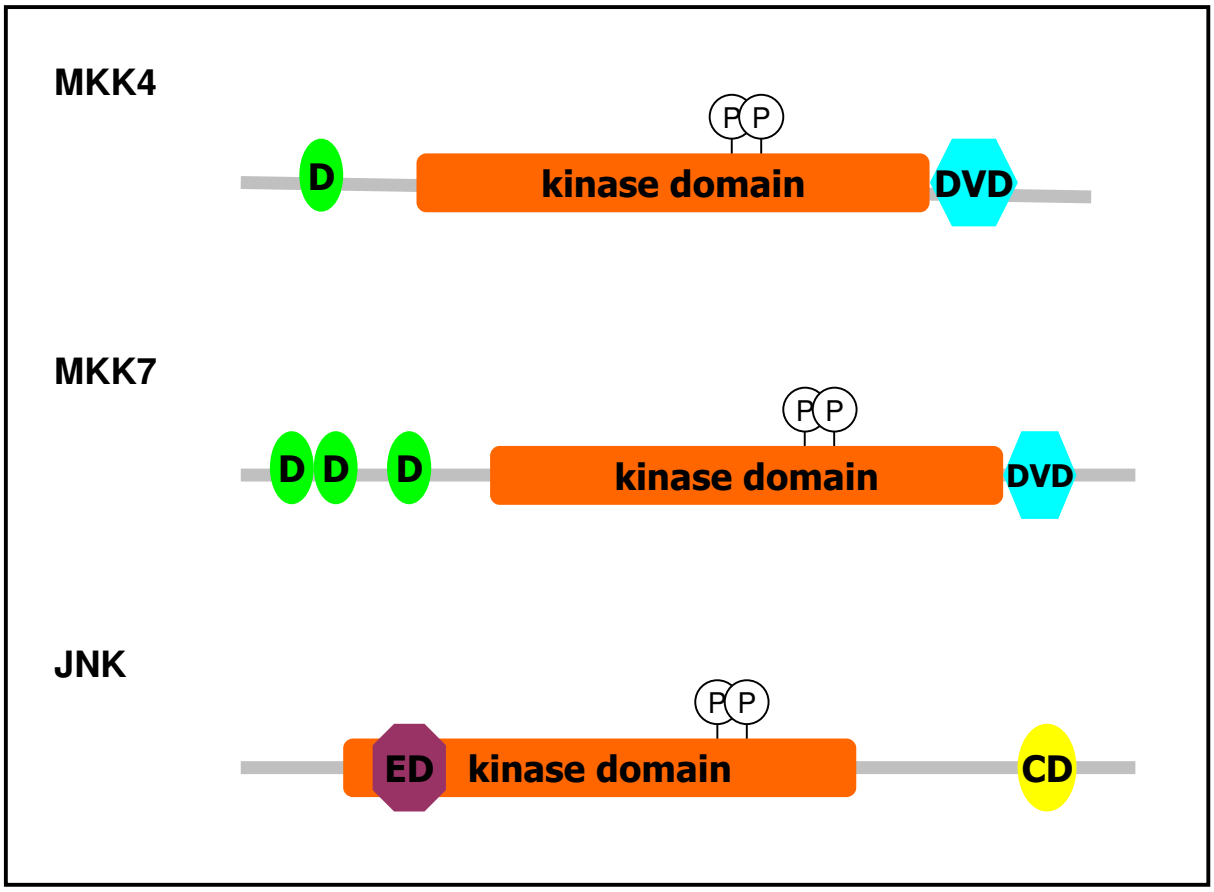

Fig. 2: Schematic illustration of the MKK4, MKK7 and JNK structures.
All three kinases contain several functional domains for activation and binding of other proteins. They are activated by phosphorylation of two residues in their kinase/catalytic domain (Ser and Thr for MKK4 and MKK7; Thr and Tyr for JNK). CD, common docking domain; D, docking domain; DVD, domain of versatile docking; ED, glutamate/aspartate domain; P, phosphorylation site.

1.2 Mitogen-activated protein kinase kinase 7

The mitogen-activated protein kinase kinase 7 (MKK7), also called stress-activated protein kinase/extracellular signal-regulated protein kinase kinase 2 (SEK2) or c-Jun N-terminal kinase kinase 2 (JNKK2) was first cloned from cDNA of murine testis with primers based on the sequence coding for the *Drosophila* mitogen-activated protein kinase kinase *hemipterous* (*hep*) (180). Subsequently, MKK7 was cloned from human and rat (80, 129, 209, 210).

Molecular characteristics- The human *mkk7* gene is located on chromosome 19 (mouse chromosome 8; rat chromosome 12; *Drosophila* (*hep*) chromosome X). By alternative splicing its transcript generates a group of protein kinases with three different N-termini (α, β and γ) and two different C-termini (1 and 2) (Fig. 3). So far, four human, six murine, one rat and three MKK7 splice variants from *Drosophila* have been described (60, 123, 180, 181, 209). They encode for proteins ranging from 347 to 469 amino acids. Human MKK7γ1 shares

98% homology with the mouse and rat protein (mouse and rat 99% homology; Drosophila *hep* transcript variant C with human 85% homology).

The **S**-K-A-**T** (Ser-Lys-Ala-Thr) motif in the kinase domain of MKK7 is phosphorylated at the serine and threonine residues by several MKKKs. Interaction of MKK7 with those upstream kinases is mediated by the domain of versatile docking (DVD) at the C-terminus (Fig. 2). MKKK binding also facilitates phosphorylation of MKK7 through conformational changes of the activation loop (173). According to the size of the N-terminus, different MKK7 splice variants contain 2 or 3 docking (D) domains for JNK binding. A comparative study on the basal activities of different murine MKK7 splice variants revealed that MKK7β and -γ have higher catalytic activities towards JNKs than MKK7α (181). This might be due to the shorter N-terminus of MKK7α, which lacks a third docking domain (79). Further *in vitro* studies showed that each MKK7 splice variant has different biochemical properties, but little is known about the functional relevance.

Functions- During embryogenesis, the *mkk7* transcript is mainly found in epithelial tissues such as skin, lung and epithelium (210). In adult humans, the *mkk7* mRNA is widely expressed in various tissues with high functional expression in the heart, liver, skeletal muscle, kidney and pancreas (209). Thus, embryos from *mkk7* knockout mice die between E11.5 and E13.5 with a disorganized liver, which contains less parenchymal hepatocytes (178, 187). Therefore, most studies were done with $mkk7^{-/-}$ mouse embryonic fibroblasts (MEFs) or chimeric mouse models. The loss of *mkk7* leads to decreased proliferation and premature cellular senescence beginning with passage 4-5 and G2/M cell cycle arrest in MEFs (187). Interestingly, knockout of *mkk4* in MEFs showed a similar phenotype but overexpression of *mkk4* in $mkk7^{-/-}$ MEFs could not compensate for the loss of *mkk7* (187). Additionally, loss of *jnk1* also has an anti-proliferative effect on MEFs and inactivation of *c-jun* caused premature senescence. This indicates that the effect of *mkk4* and *mkk7* knockout is mediated by JNKs and that both MKKs are important for these processes but carry out different tasks (179). In contrast, studies with B and T lymphocytes from chimeric $mkk7^{-/-}$/*rag2* mice showed that loss of *mkk7* enhances cell cycle progression of mast cells (155). Missing conditional and cell type specific *mkk7* knockout approaches limit the investigations of MKK7 functions *in vivo* and functional studies on single MKK7 splice variants are needed to examine further molecular characteristics.

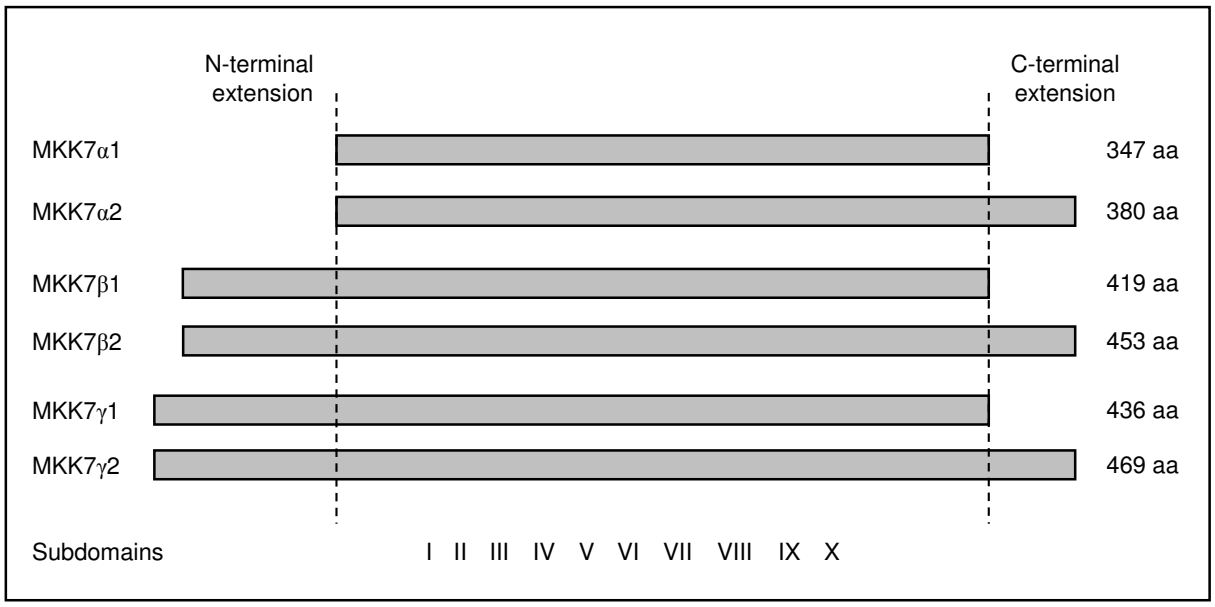

Fig. 3: Schematic illustrastion of the six murine MKK7 splice variants.
Alternative splicing of the *mkk7* transcript generates six MKK7 proteins with different C- and N-termini.

1.3 The c-Jun N-terminal kinases

The c-Jun N-terminale kinases (JNKs), also called stress-activated protein kinases (SAPKs), have first been discovered in a c-Jun binding assay with extracts from UV-stimulated HeLa cells (76). In rapid succession, all three JNK isoforms from human, mouse and rat were identified and cloned (46, 107). *Drosophila* has only one JNK (DJNK, Basket) protein, which is encoded by *basket* (*bsk*) (163).

Molecular characteristics- In mammalian genomes three genes (*jnk1*, *jnk2* and *jnk3*) encode a family of three JNK isoforms (JNK1-3) with a total of ten splice variants. The *jnk1* gene is located on human chromosome 10 (mouse chromosome 14, rat chromosome 16), *jnk2* on chromosome 5 (mouse chromosome 11, rat chromosome 10) and *jnk3* on chromosome 4 (mouse chromosome 5, rat chromosome 14). Each *jnk* gene encodes for four, or two in the case of *jnk3*, alternatively spliced transcripts, which differ in subdomain IX (α and β) and their C-termini (1 and 2). All ten mRNAs are translated into proteins of 381 to 464 amino acids with molecular weights of 46 and 54 kDa. Mouse and rat JNK2α2 are identical and share 98% homology with the human protein (73% with *Drosophila*).

JNKs are activated by concomitant phosphorylation at a threonine and a tyrosine residue within a conserved **T**-P-**Y** (Thr-Pro-Tyr) motif in the activation loop of the kinase domain by MKK4 and MKK7 (106, 199). Like all other MAPKs, JNKs have a common docking (CD) domain in their C-terminus and a glutamate/aspartate (ED) domain in their N-

terminus (Fig. 2), which enable interactions with activators (MKK4 and MKK7), inhibitory proteins (*e.g.*, mitogen-activated protein kinase phosphatases (MKPs)) and substrates (*e.g.*, c-Jun) (69).

JNKs themselves phosphorylate multiple targets. In the nucleus, various transcription factors such as c-Jun, c-Myc, activating transcription factor 2 (ATF-2) and p53 are activated by JNKs (70, 91, 125, 135). Some of these transcription factors form homo- or heterodimers to induce transcription as the activator protein-1 (AP-1) complex, a key inducer of genes encoding proteins involved in proliferation (*e.g.*, CyclinD1), differentiation (*e.g.*, c-Jun) and cell death (*e.g.*, Fas ligand (Fas-L)) (75, 159).

Cytoplasmic proteins constitute the second major pool of JNK substrates. As JNKs are involved in apoptosis, they modulate many pro- and anti-apoptotic proteins, *e.g.*, B-cell lymphoma 2 (Bcl-2), Bcl-2-associated death promoter (Bad), Bcl-2-associated X protein (Bax), B-cell lymphoma extra large (Bcl-xl) or Bcl-2-interacting mediator of cell death (Bim) (29, 113, 143). Furthermore, superior cervical ganglia 10 (SCG10) and tau, which are involved in microtubule (de-)stabilization are phosphorylated by JNKs (147, 174).

However, some targets are not only regulated by phosphorylation, but also by binding to JNKs. On the one hand, JNK-mediated phosphorylation or JNK binding activates and stabilizes substrates like transcription factors against ubiquitin-dependent degradation (111, 160); but on the other hand, JNKs also mediate ubiquitin-dependent degradation of some of their targets. These ubiquitination-dependent actions of JNKs involve their interaction with ligases, such as Itch (63).

Functions- Looking at the tissue distribution of *jnk* transcripts in humans, *jnk1* and *jnk2* are widely expressed, whereas expression of *jnk3* is mainly confined to brain, heart and testis. This restriction gave first hints for an important role of JNK3 in the nervous system.

Mice with the deletion of a single *jnk* gene are viable. Only a combined deletion of *jnk1* and *jnk2* in mice is lethal due to changes in specific natural apoptosis in the brain and a defect in neural tube morphogenesis (104, 152). Studies on *jnk* knockout mice have shown that JNKs are involved in a diversity of pathologies like diabetes, obesity, cancer, Parkinson's disease or Alzheimer's disease (14, 24, 77, 87, 88). In contrast, negative effects of *jnk* knockout on brain development, long-term potentiation, cancer, neural differentiation and regeneration have been observed (10, 20, 22, 25, 95, 104, 132, 152). Regarding the question how JNKs mediate this plethora of partially opposing functions, specificity of JNK isoforms and their targets have been investigated for a long time (11, 12). However, the last years have

provided evidence that especially signalosome assembly, cellular localisation and environmental stimuli trigger distinct JNK effects (10, 193, 216).

1.4 Regulation of JNKs by MKK4 and MKK7

Apart from phosphorylation and dephosphorylation, JNKs and their upstream kinases are regulated by post-translational modifications and they form complexes with upstream kinases or downstream targets, so called signalosomes. Scaffold proteins, repeat-motif extended proteins, often function as couplers of those complexes and determine their composition and cellular localisation.

Phosphorylation- The most obvious regulation of JNKs by MKK4 and MKK7 is their activation by phosphorylation. MKK4 and MKK7 differ in their preference for JNK phosphorylation sites. Whereas MKK4 induces phosphorylation of the tyrosine residue, MKK7 phosphorylates the threonine residue in the activation motif (100, 178). Importantly, full activation of JNK requires phosphorylation of both residues. Therefore, phosphorylation by MKK7 seems to be essential for JNK activation, while phosphorylation by MKK4 is only required for optimal JNK activation (178, 217). Furthermore, MKK7 splice variants show differences in their activation potency towards JNKs. Due to their N-terminal extension, MKK7β and –γ are strong JNK activators, whereas MKK7α only weakly phosphorylates JNKs (181).

JNK activation following different types of cellular stress can be mediated by one MKK or both activators. MKK4 is the major activator of JNKs in response to anisomycin, arsenite or heat-shock stimulation, while MKK7 strongly activates JNKs under basal conditions and after tumour necrosis factor α (TNF-α), IL-1β and thapsigargin stimulation (178). During UV irradiation and cadmiumchloride stimulation, both MKKs equally contribute to the activation of JNKs (134, 178, 208).

To stop signal transduction, mitogen-activated protein phosphatases (MKPs), also known as dual-specificity phosphatases (DUSPs), can inactivate or at least modulate JNKs, MKKs and MKKKs via dephosphorylation.

Interactions- The formation of multiple protein complexes is necessary for the regulation of JNK signalling by MKK4 and MKK7. These protein complexes consist of different combinations of MKKKs, MKKs and JNKs and can include further modulators like phosphatases or other cofactors. Some of those signalling complexes are assembled by scaffold proteins.

MKK4 and MKK7 bind to JNKs via their D-domains in the N-terminal region (78, 79, 127). This binding is very specific, as JNK1 and JNK2 do not interact with the D-domains of other MKKs (5). The intercellular concentrations of binding partners apparently determine the inhibitory or activating effect of MKKs on JNKs (97). However, interactions with MKKs enhance JNK phosphorylation but concurrently inhibit the activity of JNKs towards their downstream substrates for the time of binding.

Efficient modulation/action of JNKs requires scaffold proteins that bring MKK4 and MKK7 together with MKKKs and JNKs. The best studied group of scaffolds are the JNK-interacting proteins 1-4 (JIP-1-4) which also contribute to signal specificity. JIP-1 and JIP-2 only bind to MKK7 (198, 212), whereas JIP-3 and JIP-4 additionally bind to MKK4 (94, 109, 121). Signalosomes of JIP-1 or JIP-2 and MKK7 are found under basal conditions and increase following different types of stress like ischemia, UV irradiation or cytokine stimulation (127, 164, 198). Their abundance is always connected with a strong activation of JNKs and complexes with all three JNK isoforms have been reported.

While some biochemical properties of interactions between MKK4, MKK7 and JNKs have already been characterised, cellular functions and molecular conditions of those complexes are still to be determined. Most studies were done using *in vitro* systems, *i.e.*, independent of physiological and pathophysiological conditions. Further studies that link MKK:JNK interactions to a distinct cellular effect are necessary to understand the multiplicity of JNK-mediated functions.

1.5 PC12 cells- a versatile model for peripheral mammalian neurons

The PC12 cell line was established in 1976 by Lloyd Greene and Arthur Tischler and represents a single clonal cell line from a male rat pheochromocytoma, a tumour arising from chromaffin cells of the adrenal medulla (68). The cells synthesize and store the neurotransmitters dopamine and norepinephrine, but no epinephrine. They have a homogenous and near-diploid chromosome number of 40. PC12 cells grow adherent on collagen-coated dishes. One cell has a diameter of 15 to 30 µm. Cultured in medium that contains serum, PC12 cells have a round or polygonal shape and are comparable to adrenal chromaffin cells or sympathetic neurons. They have a doubling time of 48 to 72 h. No major changes were detected in cell growth characteristics, morphology, noradrenergic properties or growth factor sensitivity after cultivating the cells for 70 generations (68).

When cultured with serum-free medium, PC12 cells cease to proliferate (150). By addition of nerve growth factor (NGF) to serum-free medium, PC12 cells differentiate into a neuron-like phenotype (67). They undergo at least one round of division before they begin to extend branching varicose processes similar those of primary sympathetic neurons. If maintained in serum containing medium, NGF-induced differentiation is reversible. Removal of NGF is followed by degeneration of processes within 24 h and by resumption of cell multiplication within 72 h. Therefore, PC12 cells have been widely used in studying different aspects of growth factor-mediated differentiation. To induce differentiation, NGF binds to the tyrosine receptor kinase A (TrkA) and the p75 neutrophin receptor (p75) on the cellular surface (8, 102). These receptors activate different intracellular signalling cascades that usually involve the Ras/ERK1/2 pathway (144).

Apart from differentiation, apoptotic processes in PC12 cells have been examined intensively (23, 54, 144). Since it is of major interest to understand the mechanisms of neuronal cell death in several diseases, it was first necessary to establish reliable cell culture systems: only under stable conditions, it is possible to elucidate signal transduction processes that are responsible for the induction of cell death. Due to the neuronal characteristics of PC12 cells, they have been frequently used in various situations that induce neuronal apoptosis.

Another advantage of PC12 cells is that they can be transfected by various methods with high transfection efficiency and without affecting their ability to differentiate. Therefore, PC12 cells are a useful model system for many neurobiological studies.

1.6 Aims of the study

Many studies have investigated the functions of JNKs in neurons. However, it is largely unknown how this multiplicity of various and partially opposite functions is regulated. The aim of this thesis was to examine the effect of MKK4 and MKK7 on JNK signalling in neurons. Therefore, the coding sequences of MKK4 and MKK7 had to be isolated and cloned into a mammalian expression vector. As a cellular model system, PC12 cells were chosen, that should be stably transfected with MKK4 or MKK7.

In particular the following questions were addressed:

- Does overexpression of a single MKK4 or MKK7 splice variant provoke a distinct phenotype in PC12 cells?

- Which effect has a single MKK4 or MKK7 splice variant on basic cellular processes like proliferation, apoptosis or differentiation under basal and stress conditions?

- Which effect has a single splice variant of MKK4 or MKK7 on JNKs? Does it affect the activation, protein levels and localization of distinct JNK isoforms?

- Which effect has a single MKK4 or MKK7 splice variant on downstream JNK signalling, such as the activation and level of target proteins?

- Which effect has a single MKK4 or MKK7 splice variant on JNK signalosomes? Does it change the assembly or abundance of JNK signalosomes?

2 Materials and methods

2.1 Materials

Unless otherwise indicated, all solutions and dilutions were prepared in double-distilled water (DDW). All chemicals were molecular biology or *pro analysi* (*p.a.*) grade, and cell culture reagents had endotoxin levels of less than 0.01 ng/ml lipopolysaccharide. Apart from antibodies used for Western blots, Tab. 1 includes all materials together with the respective manufacturer.

Tab. 1: Materials.

Material	Manufacturer / Supplier
Acetic acid	Carl Roth; Karlsruhe, Germany
Acrylamide / bis-acrylamide solution 37.5:1	Bio-Rad; München, Germany
Agarose SeaKem LE	Biozym; Oldendorf, Germany
6-Aminocaproic acid	Merck-Schuchardt; Hohenbrunn, Germany
Ammonium persulphate (APS)	Merck; Darmstadt, Germany
Ampicillin	Stratagene; Amsterdam, Netherlands
Aprotinin	Sigma; München, Germany
Bacto-tryptone	BD Biosciences; Heidelberg, Germany
Bacto-yeast	BD Biosciences; Heidelberg, Germany
*Bam*HI	Fermentas; St. Leon-Rot, Germany
β-Glycerolphosphate	Sigma; München, Germany
Bovine serum albumin (BSA)	Boehringer; Mannheim, Germany
Boric acid	Sigma; München, Germany
BrdU incorporation assay	Roche; Mannheim, Germany
Broad Range Prestained Protein Marker	New England Biolabs; Frankfurt, Germany
Bromophenol blue	Merck; Darmstadt , Germany
Calcium chloride	Merck; Darmstadt, Germany
CASYton buffer	Schaerfe System; Hamburg, Germany
Cell culture plates (20 cm)	Sarstedt; Nümbrecht, Germany
Cell culture plates (10 cm)	Sarstedt; Nümbrecht, Germany
Cell culture plates (6 wells)	Sarstedt; Nümbrecht, Germany

Material	Manufacturer / Supplier
Cell culture plates (12 wells)	Sarstedt; Nümbrecht, Germany
Cell culture plates (24 wells)	Sarstedt; Nümbrecht, Germany
Cell culture plates (96 wells)	Sarstedt; Nümbrecht, Germany
Cell scraper	Sarstedt; Nümbrecht, Germany
Chamber slides	Nunc; Karlsruhe, Germany
3-[(3-Cholamidopropyl)dimethyl-ammonio]-1-propanesulfonate (CHAPS)	Merck; Darmstadt, Germany
ChIP-IT Control kit rat	Active Motif; Rixensart, Belgium
ChIP-IT Express Enzymatic kit	Active Motif; Rixensart, Belgium
Collagen	Biochrom; Berlin, Germany
Coomassie blue	Carl Roth; Karlsruhe, Germany
Cryotubes (2 ml)	Sarstedt; Nümbrecht, Germany
Cuvettes	Sarstedt; Nümbrecht, Germany
Diethyl pyrocarbonate (DEPC)	Sigma; München, Germany
Dimethylsulfoxide (DMSO)	Carl Roth; Karlsruhe, Germany
1,4-Dithiotheit	Carl Roth; Karlsruhe, Germany
dNTP set (10 mM each)	Fermentas; St. Leon-Rot, Germany
DreamTaq DNA Polymerase	Fermentas; St. Leon-Rot, Germany
DreamTaq Buffer (10 x)	Fermentas; St. Leon-Rot, Germany
DTT (0.1 M)	Invitrogen; Karlsruhe, Germany
Dye Reagent	Biorad; München, Germany
ECL Plus Reagents	Amersham Biosciences; Freiburg, Germany
Ethylene-diamine-tetra-acetic acid (EDTA)	Carl Roth; Karlsruhe, Germany
Ethanol *p. a.*	Carl Roth; Karlsruhe, Germany
Ethanol, technical (denatured)	Bundesmonopol für Branntwein (BfB); Offenbach, Germany
Ethidium bromide solution (10 mg/ml)	Carl Roth; Karlsruhe, Germany
Ethylene glycol-bis(2-aminomethyl)-N,N,N′,N′-tetraacetic acid (EGTA)	Merck; Darmstadt, Germany
ExactaCruz reagents	Santa Cruz; Heidelberg, Germany
Fetal calf serum (FCS)	Biochrom; Berlin, Germany
Filter paper	Whatman; Maidstone, UK
Filter unit 0.22 µm, syringe-driven	Qualilab; Bruchsal, Germany
Formaldehyde	Merck; Darmstadt, Germany

Material	Manufacturer / Supplier
Formamide	Carl Roth; Karlsruhe, Germany
G418, sulfate (solution)	Biochrom; Berlin, Germany
Glucose	Carl Roth; Karlsruhe, Germany
Glycerol	Merck; Darmstadt, Germany
Glycine	Merck; Darmstadt, Germany
HEPES	Merck; Darmstadt, Germany
*Hind*III	Fermentas; St. Leon-Rot, Germany
Horse serum	Biochrom; Berlin, Germany
Hydrochloric acid (HCL)	Carl Roth; Karlsruhe, Germany
Hyperfilm ECL	Amersham Biosciences; Freiburg, Germany
Immobilon P transfer membrane	Millipore; Eschborn, Germany
Kaiser's glycerol gelantine	Merck; Darmstadt, Germany
Kanamycin	Carl Roth; Karlsruhe, Germany
LB-Agar	Sigma; München, Germany
1 kb DNA Ladder	Invitrogen; Karlsruhe, Germany
Leupeptin	Sigma; München, Germany
Ligation buffer (10 x)	Roche; Mannheim, Germany
Magnesium chloride (RT-PCR)	Invitrogen; Karlsruhe, Germany
Magnesium chloride ($MgCl_2$)	Carl Roth; Karlsruhe, Germany
β-Mercaptoethanol	Sigma; München, Germany
Methanol	Carl Roth; Karlsruhe, Germany
MinElute PCR Purification kit	Qiagen; Hilden, Germany
4-Morpholino-propane-sulfonic acid (MOPS)	Merck; Darmstadt, Germany
Mycoplasma Stain kit	Sigma; München, Germany
NGF (2.5 S)	Alomone labs; Jeruslaem, Israel
Non-fat dry milk	Uelzena; Uelzen, Germany
Nonidet P40	Fluka Chemie; Buchs, Switzerland
NucleoBond PC 100 kit	Macherey & Nagel; Düren, Germany
NucleoBond EF 500 kit	Macherey & Nagel; Düren, Germany
NucleoSpin Plasmid QuickPure kit	Macherey & Nagel; Düren, Germany
Paraformaldehyde	Merck; Darmstadt, Germany
Phosphate buffered saline w/o Ca^{2+} and Mg^{2+} (10 x)	PAA; Cölbe, Germany

Material	Manufacturer / Supplier
PCR buffer (10 x) (RT-PCR)	Invitrogen; Karlsruhe, Germany
pEGFP-C3	Clontech; Heidelberg, Germany
Penicillin/Streptomycin solution (10,000 U/ml / 10 mg/ml)	PAA; Cölbe, Germany
Pepstatin	Sigma; München, Germany
Phenylmethylsulfonyl fluoride (PMSF)	Carl Roth; Karlsruhe, Germany
Phosphatase Inhibitor Cocktail II	Sigma; München, Germany
Pifithrin-α	Santa Cruz; Heidelberg, Germany
Piperazine-N,N'-bis(2-ethanesulfonic acid) (PIPES)	Carl Roth; Karsruhe, Germany
Pipettes (serological, sterile; 5 / 10 / 25 ml)	Sarstedt; Nümbrecht, Germany
Pipette tips (10 / 200 / 1,000 µl)	Sarstedt; Nümbrecht, Germany
Ponceau S	Sigma; München, Germany
Potassium chloride (KCL)	Carl Roth; Karlsruhe, Germany
Potassium dihydrogen phosphate	Carl Roth; Karlsruhe, Germany
Potassium disulfate	Carl Roth; Karlsruhe, Germany
2-Propanol	Carl Roth; Karlsruhe, Germany
Propidium iodide	Carl Roth; Karlsruhe, Germany
Protease Inhibitor (Complete)	Roche; Mannheim, Germany
Protein marker, prestained, broad range	New England Biolabs; Frankfurt, Germany
QIAquick Gel Extraction kit	Qiagen; Hilden, Germany
QIAquick Nucleotide Removal kit	Qiagen; Hilden, Germany
QIAshredder	Qiagen; Hilden, Germany
Random primers	Promega; Mannheim, Germany
RNase H	Invitrogen; Karlsruhe, Germany
RNeasy Plus Mini Kit	Qiagen; Hilden, Germany
RPMI-1640 medium	PAA; Cölbe, Germany
T4 DNA Ligase	Roche; Mannheim, Germany
*Sal*I	Fermentas; St. Leon-Rot, Germany
Sodium hydrogen carbonate	Sigma; München, Germany
di-Sodium hydrogen phosphate	Merck; Darmstadt, Germany
Sodium hydroxide	Merck; Darmstadt, Germany

Material	Manufacturer / Supplier
Sodium thiosulfate	Merck; Darmstadt, Germany
SuperScript II Reverse Transcriptase	Invitrogen; Karlsruhe, Germany
SP600125	Alexis; Grünberg, Germany
Sodium acetate	Sigma; München, Germany
Sodium carbonate	Sigma; München, Germany
Sodium chloride (NaCl)	Carl Roth; Karlsruhe, Germany
Sodium citrate	Carl Roth; Karlsruhe, Germany
Sodium dodecyl sulphate (SDS)	Carl Roth; Karlsruhe, Germany
Sodium hydroxide (NaOH)	Carl Roth; Karlsruhe, Germany
T4 DNA ligase	Roche; Mannheim, Germany
TaqMan Low-Density Array	Applied Biosystems; Darmstadt, Germany
TaqMan Universal PCR Mastermix	Applied Biosystems; Darmstadt, Germany
Taxol	Calbiochem; Darmstadt, Germany
TEMED	Carl Roth; Karlsruhe, Germany
Thapsigargin	Calbiochem; Darmstadt, Germany
TNF-α	Millipore; Schwalbach. Germany
Tris	Carl Roth; Karlsruhe, Germany
Triton X-100	Merck; Darmstadt, Germany
Trypan blue solution, cell culture tested	Sigma; München, Germany
Tubes (0.5 / 1.5 / 2.0 ml)	Sarstedt; Nümbrecht, Germany
Tubes for PCR	Sarstedt; Nümbrecht, Germany
Tubes, sterile (15 ml)	Sarstedt; Nümbrecht, Germany
Tubes, sterile (50 ml)	Sarstedt; Nümbrecht, Germany
Tunicamycin	Calbiochem; Darmstadt, Germany
TurboFect	Fermentas; St. Leon-Rot, Germany
Tween-20	Calbiochem; Schwalbach, Germany
Ultrapure water	Biochrom; Berlin, Germany

2.2 Centrifuges, cell culture equipment and sterilization

Centrifugation parameters are documented as “time; relative centrifugal force; temperature”, *e.g.*, “5 min; ca. 2,000 ×*g*; 4°C”. The following centrifuges were used: Biofuge fresco,

Varifuge 3.0 (all from Heraeus; Osterode, Germany), Centrifuge 5804 R (Eppendorf; Hamburg, Germany) and Mikrofuge (Neolab; Heidelberg, Germany). The Mikrofuge created a relative centrifugal force (RCF) of 2,000 ×*g* maximum. The Varifuge 3.0 and Centrifuge 5804 R displayed RCF's automatically, and the RCF's in the Biofuge fresco (maximum radius (rmax): 85 mm) were calculated using the following equation:

$$\times g = 1.118 \times \text{rmax [mm]} \times (\text{rpm}/1{,}000)^2.$$

Cell culture experiments were performed under sterile conditions (70% ethanol) in a laminar flow unit (LFU; HERAsafe; Heraeus). The cells were cultivated at 37°C and 5% CO_2 in an incubator (HERAcell; Heraeus; Osterode, Germany) and examined using an Olympus CK 2 inverted microscope (Olympus; Hamburg, Germany). All tubes and pipette tips were autoclaved (134°C, 2.2 bar, 20 min). Solutions for cell culture were either obtained sterile or autoclaved in a DS 202 autoclave (Webeco; Bad Schwartau, Germany) at 120°C and 2.0 bar for 30 min.

2.3 Culture, staining, stimulation and transfection of cells

Cells were purchased from the American Type Culture Collection (Manassas, VA, USA). Cell culture was maintained by passaging the confluent cells on 10 cm cell culture plates. Prior to use, horse serum and fetal calf serum (FCS) were inactivated by incubation at 56°C for 30 min, aliquoted and stored at –20°C. The penicillin/streptomycin solution was also stored at –20°C, while the medium was stored in a cooling chamber (4°C). The cells were provided with fresh medium every 2–3 days. The absence of mycoplasma contamination was confirmed by routine tests performed with the Mycoplasma Stain kit according to the manufacturer's instructions. After the cells had been passaged 20 times, the cultures were discarded.

2.3.1 PC12 cells

The rat PC12 pheochromocytoma cell line was derived from a transplantable rat pheochromocytoma (68). The cells were grown in RPMI-1640 medium supplemented with 10% horse serum, 5% fetal calf serum (FCS) and 1% penicillin/streptomycin solution.

Medium for transfected PC12 cells was additionally supplemented with 500 µg/ml G418 sulfate.

PC12 cells, like many other adherent cells, need a structured substrate for growing. Therefore, all plates used for cultivation and experiments were coated with collagen (0.1 mg/ml in 1x phosphate buffered saline (PBS) for proliferation; 0.01 mg/ml for differentiation). The bottom of the cell culture plates was covered with a thin layer of collagen solution, placed in the incubator for at least 1 h and then washed with PBS to remove collagen that had not adhered to the plate. Air-dried plates were stored under sterile conditions.

Since PC12 cells grow adherent, they were treated with passage EDTA before passaging. EDTA is a chelator of bivalent cations like Ca^{2+} and therefore helps to reduce cell-substrate adhesion. After washing with PBS (37°C), cells were rinsed with 2 ml passage EDTA and placed for 2 min in the incubator (37°C, 5% CO_2). Five ml of medium (37°C) was added, cells were scraped off the cell culture plate and transferred to a 15 ml tube. After centrifugation (10 min; 1000 ×*g*; r.t.), pelleted cells were first completely re-suspended in a syringe with a 21G needle attached in 2 ml of medium. Then 5 ml of medium were added and the cells were re-suspended again. After resuspension, electronic cell counts were carried out (section 2.3.2).The amount of cells, which were aliquoted into new cell culture plates depended on cell density and the diameter of the cell culture plate (Tab. 2).

For cell cycle analysis, cultures were transferred to serum-free medium for 24 h to stop proliferation (150). Cell growth was restarted by returning the cells to normal growth medium supplemented with FCS, resulting in a synchronised cell cycle.

For the production of PC12 stock aliquots, cells were harvested as described above and re-suspended in 1 ml of medium. An aliquot of the cell suspension was diluted in normal medium and cells were counted electronically. Freezing medium (RPMI-1640 supplemented with 10% FCS and 10% DMSO) was added to a final concentration of 5×10^6 cells/ml. The resulting suspension was aliquoted (1 ml) in 2 ml cryotubes which were incubated for 10 min at r.t., transferred to ice for 35 min, incubated at –20°C for 45 min and finally stored at –80°C.

For cell culture initiation, a stock aliquot was quickly thawed in a 37°C water bath. In the LFU, the cell suspension was transferred to a 10 cm plate with fresh medium (37°C). After 24 h at the latest, the medium had to be changed.

Tab. 2: PC12 cell numbers on cell culture plates.

Cell culture plate	Cells [x 10^6]
Ø 20 cm	1.5-2.5
Ø 10 cm	0.8-1.25
6-well	0.3
12-well	0.1
24-well	0.05
96-well	0.01

2.3.2 Electronic cell counting

Electronic cell counting analysis were performed by CASY TT cell counter (Schaerfe System; Hamburg, Germany). An aliquot of the cell suspension was mixed with CASYton buffer and cell number and viability were determined according to manufacturer's instructions. The CASY TT cell counter can determine the complete cell number, the ratio of cells with damaged cell membrane and the mean volume of one cell.

2.3.3 Trypan blue viability staining

Various manipulations of cells, including passaging, freezing and numerous stimulations result in cell death. To determine the number of surviving cells in a population, exclusion of the dye trypan blue can be used. Healthy cells are able to exclude this dye for a certain time, but trypan blue will quickly diffuse into cells which have lost their membrane integrity.

For trypan blue staining, control and stimulated cells were washed with PBS (37°C), rinsed with 2 ml of passage EDTA and placed for 2 min in the incubator (37°C, 5% CO_2). Five ml of medium (37°C) were added and cells were scraped off the cell culture plate and transferred to a 15 ml tube. After centrifugation (10 min; 1000 ×*g*; r.t.), the resulting pellet was thoroughly resuspended in an appropriate amount of PBS. Twenty µl of the cell suspension were mixed with 20 µl of trypan blue solution and transferred to a hemocytometer twin chamber (Omnilab; Hamburg, Germany). For reasons of accuracy, cells were not allowed to stay in the dye solution for longer than 5 min. Living cells in the 16 squares of both chambers were counted, and the percentage of viable cells was determined.

2.3.4 Flow cytometric analysis

Flow cytometry was used to determine the distribution of cells to cell cycle phases. The DNA intercalator propidium iodide binds to DNA of permeabilized cells. The amount of dye bound correlates with the content of DNA within a given cell. The relative content of DNA indicates the distribution of a population of cells throughout the cell cycle phases. Cells in the G1-phase of the cell cycle have a DNA content of 2n. Cells within the G2/M phases of the cell cyclöe have a DNA content of 4n and cells in the S-phase of the cell cycle have a DNA content greater than 2n and less than 4n.

One x 10^6 cells were harvested as described in section 2.3.1 and centrifuged at 200 x*g* and 4°C for 5 min. The medium was discarded and the cells were resuspended in 400 µl hypotonic propidium iodide solution [50 µg/ml propidium iodide; 0.1% (w/v) sodium citrate and 0.1% Triton-X-100 in Ultrapure water]. Afterwards cells were kept at 4°C in the dark until measurements. Stained cells were analysed using a FACSCalibur flow cytometer and CellQuest software (Becton Dickinson; Mountain View, CA, USA). The WinMDI (http://facs.scripps.edu/software.html) application was used for data analysis.

2.3.5 5-bromo-2-deoxyuridine (BrdU) incorporation assay

Cell proliferation was measured using a BrdU incorporation assay according to the manufacturer's instructions. 5-bromo-2-deoxyuridine is incorporated in the cellular DNA like thymidine. The immunoassay enables the quantification of cell proliferation based on the BrdU incorporation during DNA synthesis. Cells grown in a 96-well-plate (Tab. 2) were incubated with BrdU for 4 h and fixed. After incubation with an anti-BrdU-POD-antibody and the subsequent substrate reaction, absorbance at 370 nm (reference wavelength 492 nm) was measured using an ELISA reader (Model 680 microplate reader; Biorad; München, Germany).

2.3.6 Differentiation

In response to nerve growth factor (NGF), growth arrest is induced and PC12 cells differentiate into neuron-like cells with formation and elongation of neurites (67). PC12 cells were plated on collagen-coated plates (0.01 mg/ml in PBS). After 24 h, the cells were serum-starved for 72 h using medium containing 0.5% FCS and 1% penicillin/streptomycin to synchronize the cell cycle activity of the cells (150). With synchronized cells, the

differentiation process is more reproducible due to a comparatively similar NGF receptor expression on the cell surface. After 72 h, the medium was changed and supplemented with 50 ng/ml of 2.5 S NGF. The differentiating cells were provided with fresh medium containing NGF every 2–3 days. For monitoring differentiation in terms of morphological and molecular processes, cells were cultured for 5 days.

2.3.7 Neurite outgrowth

For the documentation of neurite formation and elongation, cells were photographed on day 5 of the differentiation process. To avoid artifacts of the documentation system, cells were either photographed using an Olympus CK 2 inverted microscope (Olympus; Hamburg, Germany) with a corresponding camera system (JVC; Tokio, Japan) or stained with Coomassie blue (section 2.3.8). Images were analysed using a DMR microscope (Leica; Solms, Germany) with a camera system (JVC; Tokio, Japan). The percentage of cells with neurites longer than 1.5 diameters of the cell body were counted using the software ImageJ (http://rsbweb.nih.gov/ij/).

2.3.8 Coomassie blue staining

PC12 cells at day 5 of the differentiation process (section 2.3.6) were stained with Coomassie blue to visualize the formation of neurites. Cells were plated on chamber slides (10 µl of cell solution/250 µl of medium per well) and treated with NGF (50 ng/ml) for 5 days. The medium was discarded, and the cells were rinsed with paraformaldehyde (4% in PBS, 37°C) and incubated at r.t. for 15 min. The paraformaldehyde was then discarded, and the cells were washed two times with DDW. Subsequently, the ready-to-use Coomassie blue solution was added and incubated for at least 30 min. After discarding the staining solution and washing two times with DDW, the cells were incubated in de-staining solution (10% methanol, 10% acetic acid in DDW) for at least 30 min. Finally, the cells were washed two times with DDW.

2.3.9 Incubation with inhibitors and stressors

For stimulation experiments, cells below passage number 20 were plated on 10 cm, 6-well cell culture plates or on chamber slides (250 µl of medium per well). The JNK inhibitor SP600125 (2 µM, 30 min) was added before incubation with stressors. The lyophilized

substance was dissolved in dimethyl sulfoxide (DMSO) to make up a 10 mM stock solution which was aliquoted, protected from light and stored at –20°C. The p53 inhibitor pifithrin-α (30 µM) was dissolved in DMSO to make up a 30 mM stock solution which was aliquoted and stored at -20°C. Subconfluent cells were incubated with 1.4 µg/ml tunicamycin (0.2 µg/ml stock in DMSO), 50 ng/ml TNF-α (0.1 mg/ml stock in ultra pure water), 5 µM taxol (10 mM stock in DMSO) or 5 µM thapsigargin (10 mM stock in DMSO). After the respective incubation periods, RNA or proteins were extracted.

2.3.10 Transfection

Expression of foreign genes in mammalian cells is an important technology in molecular biology for merely biochemical purposes (*e.g.*, to study protein structure-function relationships and to produce proteins at a larger scale that are normally only available in limited quantities) or for the examination of cellular processes (*e.g.*, to confirm that cloned genes can direct the synthesis of the desired proteins and to evaluate the physiological consequences of the expression of regulatory proteins). The choice of a particular expression vector and the transfection method depends on the objectives of the study. In this work, an enhanced green fluorescent protein (EGFP)-tagged vector was used so that transfected cells could easily be identified due to their green fluorescence. To deliver the nucleic acids into PC12 cells, a sterile solution of a cationic polymer (TurboFect) was used. The polymer forms compact, stable, positively charged complexes with DNA. These complexes facilitate gene delivery into eukaryotic cells and protect DNA from degradation.

For transfection PC12 cells were plated on 96-well plates (section 2.3.1). After 2 days 0.1 µg DNA per well was diluted in 10 µl RPMI-1640 medium and 0.2 µl TurboFect per well were added. This solution was incubated for 20 min at r.t.. During that time the cells on the 96-well plate were provided with fresh medium. Than 10 µl of the DNA/Turbofect mix were pipetted in each well and the plate was gently rocked to achieve an even distribution of the complexes. After 24 hours the medium was removed and replaced by fresh medium containing 500 µg/ml G418 sulfate for selection of transfected cells.

There are two possibilities of expressing foreign DNA in mammalian cells: Cells can either be transfected transiently or stable clones can be generated. However, to examine effects of the recombinant proteins, the transfection efficiency has to be high, which is usually not the case with PC12 cells. Therefore, stable cell clones were established in this study by selection with G418 (section 2.3.1).

2.4 Processing of PC12 cells for RNA extraction

2.4.1 Experimental precautions to minimize RNA degradation

To minimize RNase activity during RNA extractions, several precautions were taken. Molecular biology grade chemicals were used to prepare buffers. All solutions were made up in DDW containing 0.1% diethylpyrocarbonate (DEPC) and were autoclaved prior to use. All tubes, pipette tips etc. were bought RNase-free. Samples were kept on ice wherever possible and all reagents were added on ice, since RNases are less effective at low temperatures.

2.4.2 Harvesting cells

PC12 cells were harvested from the respective cell culture plates. The medium was discarded and the cells were washed with PBS (37°C). After removing the PBS very carefully, an appropriate amount of RLT Plus buffer (including 1% β-mercaptoethanol) (RNeasy Plus kit, Qiagen) was pipetted on the plates (1 ml for 6 cm plates, 3 ml for 10 cm plates) and the PC12 cells were scraped off the plates using a sterilized (70% ethanol) rubber cell scraper. The resulting cell extracts were transferred to 1.5 ml tubes and either immediately processed for RNA extraction (section 2.5) or stored at -80°C until extraction.

2.5 Isolation of RNA

2.5.1 RNA extraction

RNA extraction from cells was performed using the RNeasy Plus Mini kit with an optimized protocol. The cell lysates were pipetted into a QIAshredder spin column placed in a 2 ml collection tube, and centrifuged (2 min; 16,000 x*g*; r.t.) to homogenize the lysate. For DNA removal, the homogenized lysate was transferred to a gDNA Eliminator spin column and centrifuged (30 sec; 16,000 x*g*; r.t.). One volume of 70% ethanol was added to the flow-through, and mixed by pipetting. The sample was transferred to an RNeasy spin column and centrifuged (30 sec.; 16,000 x*g*; r.t.) for precipitation of RNA. The precipitated RNA on the column membrane was washed once with 700 µl RW1 buffer, and twice with 500 µl RPE buffer (including ethanol) (30 sec.; 16,000 x*g*; r.t.) to remove salts. After the RNeasy spin column has been transferred to a clean collection tube, the membrane was dried by centrifugation (3 min; 16,000 x*g*; r.t.). For elution of RNA, the RNeasy spin column was transferred to a clean collection tube and 40 µl RNase-free water was directly pipetted on the

spin column membrane. After 1 min. incubation at r.t. the RNeasy spin column was centrifuged for 1 min at 16,000 x*g* and r.t.. The isolated RNA was stored at -80°C.

2.5.2 RNA quantification and quality control

The RNA sample was diluted 1:25 in RNase-free water. RNA concentrations were determined by measuring the absorbance at 260 nm (A_{260}) against a blank of RNase-free water in a photometer (BioPhotometer; Eppendorf; Hamburg, Germany). An absorbance of 1 unit at 260 nm corresponds to 40 µg/ml of RNA in water. Therefore, the RNA concentration c_{RNA} could be determined using the following equation:

$$c_{RNA} = 40 \times A_{260} \times \text{dilution factor (}e.g.\text{, 25)}$$

The ratio of the absorbances at 260 nm and 280 nm (A_{260}/A_{280}) allows to estimate the purity of RNA with regard to protein contaminants that also absorb in the UV. A ratio of 1.6–2.0 indicates pure RNA (in water). In order to exclude genomic DNA contamination, control reverse transcription polymerase chain reaction (RT-PCR) experiments were performed in which no reverse transcriptase (RT) was added prior to a PCR step with primers for H2A.z (section 2.6).

2.5.3 RNA agarose gel

To assess the integrity of isolated RNA, an aliquot of the RNA sample was analysed with a denaturing agarose gel. Intact total RNA run on a denaturing gel has sharp, clear 28S and 18S rRNA bands. The 28S rRNA band should be approximately twice as intense as the 18S rRNA band. This 2:1 ratio (28S:18S) is a good indication that the RNA is completely intact. Partially degraded RNA has a smeared appearance, lacks the sharp rRNA bands, or does not exhibit the 2:1 ratio of high quality RNA. Completely degraded RNA appears as a very low molecular weight smear.

Formaldehyde agarose gels (1.5%) were performed with MOPS buffer [40 mM 4-morpholino-propane-sulfonic acid (MOPS; pH 7.0), 10 mM sodium acetate, 1 mM EDTA] and 20% formaldehyde. Two µg of RNA was filled up to 10 µl with ultrapure water and 10 µl of RNA loading buffer [40% (v/v) formamide, 20% (v/v) saturated bromophenol blue solution, 5% (v/v) formaldehyde and 0.75% ethidium bromide in MOPS buffer] were added.

The RNA samples were incubated for 5 min. at 65°C to denaturate the RNA. The gels were run in MOPS buffer at a current voltage of 60 V for 3 h. Bands were visualized with 312 nm UV light (Image Master VDS; BioRad; München, Germany).

2.6 Reverse transcription polymerase chain reaction (RT-PCR)

2.6.1 Reverse transcription of mRNA

Reverse transcription polymerase chain reaction (RT-PCR) is a method in which a RNA-dependent DNA polymerase (the reverse transcriptase, RT) is used to selectively transcribe mRNA into complementary DNA (cDNA). The RT can start from random primers binding to the polyadenylated tail of the mRNAs. The resulting cDNAs can then be selectively amplified by PCR. In this study, the SuperScript II First-Strand Synthesis System for RT-PCR was used to produce cDNA.

The RT reaction was carried out in a final volume of 20 µl. For each sample, 500 ng of RNA (section 2.5) were diluted in a volume of 11.5 µl with ultrapure water in a single PCR tube. The Random primer solution (0.5 µl) was added to each sample, incubated for 5 min at 65°C in a thermocycler (Personal Cycler; Biometra; Göttingen, Germany) and chilled on ice in order to eliminate RNA secondary structures and to allow binding of the Random primers to the polyadenylated tails of the mRNAs. Meanwhile, the RT master mix was prepared on ice as described in Tab. 3. After the samples had been chilled on ice, 7 µl of the RT master mix was added to each sample.

Tab. 3: Composition of the RT-PCR master mix.

Component	Quantity (for 7 µl per sample)
PCR Buffer (10 x)	2 µl
dNTP Mix (10 mM)	1 µl
DTT (0.1 M)	2 µl
$MgCl_2$ (25 mM)	2 µl

Samples were incubated in the thermocycler at 25°C for 2 min, then 1 µl SuperScript II RT was added to each sample. Subsequently, incubation in the thermocycler at 25°C was continued for 10 min followed by 42°C for 50 min and 70°C for 15 min. This rise in

temperature inactivated the RT and denatured RNA-cDNA hybrids. After addition of 1 µl RNase H for a final 20 min incubation in the thermocycler at 37°C, samples were either used immediately in subsequent PCRs or stored at –20°C until required.

2.6.2 PCR

The cDNA produced in the RT reaction (section 2.6) was amplified in a total volume of 50 µl in a thermocycler. 1 µl of the cDNA sample was pipetted into single PCR tubes and placed on ice. The PCR master mix (Tab. 4) was prepared on ice, and the respective amount of the master mix was added to each sample. The final PCR mix contained 1 µl of the RT products, 0.2 mM of each dNTP, 0.2 µM of each primer and 2.5 units of Taq DNA Polymerase.

Tab. 4: Composition of the PCR master mix.

Component	Quantity (for 50 µl per sample)
Autoclaved DDW	40.75 µl
DreamTaq buffer (10 x)	5 µl
dNTP solution (10 mM)	1 µl
Forward primer (10 µM)	1 µl
Reverse primer (10 µM)	1 µl
DreamTaq DNA Polymerase	0.25 µl (1 unit)

All primers were designed using the software Primer 3 Software Distribution (Whitehead Institute/Howard Hughes Medical Institute; Boston, MA, USA). The size of the amplicons ranged from 129 bp to 835 bp with different annealing temperatures depending on the DNA sequence (Tab. 5). Therefore, different PCR programs had to be used for most PCRs.

Initially, one incubation at 94°C for 5 min was performed to denature the cDNA template. The denaturation step was followed by repeated cycles, each consisting of a denaturation step in which double-stranded DNA was melted to single strands (94°C for 1 min), an annealing step for binding of the primers to their specific recognition sites on the template (1 min), and an extension step (72°C) where new strands of DNA were produced by DNA polymerase extension of the primers. Finally, an additional extension step (72°C, 10 min) was carried out to ensure that all DNA produced was double-stranded.

For each RT-PCR experiment, a primer pair which was specific for the target sequence and a primer pair which resulted in amplification of an ubiquitously occuring endogenous cellular component, the histone H2A.z, were selected. H2A.z is the only histone which is not regulated in its expression during the differentiation of rat neurons (139), and it was amplified to normalize for varying efficiencies in RNA isolation and reverse transcription. The absence of contamination was checked by negative control assays, in which RNA in the RT reaction and cDNA in the PCR were replaced by DEPC-DDW. Genomic DNA contamination had already been excluded by PCR for H2A.z in minus-RT reactions.

Tab. 5: Primer pairs and reaction conditions for PCR amplification.

Primer	Sequence (5'→3')	T_A [°C]	Cycles	Amplicon [bp]
H2A.z_for	CGTATTCATCGACACCTGAAA	55	22	282
H2A.z_rev	CTGTTGTCCTTTCTTCCCAAT			
GAPDH_for	AACGACCCCTTCATTGAC	53	31	835
GAPDH_rev	TCCACGACATACTCAGCAC			
p21/WAF_for	TGGACAGTGAGCAGTTGAGC	54	27	129
p21/WAF_rev	ACACGCTCCCAGACGTAGTT			
CyclinD1_for	ATTGAAGCCCTTCTGGAGTCAAGCC	58	27	420
CyclinD1_rev	TCTATTTTTGTAGCACCCCCCCGTC			
JNK1_for	ATGCTAAGCGAGCCTACCG	55	30	621
JNK1_rev	TCTCAAAGCTATAGCCAGCG			
JNK2_for	ACCTCCTCTACCAGATGCT	58	27	357
JNK2_rev	TGAACTCTGCGGATGGTG			

The specificity of the primer pairs was verified by comparative alignment using the BLAST database (http://www.ncbi.nlm.nih.gov/BLAST/) at the National Center for Biotechnology Information (NCBI; Bethesda, MD, USA). All amplicons were cloned and sequence verified using the GATC Biotech AG (Konstanz, Germany) sequencing service.

RT-PCR products were visualized by agarose gel electrophoresis. One % (w/v) or 1.5% (w/v) agarose gels were prepared with 1 × Tris-boric acid-EDTA buffer [TBE; 0.9 M Tris, 0.9 M boric acid and 20 mM EDTA]. The 1 × TBE buffer was set up by diluting a 10 × concentrate with DDW. After dissolving the required amount of agarose by heating in a

microwave oven, 5 µl/100 ml of a 10 mg/ml ethidium bromide stock solution was added (final concentration: 0.5 µg/ml). 10 × loading buffer [0.25% (v/v) bromophenol blue and 30% (v/v) glycerol in DDW] was prepared and added to all samples, resulting in a 1 × final concentration. The 1 kb DNA Ladder was used as a marker. The gels were run in 1 × TBE buffer at 80 mV for ca. 60 min (Wide Mini-Sub Cell GT, Biorad; München, Germany). Bands were visualized with 312 nm UV light (Image Master VDS; Biorad; München, Germany).

2.7 TaqMan Real-Time-quantitative PCR (QRT-PCR)

TaqMan Real-Time PCR gene expression profiling was done by using the Applied Biosystems 7900HT Fast Real-Time System with TaqMan Low-Density Arrays, which is a 384-well micro-fluidic card pre-loaded with optimised probes and primers for selected genes. Relative quantification analysis was performed with ABI Prism SDS 2.1.1 software (Applied Biosystems; Darmstadt, Germany). All experiments were performed in technical triplicates for each of the three biological replicates in 384 well plates. The QRT-PCRs were performed in cooperation with Dr. Robert Häsler from the Institute of Clinical Molecular Biology at the University Hospital Schleswig-Holstein Campus Kiel.

TaqMan probes depend on the 5'- nuclease activity of the DNA polymerase used for PCR to hydrolyze an oligonucleotide that is hybridized to the target amplicon. TaqMan probes are oligonucleotides that have a fluorescent reporter dye attached to the 5' end and a quencher moeity coupled to the 3' end. These probes are designed to hybridize to an internal region of a PCR product. In the unhybridized state, the proximity of the fluor and the quench molecules prevents the detection of fluorescent signal from the probe. During the elongation step of the PCR, the 5'- nuclease activity of the polymerase cleaves the probe. This leads to the release of the fluorescent dye from the quencher and to an increase in fluorescence that is proportional to the exponentially amplified amount of cDNA. The CT (cycle threshold)-value of a sample indicates the number of cycles needed to reach defined fluorescence intensity above background levels.

All experiments were performed with TaqMan Universal PCR Mastermix. Mastermix (4.5 µl), fluorescently labeled probe (0.2 µl; 10 µM) and forward and reverse primers (0.15 µl; 20 µM) were added to each plate well. The final reaction volume was set to 10 µl. The endogenous control 18s was used for normalization. Normalized delta (Δ) cycle threshold (CT) values were then subjected to evaluation of statistical significance ($p < 0.05$) of differential expression compared to control using the Wilcoxon test. Fold changes were

calculated using the ΔΔCT method, whereby linoleic acid intervention values were used as reference (control). The relative expression of each sample was calculated using the $2^{-\Delta\Delta CT}$ method:

Relative expression = $2^{-(S\Delta CT - C\Delta CT)}$

ΔCT = (CT(GOI) – CT(HKG))

SΔCT - CΔCT = control value (C) is subtracted from sample value (S)

GOI : gene of interest

HGK: house keeping gene

S: sample

C: control

2.8 Cloning of cDNA fragments

2.8.1 General principles and procedure

Molecular cloning is defined as the insertion of a DNA fragment – either genomic DNA or cDNA – into a vector which allows amplifying and modifying this fragment. Since this study focused on the effects of recombinant protein expression, cDNA was used.

First, RNA was extracted from PC12 cells (section 2.5.1), transcribed into cDNA and amplified by PCR using Taq polymerase (section 2.6). The cDNA was purified and ligated into the mammalian expression vector pEGFP-C3, which was transferred into competent bacteria. Positive bacterial clones were used for endotoxin-free plasmid extraction, which finally yielded the plasmid for the transfection of PC12 cells.

The choice of a particular expression vector depends on the cell culture system used. For neuronal cells, which are difficult to transfect, it is advisable to use expression vectors that encode fluorescence tagged fusion proteins to facilitate detection and selection of transfected cells. Therefore, the pEGFP-C3 vector was used in this study.

2.8.2 Production of competent *E. coli* DH5α cells

DH5α is a versatile *E. coli* strain that can be used in many cloning applications. For culturing DH5α, LB liquid medium was set up as follows: 10 g of Bacto tryptone, 5 g of Bacto yeast extract and 5 g of sodium chloride were dissolved in 1 l of DDW and the pH was adjusted to

7.2. LB agar medium for culture plates was produced by dissolving 16 g of purchased LB Agar in 500 ml of DDW and adjusting the pH to 7.2. Both LB medium and LB agar were autoclaved prior to use or plating the agar on Petri dishes, respectively.

For the production of DH5α stock aliquots, single colonies were picked from a freshly streaked out plate and cultures were inoculated in 2–5 ml LB medium. The cultures were placed in the incubator (Innova 4000; New Brunswick Scientific; Amsterdam, The Netherlands) for 12–14 h at 37°C with vigorous shaking (200 rpm). Subsequently, 1.66 ml of the bacteria solution was transferred into cryotubes, mixed with 0.344 ml 86% (v/v) sterile glycerol. The cryotubes were snap-frozen in liquid nitrogen and stored at –80°C.

For the production of competent DH5α, a starter culture was inoculated with bacteria from a stock aliquot (3 ml LB, 37°C and 200 rpm overnight). Subsequently, cells were streaked out on LB agar and placed in an incubator at 37°C overnight. A single colony was picked and another overnight culture was inoculated with bacteria from this colony (3 ml LB, 37°C, 200 rpm). The overnight culture was diluted in LB medium (1:100) and incubated (37°C, 200 rpm) until an OD_{600} of 0.3–0.4 was reached. The OD_{600} was measured with 1 ml aliquots in disposable plastic cuvettes in a spectrophotometer (U-2000; Hitachi; Wiesbaden, Germany). The bacteria were placed on ice for 10 min before centrifugation (10 min; 1,000 × *g*; 4°C). The supernatant was discarded and the pellets were re-suspended in an appropriate amount of 100 mM $MgCl_2$ (1 ml of $MgCl_2$ solution for a pellet obtained from 25 ml of cell suspension). All bacteria were transferred into one tube and stored at 4°C overnight. Subsequently, sterile glycerol was added to a final concentration of 15% (v/v). The bacteria-glycerol solution was distributed in pre-chilled 1.5 ml tubes (200 µl aliquots) and stored at -80°C.

2.8.3 Generation of cloning primers and selection of restriction enzymes

Before generating cloning primers, the coding sequences of *mkk4* and *mkk7* (Genbank accession numbers AY880882 and AY879265) were screened for restriction sites with the software WebCutter 2.0 (http://tools.neb.com/NEBcutter2/). Subsequently, the multiple cloning site of the vector was analysed, and two restriction sites that were absent in the respective *mkk* sequence were chosen. The sequence of the 5'-restriction site was placed at the front of the sense primer, and the 3'-restriction site was placed at the back of the antisense-primer (Tab. 6). It was also important to match the annealing temperatures T_A, which was done by using the following formula:

$$T_A = 4 \times (\text{number of G and C}) + 2 \times (\text{number of A and T})$$

Restriction enzymes or restriction endonucleases are part of bacterial defence systems which recognize and cut foreign DNA. The recognition sites consist of palindromic sequences of 4–8 base pairs. Type II restriction enzymes reliably cut DNA sequences at defined sites and are therefore used for restriction digestion in molecular biology. Tab. 7 lists the restriction enzymes used in this study.

Tab. 6: Cloning primers.

Primer name	Sequence (5'→3')
MKK4_rat_*Hind*III_for	ATGGTAAAGCTTATGGCGGCTCCGAGCC
MKK4_rat_*Bam*HI_rev	ATGGTAGGATCCCTAGTCGACATACATG GGAGAGCTGG
MKK7_rat_*Hind*III_for	ATGGTAAAGCTTATGGCGGCGTCCTCCC
MKK7_rat_*Bam*HI_rev	ATGGTAGGATCCCTACCTGAAGAAGGG CAGATGGTG

Tab. 7: Restriction enzymes.

Restriction enzyme	Recognition site
Hind III	A↓AGCTT
Bam HI	G↓GATCC

2.8.4 Amplification and purification of a PCR product

PCR (section 2.6.2) was always performed with two identical samples (50 µl each). Before pooling the samples, a 10 µl aliquot of each reaction was removed to verify the size of the amplicon and the absence of nonspecific bands on an agarose gel (section 2.6.2). For cloning, 90 µl of the PCR reaction was purified by the MinElute PCR Purification kit to purify the DNA from primers, nucleotides, polymerases and salts. PB buffer (450 µl) was added to the PCR reaction (90 µl), mixed, loaded on a MinElute spin column and centrifuged (1 min; 16,000 x*g*; r.t.). The flow-through was discarded and the column was washed with 750 µl PE buffer (including ethanol) (1 min; 16,000 x*g*; r.t.). After the flow-through was discarded, the MinElute spin column was centrifuged again (1 min; 16,000 x*g*; r.t.) to dry the column

membrane. For elution of cleaned DNA, the MinElute spin column was placed in a clean tube and 10 µl EB buffer was pipetted to the center of the column membrane. Before centrifugation (1 min; 16,000 x*g*; r.t.) the column was incubated for 1 min at r.t..

DNA concentration was determined by measuring the absorbance of a diluted aliquot at 260 nm (A_{260}) against a blank of ultrapure water. An absorbance of 1 unit at 260 nm corresponds to 50 µg of DNA per ml water. Therefore, the DNA concentration c_{DNA} was determined as follows:

$$c_{DNA} = 50 \times A_{260} \times \text{dilution factor (}e.g.\text{, 200)}$$

Similar to RNA, the ratio of the readings at 260 nm and 280 nm (A_{260}/A_{280}) provides an estimate of the purity of DNA with respect to contaminants that absorb in the UV, such as proteins. A ratio of 1.6–2.0 indicates pure DNA in water.

2.8.5 Restriction digestion

For cloning as well as for insert analysis of the resulting plasmids, restriction digestions were performed. The volumes and amount of DNA used depended on the purpose of the experiment. All components (Tab. 8) were added in the indicated order to a single sterile 1.5 ml tube. For mini preparation, test digestions and for general restriction digestions with 1 µg plasmid DNA, the samples were incubated for 1 h at 37°C. For preparative digestions, the incubation time was prolonged to 2.5 h. Subsequently, all samples were analysed on a 1% agarose gel. A 10 × concentration of loading buffer (see section 2.6.2) was prepared and added to all samples to result in a 1 × final concentration. The gels were run in 1 × TBE buffer at 100 mV for approximately 90 min and analysed as described above.

Tab. 8: Composition of a general digestion reaction.

Component	Quantity (for 10 µl per sample)
DDW (autoclaved)	7.5 µl
Plasmid DNA (1 µg/µl)	1 µl
Buffer (10 x)	1 µl
Restriction enzyme (10 U/ml)	0.5 µl

2.8.6 Purification of a digestion reaction

Before further enzymatic hydrolysis of digested PCR products (section 2.6.2) or plasmid DNA (section 2.8.9), the DNA was purified from restriction enzymes, nucleotides and salts using the QIAquick Nucleotide Removal kit. First, 10 volumes of PN buffer were added to 1 volume of digestion reaction, mixed and pipetted on a QIAquick spin column. After centrifugation (1 min; 16,000 x*g*; r.t.) the bound DNA was washed with 750 µl PE buffer (including ethanol) (1 min; 16,000 x*g*; r.t.). The flow-through was discarded and the QIAquick spin column was centrifuged again to dry the membrane (1 min; 16,000 x*g*; r.t.). For elution of DNA, the QIAquick column was placed in a clean tube, 30 µl of EB buffer was pipetted to the center of the membrane and centrifuged (1 min; 16,000 x*g*; r.t.) after 1 min incubation at r.t..

After a second digestion, the digested PCR products and plasmid DNA were analysed on a 1% agarose gel to verify the digestion and isolate the DNA fragment of interest. For purification of DNA fragments, the QIAquick Gel Extraction Kit was used. After running the agarose gel (section 2.6.2), the DNA fragment is excised from the gel with a clean scalpel. The gel slice was weighted in a tube and 300 µl QG buffer were added per 100 mg gel. In order to dissolve the gel, the sample was incubated for 10 min at 50°C and vortexed every second minute. After the agarose has dissolved completely, 1 volume of isopropanol was added and the sample was mixed by pipetting. To bind the DNA, the sample was pipetted onto a QIAquick column and centrifuged (1 min; 16,000 x*g*; r.t.). After the flow-through was discarded, the DNA was washed with 750 µl PE buffer (1 min; 16,000 x*g*; r.t.). The column membrane was dried by centrifugation (1 min; 16,000 x*g*; r.t.). For DNA elution the QIAquick column was placed in a clean tube and 30 µl EB buffer were pipetted to the center of the membrane. After incubation for 1 min at r.t. the column was centrifuged for 1 min at 16,000 x*g* and r.t..

2.8.7 Ligation of DNA fragments into the pEGFP-C3 vector

For ligation of the pEGFP-C3 vector and a DNA fragment, both had to be cut by restriction enzymes and purified carefully to allow efficient ligation (sections 2.8.5 and 2.8.6). The optimum molar ratio of insert and vector was 3:1. The required amount of the DNA fragment (in ng) was determined as follows:

$$100\ \text{ng vector} \times (\text{kb insert} / \text{kb vector}) \times \text{molar ratio of insert / vector} = \text{ng insert}$$

The appropriate amounts of vector and insert were mixed and filled up with autoclaved DDW to 13 µl. The ligation buffer (1.5 µl; 10 x) and 0.5 µl T4 DNA ligase were added. Samples were placed in a thermocycler, incubated for 30 min at r.t., and subsequently for at least 12 h at 15°C. To avoid exonuclease activity of the T4 ligase, the ligation mix was stored at –20°C.

2.8.8 Heat-shock transformation of *E. coli* DH5α cells

For optimal transformation efficiency, 10 ng of plasmid DNA (section 2.8.9) or 1 µg of ligation product (section 2.8.7) were used. To validate the quality of the competent cells, an appropriate vector for the respective antibiotic was used as a positive control. Competent DH5α cells were slowly thawed on ice. The appropriate amount of plasmid DNA or ligation product was added and the cells were kept on ice for 30 min. Subsequently, the cells were incubated at 42°C for 2 min and immediately placed back on ice for another 2 min. After adding 800 µl of pre-warmed LB medium, the cells were incubated at 37°C and 200 rpm for 1 h. The bacteria suspension (100 µl or 500 µl) was streaked out on agar plates which contained the selective antibiotic to inhibit growth of non-transformed bacteria. The plates were placed in the incubator (37°C) overnight. When single colonies were detected after overnight incubation, plates were stored at 4°C to inhibit further growth of the colonies.

2.8.9 Preparation of plasmid DNA

2.8.9.1 Mini preparation of plasmid DNA

For small scale purification of plasmid DNA, 5 ml LB medium containing the selective antibiotic were inoculated with a single clone and incubated overnight (37°C, 200 rpm). Afterwards the plasmid DNA was isolated from 3 ml bacteria suspension with the NucleoSpin Plasmid QuickPure kit according to the manufacturer's instruction. The procedure is based on a modified alkaline lysis that was first described in 1979 by Birnboim and Doly (9). The purity and concentration of isolated plasmid DNA was determined by measuring the absorbance at 260 nm in a photometer (section 2.8.4). Plasmid DNA was stored at -20°C. The remaining 2 ml bacteria suspension were stored at 4°C until analysis of the insert size had shown whether the clone contained the desired insert. In this case, the leftover bacteria suspension was used for producing glycerol stocks (see section 2.8.2).

2.8.9.2 Midi preparation of plasmid DNA

For cDNA sequence verification by GATC Biotech AG (Konstanz, Germany) and further experiments, plasmid DNA was isolated using the NucleoBond PC 100 kit according to the manufacturer's specifications. Since the plasmids used in this study had a high copy number, overnight cultures of 25 ml LB (37°C, 200 rpm) with the selective antibiotic were sufficient for midi preparation.

The bacteria were harvested by centrifugation (15 min; 6,000 ×*g*; 4°C). The pellet was resuspended in 4 ml of Buffer 1, 4 ml of Buffer 2 were added and the tube was inverted 4–6 times to gently mix its contents. After incubating the sample for 5 min at r.t., 4 ml of pre-chilled Buffer 3 were added and the sample was mixed again by inverting the tube. The lysate was poured into the Qiafilter cartridge and incubated for 10 min at r.t.. During incubation, a Qiagen-tip 100 was equilibrated with 4 ml of Buffer QTB. After the 10 min incubation, the lysate was filtered using the Qiafilter cartridge and loaded on the equilibrated Qiagen-tip 100. After the lysate had passed through the resin by gravity flow, the Qiagen-tip was washed two times with 10 ml of Buffer QC. Subsequently, the plasmid DNA was eluted with 5 ml of Buffer QF, transferred to a fresh 15 ml tube and mixed with 3.5 ml of 2-propanol. To precipitate the plasmid DNA, the mixture was distributed into sterile 1.5 ml tubes (830 µl each) and centrifuged (30 min; 16,000 ×*g*; 4°C). The resulting pellets were washed with 100 µl of ethanol (70%) and centrifuged again (10 min; 16,000 ×*g*; 4°C). After air-drying, the pellets were dissolved in 50–100 µl of ultrapure water and the yield was determined (section 1.8.4.). The remaining DNA was stored at –20°C until use.

2.8.9.3 Endotoxin-free maxi preparation of plasmid DNA

For transfection experiments, plasmid DNA must be free of endotoxins. To obtain this standard, the NucleoBond EF 500 protocol for high copy plasmids was used. Overnight cultures in 100 ml LB containing the selective antibiotic were inoculated (37°C, 200 rpm). The bacteria were harvested by centrifugation (15 min; 6,000 ×*g*; 4°C) and the pellet was resuspended in 10 ml of Buffer P1. Subsequently, 10 ml of Buffer P2 were added and the tube was inverted 4–6 times for gentle mixing. The sample was incubated at r.t. for 5 min. Ten ml of pre-chilled Buffer P3 was added and the sample was mixed by inverting the tube. The lysate was poured into the Qiafilter cartridge and incubated for 10 min at r.t.. Subsequently, the lysate was filtered into a 50 ml tube, and 2.5 ml of Buffer ER were added to remove the endotoxins. The tube was inverted to mix its contents and placed on ice for 30 min. During

incubation, a Qiagen-tip 500 was equilibrated with 10 ml of Buffer QTB. The cleared endotoxin-free lysate was loaded on the equilibrated Qiagen-tip. The lysate was allowed to enter the resin by gravity flow. Subsequently, the Qiagen-tip 500 was washed twice with 30 ml of Buffer QC. After elution with 15 ml of Buffer QN, the plasmid DNA was transferred to a fresh 50 ml tube and mixed with 10.7 ml 2-propanol. For precipitation, the plasmid DNA was distributed in sterile 1.5 ml tubes (830 µl each) and centrifuged (30 min; 16,000 ×*g*; 4°C). The resulting pellets were washed with 100 µl of 70% (v/v) ethanol and centrifuged again (10 min; 16,000 ×*g*; 4°C). Air-dried pellets were dissolved in 50–100 µl of Ultrapure water, the yield was determined and the DNA was stored at –20°C.

2.8.9.4 Plasmid purification

After restriction digestion and analysis on an agarose gel, the fragments had to be purified for further use. To guarantee a high standard of purity, the QIAquick Gel Extraction kit was used (section 2.8.6). The agarose gels used for this extraction contained minimal amounts of ethidium bromide in order to avoid mutations caused by this dye.

2.8.10 Sequence verification

The Taq DNA polymerase synthesizes DNA very quickly, but it has a high error rate as compared to other DNA polymerases, such as Pfu. Therefore, it is necessary to verify the cloned sequences. In this study, all cloned cDNAs (ligated into pEGFP-C3) were sent to GATC (Konstanz, Germany) for sequence verification. The standard run was used. Before sequencing, the plasmid DNA was extracted by NucleoBond PC 100 plasmid preparation (section 2.8.9).

2.9 Denaturing protein extraction and protein quantification

2.9.1 Harvesting cells

After discarding the medium and washing the cells with PBS, PC12 cells were rinsed again with 800 µl PBS and scraped off the plates using a 70% ethanol-sterilized rubber cell scraper. The cell suspension was transferred to a sterile 1.5 ml tube and centrifuged (1 min; 2,000 ×*g*; r.t.). The supernatant was discarded and the pellet was used for protein extractions.

2.9.2 Denaturing extraction of whole cell proteins

Denatured protein extracts were prepared using a Tris-buffered sodium dodecyl sulfate (SDS) lysis buffer containing 1% (v/v) SDS, 10 mM Tris (pH 7.4), Protease Inhibitor complete (1 tablet for 10 ml of extraction buffer) and 1% Phosphatase Inhibitor Cocktail II in autoclaved DDW. The cell pellet sitting in a 1.5 ml tube was resuspended in 50–300 µl of lysis buffer (depending on the size of the pellet), incubated for 5 min at 95°C in a heating block (Thermomixer 543; Eppendorf; Hamburg, Germany) and chilled on ice. The sample was then sonicated twice for 5 s using a MS 72 sonotrode in a Sonopuls GM 70 sonicator (Bandelin; Berlin, Germany) and placed on ice again. Insoluble material was removed by centrifugation (15 min; 16,000 ×*g*; 4°C). The supernatant was transferred to a new 1.5 ml tube, and an aliquot was removed for determining the protein concentration. Protein extracts were aliquoted (in order to avoid repeated freeze-thaw cycles which can lead to loss of phosphate groups from phosphorylated proteins), snap-frozen in liquid nitrogen and stored at –80°C.

2.9.3 Denaturing extraction of nuclear proteins

To analyse nuclear proteins or the translocation of cytoplasmic proteins to the nucleus, cytoplasmic and nuclear proteins were extracted separately. Cells were harvested and washed in lysis buffer without Nonidet [10 mM HEPES, 10 mM KCl and 1.5 mM $MgCl_2$]. To lyse the cell membranes, cell pellets were resuspended in lysis buffer supplemented with Nonidet (0.1% v/v) and placed on ice for 10 min. The amount of lysis buffer was dependent on the size of the pellet (80–250 µl). After centrifugation (5 min; 12,000 ×*g*; 4°C), the supernatants containing the cytoplasmic proteins were transferred to a sterile 1.5 ml tube and SDS from a 10% stock solution was added to a final concentration of 1% SDS. Nuclear proteins were extracted by resuspension of the nuclear pellets in denaturing lysis buffer (section 2.9.2). Again, the amount of lysis buffer (50–100 µl) depended on the size of the cell pellet. From this point onwards, the cytoplasmic and the nuclear samples were treated as described for whole cell lysates in section 2.9.2.

2.9.4 Non-denaturating extraction of whole cell proteins

To analyse cytoplasmic proteins for Caspase-3 cleavage, cells were extracted under non-denaturating conditions. PC12 cells were harvested and lysed with CHAPS cell extract buffer [50 mM PIPES/NaOH (pH 6.5), 2 mM EDTA, 0.1% CHAPS, 5 mM DTT, 20 µg/ml

leupeptin, 10 µg/ml aprotinin, 10 µg/ml pepstatin, and 1 mM PMSF]. The cell pellet sitting in a 1.5 ml tube was resuspended in 20–30 µl of lysis buffer (depending on the size of the pellet) and snap-frozen in liquid nitrogen. After thawing, the pellet was snap-frozen in liquid nitrogen and thawed for another two times. Insoluble material was removed by centrifugation (15 min; 16,000 ×*g*; 4°C). The supernatant was transferred to a new 1.5 ml tube, and an aliquot was removed for determining the protein concentration. Protein extracts were aliquoted (in order to avoid repeated freeze-thaw cycles), snap-frozen in liquid nitrogen and stored at –80°C.

2.9.5 Non-denaturating extraction of whole cell proteins for immunoprecipitations

To analyse protein-protein interactions, cells were extracted under non-denaturating conditions to keep them in their native conditions. PC12 cells were harvested and resuspended in native lysis buffer [20 mM Tris (pH 7.6), 250 mM NaCl, 3 mM EDTA, 3 mM EGTA, 0,5% (v/v) Nonidet P40, 1% (v/v) phosphatase inhibitor, 1% (v/v) β-glycerolphosphate and 1% (v/v) protease inhibitor]. After incubation on ice for 30 min, the lysate was centrifuged to remove insoluble material (15,000 x*g* for 15 min). The supernatant was transferred to a new 1.5 ml tube, and an aliquot was removed for determining the protein concentration. Protein extracts were aliquoted (to avoid repeated freeze-thaw cycles), snap-frozen in liquid nitrogen and stored at –80°C.

2.9.6 Determination of protein concentrations

Protein concentrations were determined using Dye Reagent (Bio-Rad; München, Germany), a variant of Bradford's colorimetric assay. The Bradford assay is based on the shift of the absorbance maximum for an acidic solution of Coomassie Brilliant Blue G-250 from 465 nm to 595 nm when the dye binds to proteins. The assay was performed in disposable plastic cuvettes.

A protein standard was produced by serial dilution of a 1.2 mg/ml bovine serum albumin (BSA) stock solution in autoclaved DDW (0.1 to 0.6 mg/ml). Samples were diluted 1:20 or 1:50 in autoclaved DDW. Afterwards, 20 µl of sample or standard were pipetted into a cuvette and one cuvette was blanked with 20 µl of DDW. To prepare the working solution, the Dye Reagent stock solution was diluted 1:5 with DDW. One ml of the working solution was added to each cuvette. All cuvettes were vortexed to start the reaction and incubated at r.t.

for 10 min. The absorbance at 595 nm (A_{595}) was measured using a spectrophotometer (U-2000; Hitachi; Wiesbaden, Germany).

2.9.7 Immunoprecipitation (IP) and immunodepletion (ID)

For immunoprecipitation (IP) and immunodepletion (ID), native cell lysates (section 2.9.5) were prepared from subconfluent cells. One hundred fifty µg of total proteins were used for IP and ID with the ExactaCruz reagents. All steps were performed at 4 °C if not mentioned otherwise. The samples were pre-cleared for 30 min with the appropriate pre-clearing Matrix. The antibody-IP matrix complex was formed by incubation of 1 µg primary antibody with 50 µl of the appropriate IP matrix in 500 µl of PBS for 1 h. The IP antibody-IP matrix complex was washed twice with cold PBS, the pre-cleared sample was mixed with the antibody-IP matrix complex and incubated overnight. The negative control was prepared by incubation of the antibody-IP matrix complex with native lysis buffer. After centrifugation, the supernatants with the ID samples were collected for Western blots, while the pellets containing immobilized proteins with IP matrix complexes were washed three times with PBS. The immobilized proteins were dissociated with 5 x reducing electrophoresis buffer in 20 µl of ultra-pure water at 95 °C for 3 min. The supernatants from the dissociation were carefully loaded onto 12% (v/v) SDS-gels (section 2.10.1) whereas the matrix was removed by centrifugation.

2.9.8 Chromatin immunoprecipitation (ChIP)

Chromatin immunoprecipitation (ChIP) was performed using the ChIP-IT Express Enzymatic kit according to the manufacturer's instructions. Chromatin samples were immunoprecipitated with a p53 antibody (Oncogene). An RNA polymerase II antibody was used as a positive control and an IgG antibody as a negative control following the protocol of the ChIP-IT control kit rat. PCR was performed on input DNA, DNA immunoprecipitated with the control antibodies and DNA immunoprecipitated with the p53 antibody. ChIP PCR was done using β-Actin control primers and the following primers: 5'-GGGAGTGGTC ATTAGGTCTG-3' and 5'-GGGTGGTATTTGGAGTTCAG-3'. These primers flank a p53-binding site in the promoter region of the rat *p21* gene. PCR was performed with the DreamTaq PCR reagent system and PCR fragments were analysed on a 1.5% (w/v) agarose gel (section 2.6.2).

2.10 Sodium dodecyl sulfate polyacrylamide gel electrophoresis (SDS-PAGE) and Western blot

2.10.1 SDS-PAGE

The principle of SDS-PAGE is based on the fact that SDS-treated proteins are denatured and negatively charged in proportion to their molecular weights, which allows electrophoretic separation of SDS-treated proteins according to their size in the molecular sieve of a polyacrylamide gel. Polyacrylamide gels were prepared by co-polymerization of acrylamide monomers with the cross-linker bis-acrylamide, which was catalyzed by ammonium persulphate (APS; 10% (w/v) in DDW, stored at 4°C in the dark) and initiated by N,N,N',N'-tetramethylethylenediamine (TEMED). For better resolution, a short stacking gel was set on top of the main resolving gel. Differences in composition between these two gels resulted in concentration of the protein samples into narrow bands in the stacking gel and separation of the bands according to their size in the resolving gel.

Glass plates for a MiniProtean3 Vertical PAGE chamber (Biorad; München, Germany) were cleaned with warm water and 70% (v/v) ethanol. The glass plates were clamped together and placed in a vertical position on the benchtop. Depending on the molecular weight of the protein to be analysed, different acrylamide (Acrylamide/bis-acrylamide solution 37.5:1) percentages were used for preparation of the resolving gels [4 x resolving buffer; 1.5 M Tris (pH to 8.8 with HCl), 0.4% SDS]. The catalyst TEMED was added last to the resolving gel mix (Tab. 9) prepared in a 15 ml tube, and after thorough vortexing, the gel mix was pipetted carefully between the gel plates using a 10 ml pipette. For a smooth interface between resolving and stacking gel, the resolving gel was overlayered with DDW and allowed to solidify for 10–30 min (depending on the acrylamide percentage).

Tab. 9: Composition of resolving gels for SDS-PAGE.

Target protein size	10-30 kDa	30–60 kDa	60–100 kDa	> 100 kDa
Components	**15% gel**	**12% gel**	**10% gel**	**7.5% gel**
Acrylamide	5 ml	4 ml	3.3 ml	2.5 ml
resolving buffer (4 x)	2.5 ml	2.5 ml	2.5 ml	2.5 ml
Autoclaved DDW	2.4 ml	3.4 ml	4.1 ml	4.9 ml
TEMED	10 µl	10 µl	10 µl	10 µl
APS (10%)	100 µl	100 µl	100 µl	100 µl

The standard width of the resolving gel was 6 cm. When the gel had polymerized, the DDW layer was removed and residual liquid on the gel interface was carefully removed using strips of filter paper. Subsequently, the stacking gel [4 x stacking buffer; 0.5 M Tris (pH to 6.8 with HCl), 0.4% SDS] was prepared and pipetted over the solidified resolving gel (Tab. 10). A 15-well-comb was added, and the stacking gel was allowed to solidify for ca. 30 min.

Tab. 10: Composition of 3% stacking gels for SDS-PAGE.

Component	Quantity
Acrylamide	0.6 ml
stacking buffer (4 x)	1.5 ml
Autoclaved DDW	3.9 ml
Bromophenol blue	5 µl
TEMED	6 µl
10% APS[4]	60 µl

In the meantime, protein samples were diluted with autoclaved DDW in order to obtain 20 µg of total protein in a volume of 8 µl. 2 µl of 5 × SDS sample buffer were added, and the samples were heated to 95°C for 5 min (Thermomixer 543; Eppendorf; Hamburg, Germany). The 5 × SDS sample buffer contained 312.5 mM Tris (pH to 6.8 with HCl), 10% SDS, 10% β-mercaptoethanol, 50% glycerol and some crystals of bromophenol blue. After the final denaturation in sample buffer, samples were placed on ice until the gel was loaded.

After the stacking gel had polymerized, the comb was removed and the gel plates were attached to the vertical SDS-PAGE chamber. The buffer reservoirs were filled with 1 × protein electrophoresis buffer [25 mM Tris (pH 8.3), 192 mM glycine, 0.1% SDS; diluted from a 10 × stock solution], and the wells of the stacking gel were rinsed with electrophoresis buffer using a pipette. After the wells were free of residual gel particles, the samples (10 µl of sample containing 20 µg of protein) were loaded into the wells. Broad range pre-stained protein marker (5 µl) was loaded into separate wells in order to estimate the molecular weights of bands detected by subsequent Western blotting. The samples were run through the stacking gel at a constant current of 15 mA per gel for 30 min (Power Supply 250 EX; Invitrogen; Karlsruhe, Germany). After the samples had entered the resolving gel, the current was raised to 30 mA per gel. Usually, gels were run for 30 min after the tracking dye had

passed the end of the gel. Finally, gels were removed from the gel plates, the stacking gel was discarded, and the resolving gels were used for Western blots.

2.10.2 Western blot

In Western blotting experiments, proteins are transferred from a SDS-PAGE gel (section 2.10.1) to a synthetic membrane, on which specific proteins are subsequently detected by enzyme-tagged antibodies. In order to prevent non-specific attachment of antibodies to the membrane, the protein-binding capacity of the membrane is first saturated by incubation in non-fat milk or a BSA solution. After that, target proteins are labeled by hybridization with a primary IgG antibody (pAB; *e.g.*, produced in mice) and detected by a secondary antibody directed against IgG (sAB; *e.g.*, total mouse IgG). This secondary antibody is fused with an enzyme, *e.g.*, a horseradish peroxidase (HRP), which converts a chemiluminescence substrate. The chemiluminescence detected by highly sensitive films is proportional to the amount of secondary antibody bound to the primary antibody, the binding rate of which is in turn proportional to the amount of target protein present on the Western blotting membrane.

In the present study, proteins were transferred to a polyvinylidene difluoride (PVDF) membrane by semi-dry blotting using a semi-dry electroblotter. Three different transfer buffers were prepared, namely cathode buffer [25 mM Tris, 40 mM 6-aminocaproic acid, 20% methanol], anode buffer 1 [30 mM Tris, 20% methanol] and anode buffer 2 [300 mM Tris, 20% methanol]. For each gel, 15 pieces of blotting paper were cut to the size of the gel (9 × 6 cm) and pre-soaked in cathode buffer (6 pieces), anode buffer 1 (3 pieces) and anode buffer 2 (6 pieces), respectively. The Immobilon P PVDF membrane was cut to the size of the gel, marked for orientation and pre-soaked in 100% methanol for 3 min. After rinsing the membrane in DDW for 2 min to elute the methanol, it was equilibrated in anode buffer 1 until use. The six cathode buffer-soaked filter papers were placed in a stack on a glass plate with the SDS-PAGE gel on top. The equilibrated membrane was then placed in close contact with the gel, taking care not to leave air-bubbles in between. The ‘sandwich’ was completed by stacking the remaining pieces of filter paper (pre-soaked in anode buffers 1 or 2, respectively) on the membrane. Finally, the blotting ‘sandwich’ was turned around and placed into the semi-dry transfer unit (Pegasus; Phase; Lübeck, Germany) in which the lid is the cathode.

Proteins were transferred to the PVDF membrane using a constant current of 0.8 mA/cm^2 for 50 min (protein size 10-30 kDa), 1 h (protein size 30–80 kDa) or 1.5 h (> 80 kDa). Following transfer, the membrane was washed for 15 min in TBST buffer [20 mM Tris,

137 mM sodium chloride, 0.1% Tween-20]. TBST was prepared by diluting a 10 × TBS stock solution [200 mM Tris, 1.37 M sodium chloride] in DDW and adding 0.1% (v/v) of the detergent Tween-20.

Blocking, hybridization and washing steps were performed in petri dishes or smaller vessels (depending on the size of the blot membrane) on a rotator (Polymax 2040; Heidolph; Kehlheim, Germany). The membrane was placed in an appropriate vessel with the protein side up, and blocking solution (BS; 4% non-fat dry milk dissolved in TBST) was added. Membranes were incubated in this solution for 1 h at r.t. and subsequently hybridized with the primary antibody at 4°C overnight. The next morning, the primary antibody solution was discarded and unbound antibody was removed by washing the membranes once for 15 min and twice for 5 min each with TBST. Subsequently, the membrane was incubated with a dilution of secondary antibody (anti-rabbit (NEB/CST) or anti-mouse (Amersham Biosciences; Freiburg, Germany)) for 30 min at r.t.. After discarding the secondary antibody solution, the membrane was washed four times for 5 min each with TBST. All hybridization parameters are listed in Tab. 11.

Tab. 11: Primary and secondary antibodies for Western blots.

pAB	Manufacturer[1]	Dilution and buffer	sAB	Dilution and buffer
ATF-2	SC	1:500 in TBST	rabbit	1:5000 in BS
Bax	SC	1:3000 in 1% BS	rabbit	1:8000 in BS
Bcl-2	SC	1:3000 in 1% BS	mouse	1:2000 in 2% BS
Bcl-xl	CST	1:1000 in TBST	rabbit	1:2000 in 2% BS
Bim	BD	1:2000 in 2% BS	rabbit	1:2000 in 2% BS
Caspase-3	SC	1:1000 in BS	rabbit	1:6000 in BS
c-Jun	SC	1:1000 in TBST	rabbit	1:2000 in BS
Cleaved Caspase-3	CST	1:1000 in BS	rabbit	1:2000 in BS
c-Myc	SC	1:1000 in TBST	rabbit	1:1000 in 2% BS
Cyclin D1	BD	1:1000 in TBST	mouse	1:6000 in BS
Fas	SC	1:1500 in 2% BS	rabbit	1:5000 in 2% BS
Fas-L	SC	1:1000 in 1% BS	rabbit	1:2000 in 2%BS
JIP-1	SC	1:1000 in TBST	rabbit	1:2000 in 2% BS
JNK	CST	1:1000 in TBST	rabbit	1:2000 in 2% BS

pAB	Manufacturer[1]	Dilution and buffer	sAB	Dilution and buffer
JNK1	BD	1:1000 in TBST	mouse	1:3000 in 1% BS
JNK2	E	1:5000 in TBST	rabbit	1:3000 in 2% BS
MKK4	SC	1:1000 in TBST	rabbit	1:2000 in 1% BS
MKK7	CST	1:1000 in 1% BS	rabbit	1:2000 in 2% BS
p21/WAF	SC	1:1000 in TBST	mouse	1:2000 in 2% BS
p38	SC	1:1000 in BS	rabbit	1:5000 in BS
p53	BD	1:1000 in TBST	mouse	1:1500 in 1% BS
Phospho-ATF-2	CST	1:1000 in TBST	rabbit	1:1000 in 2% BS
Phospho-c-Jun	CST	1:1000 in TBST	rabbit	1:2000 in 2% BS
Phospho-c-Myc	CST	1:1000 in TBST	rabbit	1:2000 in 2% BS
Phospho-JNK	P	1:2000 in BS	rabbit	1:2000 in BS
Phospho-MKK4	SC	1:1000 in TBST	rabbit	1:5000 in 2% BS
Phospho-MKK7	CST	1:1000 in 1% BS	rabbit	1:2000 in 2% BS
Phospho-p38	P	1:2000 in BS	rabbit	1:2000 in BS
Phospho-p53	CST	1:1000 in TBST	mouse	1:1500 in 1% BS
β-Actin	S	1:5000 in TBST	mouse	1:3000 in TBST

[1]) Manufacturer: P (Promega; Mannheim, Germany); CST (New England Biolabs / Cell Signaling Technology; Frankfurt, Germany); SC (Santa Cruz Biotechnology; Heidelberg, Germany); S (Sigma; München, Germany); E (Epitomics; Hamburg, Germany); BD (BD Biosciences; Heidelberg, Germany).

After the last washing step, TBST was allowed to drip off the membrane, and the membrane was placed with the protein side up on a glass plate. For a 6 × 9 cm (standard sized) membrane, 1 ml of ECL Plus HRP substrate was prepared immediately prior to use by mixing 0.975 ml of ECL Plus Reagent A with 25 µl of ECL Plus Reagent B. The membrane was carefully covered with the HRP substrate solution and incubated for 3 min. Subsequently, all HRP substrate was allowed to drip off the membrane and the membrane was placed inside the plastic pocket of a film cassette. The chemiluminescence on the membranes was detected by exposing the membranes to Hyperfilm ECL films in a darkroom. All membranes were exposed to film for varying lengths of time, and only films generating subsaturating levels of

intensity were selected for densitometrical and statistical evaluation. Films were developed and fixed by a film processor (Curix 60; Agfa, Köln, Germany).

2.10.3 Stripping of Western blot membranes

In order to allow repeated hybridizations of the same Western blotting membrane (section 2.10.2) with different antibodies, *e.g.*, 'phospho-specific target' antibodies and 'total target protein' antibodies, the membrane was stripped in between. The stripping stock solution consisted of 2% SDS and 62.5 mM Tris; 100 mM β-mercaptoethanol were added prior to use. Membranes were stripped for 20 min at 50°C and 25 rpm in an incubator (Innova 4000; New Brunswick Scientific; Amsterdam, The Netherlands) and washed at least twice for 10 min each with TBST. Subsequently, the membrane was blocked again with 4% milk and the next hybridzation was performed.

2.10.4 Ponceau S staining of Western blot membranes

Ponceau S is the only staining method which is completely compatible with all procedures of immunological probing, because the stain is transient and can be washed away so that it does not interfere with subsequent detection of antigens. Ponceau S is normally used for visual evidence that electrophorectic transfer of proteins has taken place. In the present study, it was also used to normalize for the amount of proteins in each lane, since there is no housekeeping protein which is reliable in every stage of neuronal differentiation. After the ECL reaction, membranes (section 2.10.2) were washed twice with TBST and then stained with Ponceau S for 20 min. The staining solution was re-used several times. Stained membranes were washed twice with DDW for 5 min each before air-drying. After scanning the stained membranes (ScanJet IIc; Hewlett Packard; Böblingen, Germany), the protein contents of the lanes were quantified using the densitometry software QuantityOne (Biorad, München, Germany).

2.11 Statistical analysis and replication of the experiments

Unless otherwise indicated, all experiments were carried out independently 3 to 6 times. Statistical analysis was performed with GraphPad Prism software (www.graphpad.com) using one-way analysis of variance with repeated measures. Means were compared using the post-

hoc Bonferroni test, and significance was defined for $p \leq 0.05$. Data were expressed as means ± standard deviation.

3 Results

3.1 Stable transfection of PC12 cell lines

This first part deals with the preparatory work for the functional characterisation of MKK4 and MKK7. It contains the cloning of different splice variants of *mkk4* and *mkk7* and the generation of stably transfected cell clones. As a cellular system, the rat pheochromocytoma cell line PC12 was used. Cultured in medium that contains serum PC12 cells are comparable to adrenal chromaffin cells or sympathetic neurons. By addition of nerve growth factor (NGF) to serum-free medium neuronal differentiation can be induced in PC12 cells (67). Stably transfected PC12 cells enable the investigation of MKK4 and MKK7 functions under naïve and differentiated conditions.

3.1.1 Cloning of MKK4 and MKK7 expression vectors

In order to study the influence of MKK4 and MKK7 on JNK activity and function, the coding sequences of rat *mkk4* and *mkk7* were cloned into the mammalian expression vector pEGFP-C3. So far only one gene product of *mkk4* was identified from all species (115). In the case of *mkk7* four human and six murine MKK7 splice variants (α1; α2; β1; β2; γ1 and γ2) have been described so far, but only one rat MKK7 splice variant that is equivalent to MKK7β1 (60, 123, 180, 209).

For generation of MKK4 and MKK7 constructs, the coding sequences for both proteins were amplified from PC12 cell cDNA. Amplification of the complete coding sequences under optimized PCR conditions revealed the expected bands of 1191 bp (*mkk4*) and 1257 bp (*mkk7*) corresponding to protein sequences of 397 (MKK4) and 419 (MKK7) amino acids, respectively (Fig. 4A).

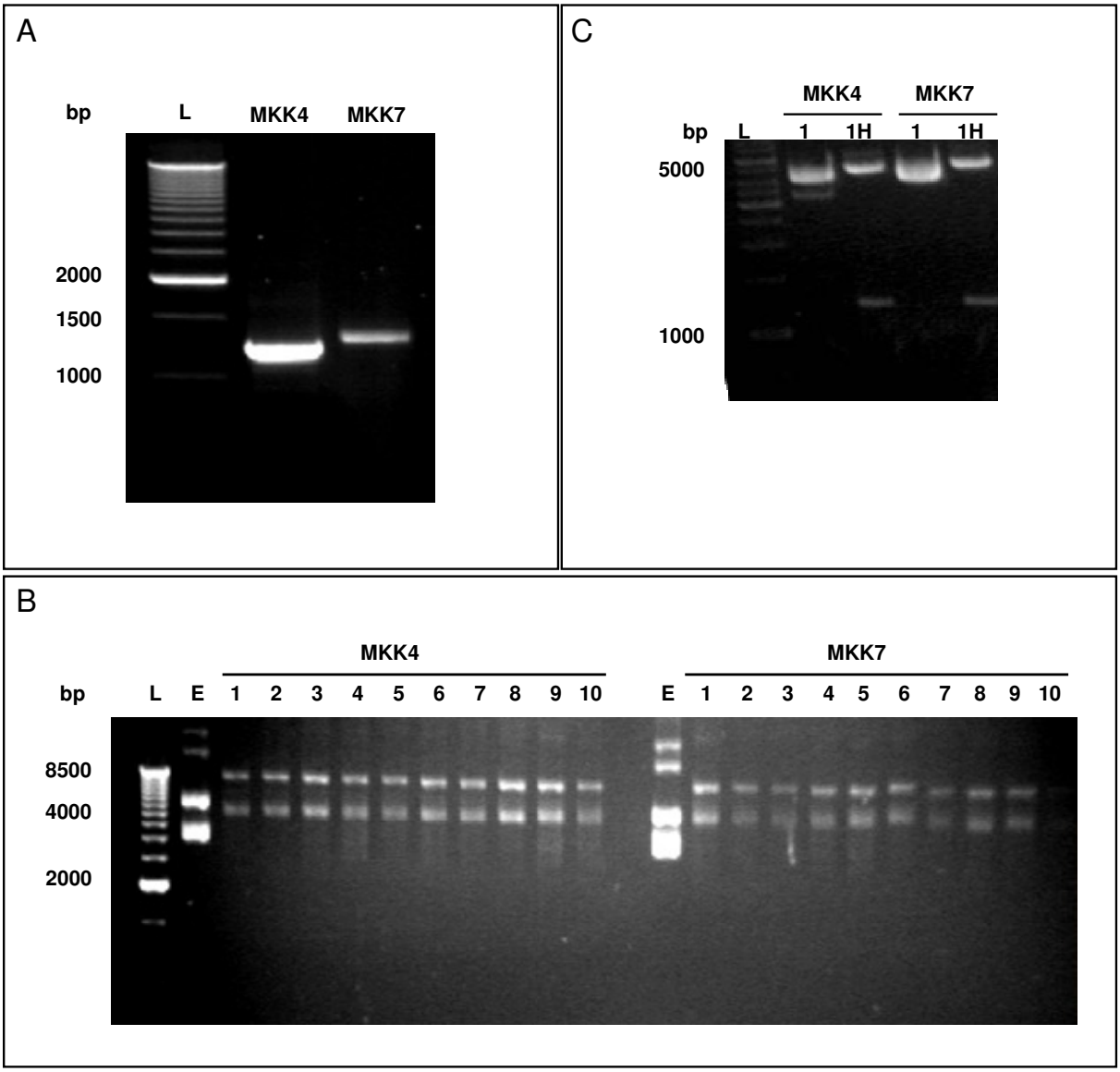

Fig. 4: Cloning of *mkk4* and *mkk7* into the expression vector pEGFP-C3.
A, Amplification of coding sequences for *mkk4* and *mkk7* from PC12 cell cDNA.
B, Plasmid DNA of single colonies of MKK4-pEGFP and MKK7-pEGFP clones.
C, *Bam*HI and *Hind*III enzymatically hydrolyzed DNA from MKK4-pEGFP and MKK7-pEGFP plasmid DNA. L, DNA ladder; E, pEGFP-C3; 1-10, number of the clone; 1H, enzymatically hydrolyzed DNA of clone 1.

For expression of MKK4 and MKK7 in PC12 cells, the mammalian expression vector pEGFP-C3 was chosen. The pEGFP-C3 plasmid enables the expression of a gene of interest under the control of a strong SV40 early promoter. Additionally, genes cloned into the multiple cloning site of pEGFP-C3 are expressed as fusion proteins with EGFP at the C-terminus, which entails a green fluorescence of the protein and allows its localization *in vivo*. Thereby, the green fluorescence is a marker for the transfection efficiency.

The enzymatically hydrolyzed *mkk4* and *mkk7* cDNAs were ligated into the enzymatically hydrolyzed mammalian expression vector pEGFP-C3. The PC12 *mkk4* and *mkk7* cDNA were cloned in-frame with the EGFP coding sequence without a stop codon. Transformation of the constructs into *E. coli* DH5α and plating of transformed bacteria resulted in 50-80 clones of every construct. Ten single colonies of every clone were picked and plasmid DNA was isolated. All plasmids of the 20 picked colonies had a larger size as the empty pEGFP vector (Fig. 4B).

To confirm the presence of an insert in the plasmids, the DNA was enzymatically hydrolyzed with *Bam*HI and *Hind*III. All clones showed the expected fragment (Fig. 4C). In order to verify the sequence of the clones, plasmid DNA was send to GATC Biotech AG. Sequencing revealed some clones with the right and in-frame sequence for *mkk4* and *mkk7* from rat.

One cloned construct contained the known rat *mkk4* sequence (MKK4) with an additional 30 bp segment within the 5' coding region (MKK4Δ). This 30 bp exon encodes a 10 amino acid fragment (Fig. 5).

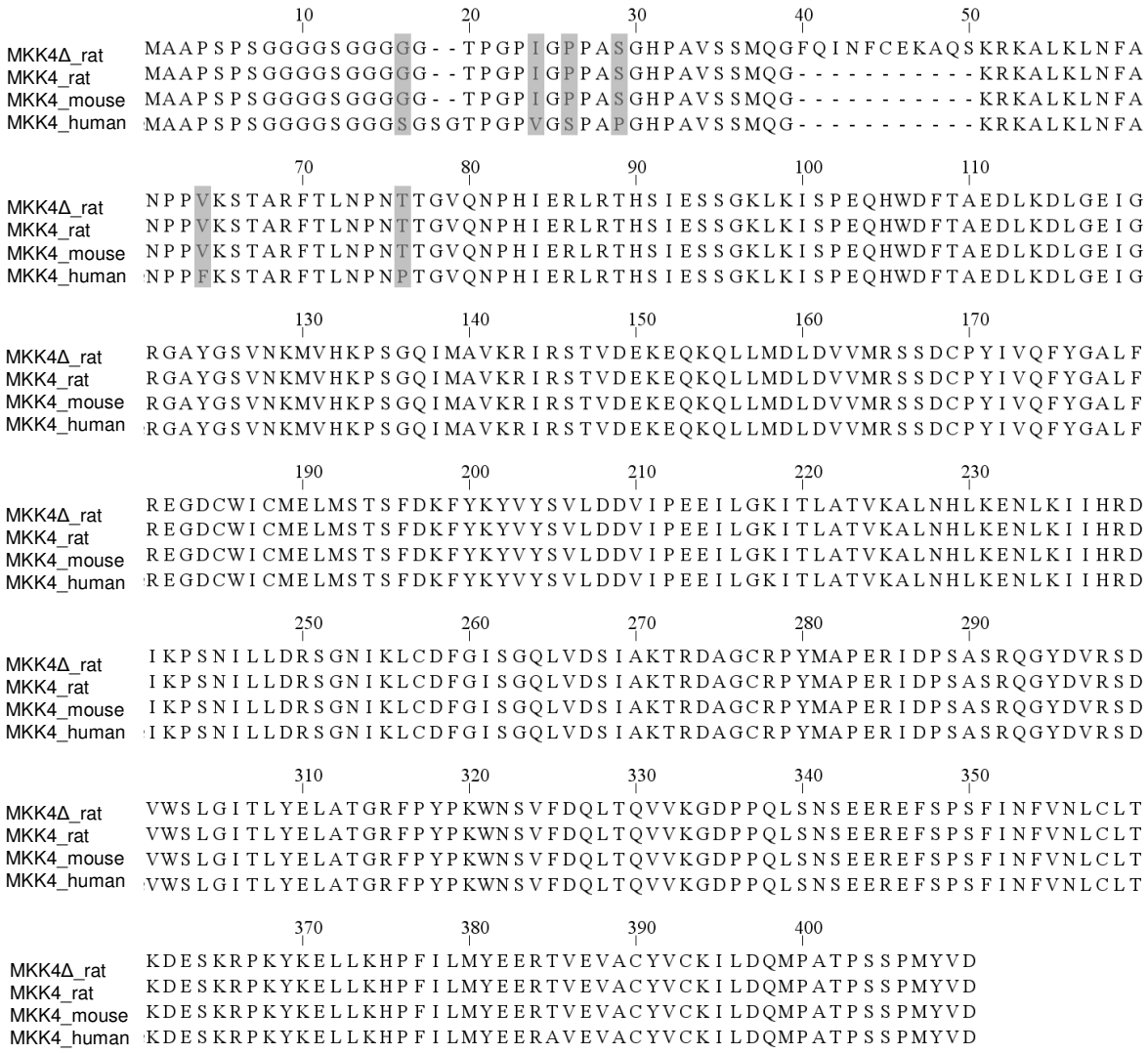

Fig. 5: Sequence alignment of MKK4.
The primary sequence of the novel MKK4Δ from PC12 cells (rat) compared to MKK4 from PC12 (rat), mouse and human. Differences between the species are highlighted in grey.

Analyzing different amplicons from PC12 cDNA, the established MKK7 splice variant (MKK7β1) and a novel splice variant (MKK7γ1) were identified. Sequence analysis and alignment studies revealed a 99% homology to mouse MKK7γ1 (Fig. 6). Compared to the MKK7β1 sequence, the novel rat splice variant includes a fragment of 16 additional amino acids in the N-terminal region. Examination of the rat *mkk7* genomic sequence shows that the unique 48 bp insert is a complete exon, indicating that this variant is not only expressed in PC12 cells, but also in the rat and is not a PCR artefact.

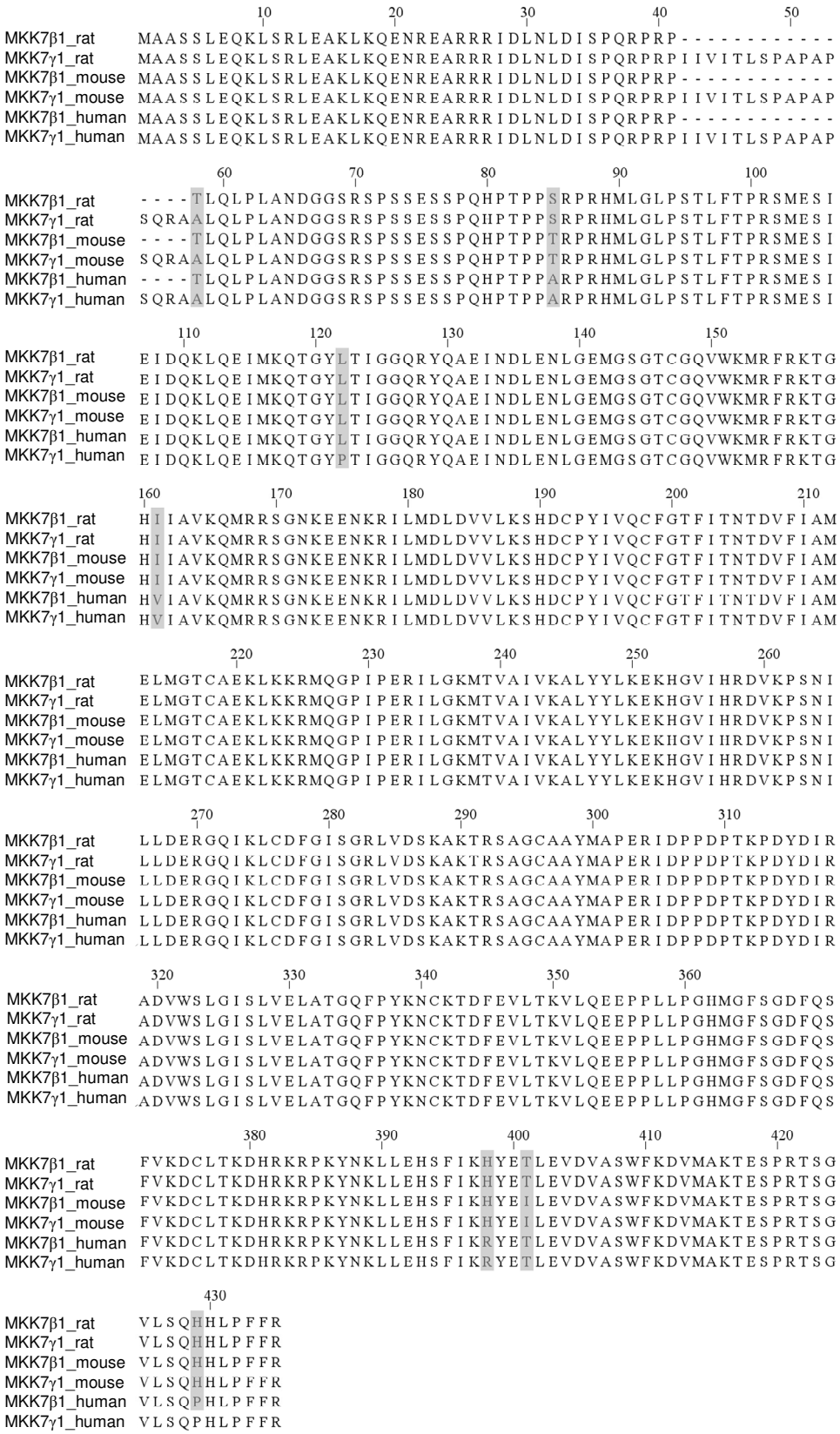

Fig. 6: Sequence alignment of MKK7.
The primary sequence of the novel MKK7γ1 from PC12 cells (rat) compared to MKK7β1 from PC12 (rat) and both splice variants of MKK7 from mouse and human. Differences between the species are highlighted in grey.

3.1.2 Stable transfection of PC12 cells with MKK4 and MKK7 constructs

First of all, PC12 cells were tested for G418 (Geneticin) sensitivity. At 500 µg/ml G418 all non-transfected PC12 cells died, while transfection with pEGFP-C3 (vector), MKK4-pEGFP, MKK4Δ-pEGFP, MKK7β1-pEGFP or MKK7γ1-pEGFP protected the cells and allowed the selection of transfected cells, which usually took 6 weeks. Ten different cell clones for every construct were cultured until they arrived the maintenance culture state. After freezing some stocks of every cell line, 5 cell clones were screened for the expression of the transfected pEGFP constructs. Western Blot analysis revealed different protein levels for every construct (Fig. 7).

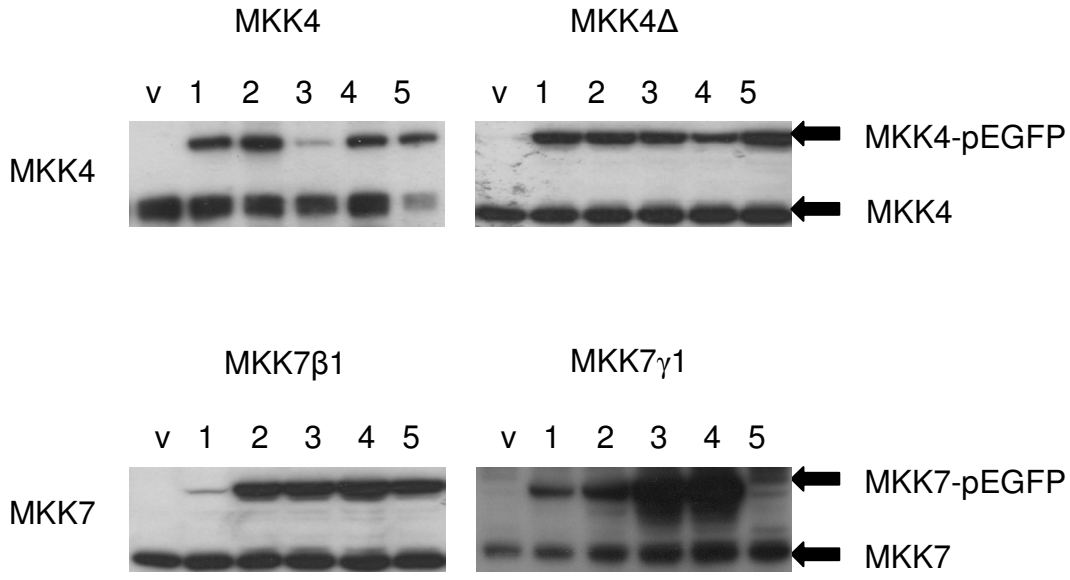

Fig. 7: Protein levels of the transfected pEGFP constructs in PC12 cells.
Protein levels of endogenous and exogenous MKK4 and MKK7 in different stably transfected PC12 cell clones were analysed by Western blots from whole cell extracts. v, vector (pEGFP-PC12); 1-5, number of the cell clone.

3.2 Functional analysis of MKK7γ1 in naïve PC12 cells

After the generation of stably transfected PC12 cell lines, functional analysis of MKK4, and MKK7 and their splice-variants could be carried out. MKK7 is the only direct upstream kinase of JNKs that exclusively activates JNKs (181). Having identified a so far undescribed splice variant of MKK7 in rat, the first set of experiments was performed with MKK7γ1-transfected naïve PC12 cells in order to address the influence of MKK7γ1 on JNK signalling.

3.2.1 MKK7γ1 under normal cell growth conditions

3.2.1.1 Characterisation of MKK7γ1-transfected PC12 cells

First of all, vector- and MKK7γ1-transfected PC12 cells were monitored with regard to cell morphology, growth characteristics, and the expression status of MKK7.

No morphological changes were detected (Fig. 8); under normal growth conditions, both vector- and MKK7γ1-transfected cells revealed a round or polygonal shape and did not spontaneously extend processes. However, the cell cultures transfected with MKK7γ1 contained more cell debris and dead cells than the vector-transfected cell cultures.

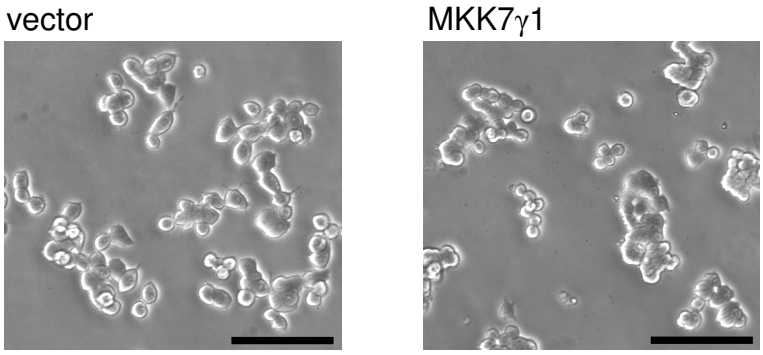

Fig. 8: Cell morphology of vector- and MKK7γ1-transfected PC12 cells.
Light microscopic images of vector- and MKK7γ1-transfected PC12 cells. Both were kept under the same culture conditions. Bars, 50 µM.

To examine whether this microscopic observation is reflected in cell numbers, electronic cell counting was carried out. Indeed, stable transfection of PC12 cells with

MKK7γ1 caused a significant decrease in viable cells by 29% compared with vector-transfected cells under normal growth conditions (Fig. 9).

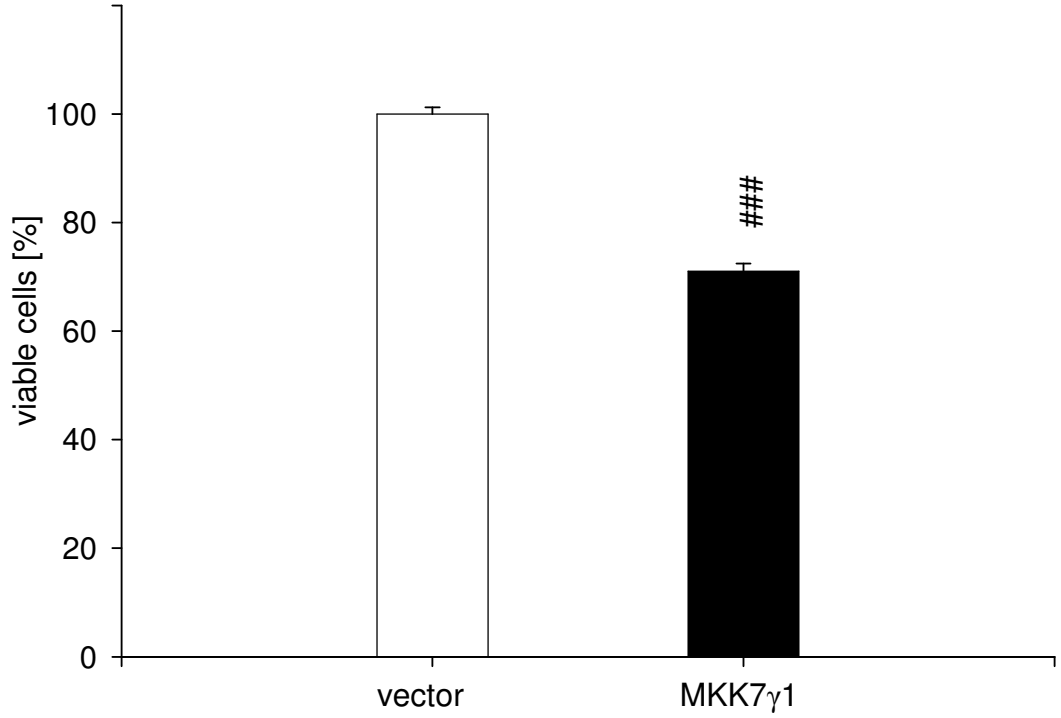

Fig. 9: Viability of vector- and MKK7γ1-transfected PC12 cells.
Electronic cell counts of vector- and MKK7γ1-transfected PC12 cells. Both were kept under the same culture conditions. The data represents six independent experiments with ternary ascertainment. ###, $p < 0.001$ for effect of transfection with MKK7γ1 vs. vector.

Additionally, stable clones were screened for MKK7 protein levels and activation by Western blot analysis. For activation of MAP2Ks/MAPKs, the characteristic **Ser**-Ile-Ala-Lys-**Thr/Thr**-X-**Tyr** activation motives must be phosphorylated on both residues. Therefore, the antibodies used for detection of active MAP2Ks/MAPKs were specific for the dual-phosphorylated forms. After determining phosphorylation levels of MAP2Ks/MAPKs, blot membranes were stripped and re-hybridized with antibodies directed against total kinase protein to normalize for kinase protein contents.

The transfection with pEGFP or MKK7γ1-pEGFP did not change the amount and phosphorylation of endogenous MKK7 (Fig. 10). Furthermore, the amount of MKK7γ1 protein produced by transfected cells was comparable with that of endogenous MKK7, whereas phosphorylation of exogenous MKK7γ1 was slightly reduced compared to endogenous MKK7 activation.

Importantly, the protein level of the second direct JNK activator MKK4 was reduced, but basal MKK4 activity was unchanged by transfection with MKK7γ1. The protein amounts and activation of JNKs, as the only direct downstream targets of MKK7, were investigated by Western blots. Importantly, PC12 cells only express JNK1 and JNK2, but not JNK3 (124). Whereas total JNK1 and JNK2 protein were only slightly increased after MKK7γ1-transfections, the amount of phosphorylated JNK1 and JNK2 was substantially increased (Fig. 10).

Activated JNKs phosphorylate a multiplicity of proteins (reviewed by (12)). Transcription factors are the best known substrates thereof. Under normal cell growth conditions, both protein levels and phosphorylation of c-Jun and the tumour suppressor p53 were increased after transfection with MKK7γ1. However, in the case of the proto-oncogene c-Myc, protein and activation level were decreased in MKK7γ1-transfected cells (Fig. 10)

These results show that transfection with MKK7γ1 causes a high basal level of JNK activity and changes in protein levels and phosphorylation of associated transcription factors, which might induce a subsequent alteration in expression of target genes.

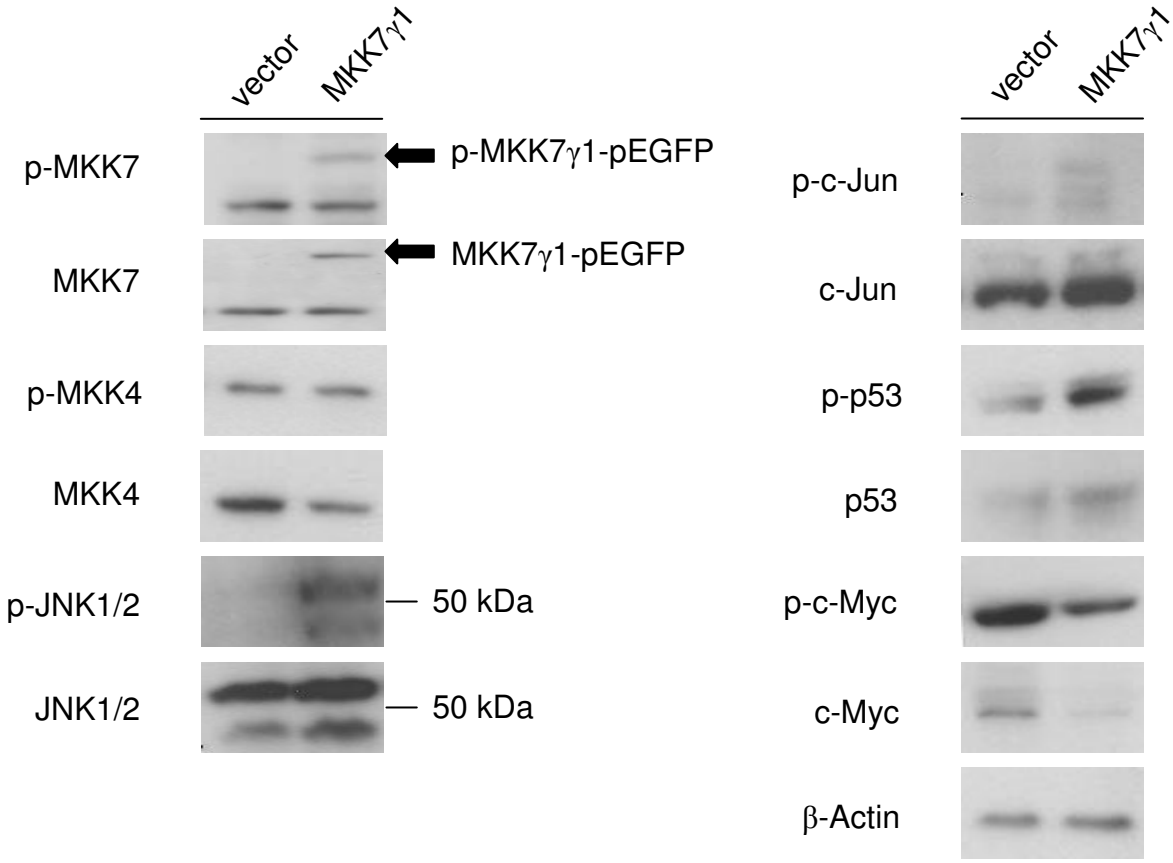

Fig. 10: Protein levels and phosphorylation of JNK1/2, their direct upstream kinases MKK4 and MKK7 and some of their direct downstream targets.
Whole cell lysates (20 µg) from vector- and MKK7γ1-transfected PC12 cells were immunoblotted against JNK1/2, their upstream kinases (MKK4 and MKK7) and some of their downstream targets (c-Jun, p53 and c-Myc). The Western blot membrane was first immunoblotted with phospho-specific antibodies (p-), than stripped and immunoblotted with an antibody directed against the total protein. Both cell lines were kept under the same conditions. β-Actin was used as a loading control. Western blots are representative for five independent experiments.

3.2.1.2 Cell proliferation

The next step was to verify if the MKK7γ1-induced decrease in cell number can be ascribed to changes in cell proliferation. Therefore, 5-bromo-2-deoxyuridine (BrdU) incorporation assays were performed. PC12 cells were transferred to serum-free medium for 24 h to stop proliferation. Cell growth was restarted by returning cells to normal growth medium supplemented with horse and fetal calf serum, resulting in a synchronized cell cycle (150).

The transfection with MKK7γ1 reduced BrdU incorporation to 78% compared to vector controls (Fig. 11). These findings indicate that an increase in MKK7γ1 protein inhibits cell proliferation in PC12 cells under normal cell growth conditions. Consequently, the

observed decrease in cell numbers of MKK7γ1-transfected PC12 cells is attributable to a lowered cell proliferation.

Next, the protein levels of the cell cycle regulators $p21^{WAF1/CIP1}$ (p21) and CyclinD1 was examined. p21 negatively regulates the cell cycle by inhibiting the activity of cyclin-dependent kinases (65, 98), whereas CyclinD1 is an important promoter of cell cycle progression (112). Indeed, the cell cycle inhibitor p21 was strongly up-regulated in MKK7γ1-transfected cells, whereas CyclinD1 was down-regulated compared to vector-transfected cells (Fig. 12).

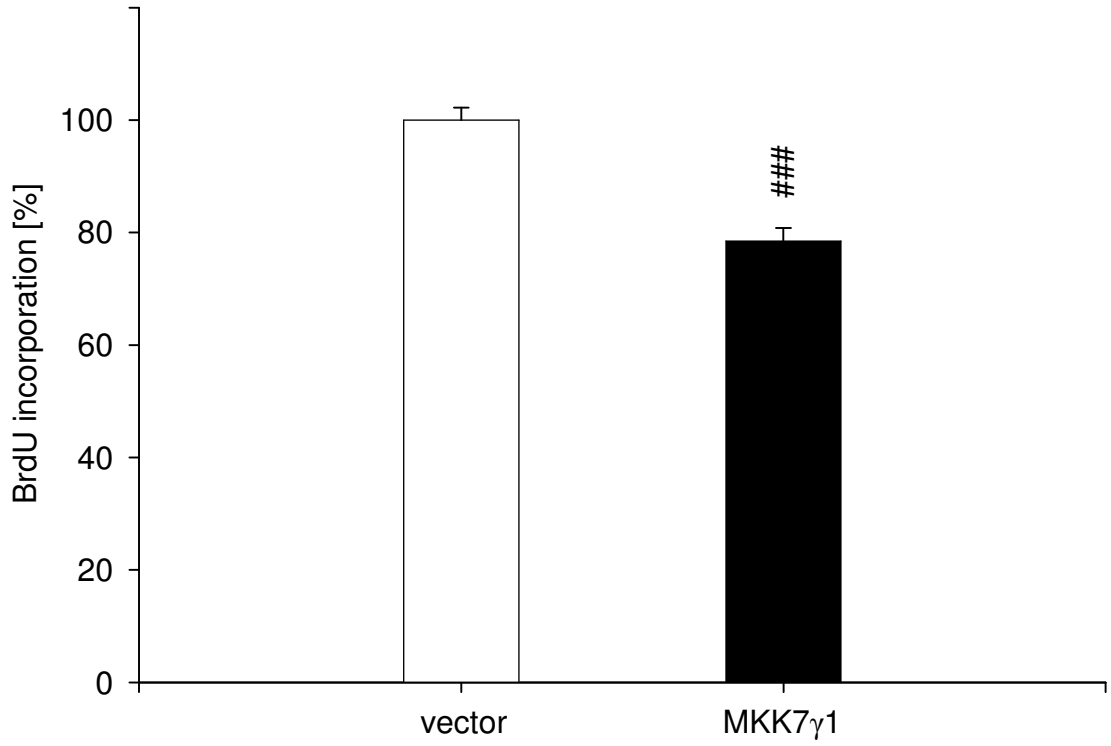

Fig. 11: Proliferation of vector- and MKK7γ1-transfected cells.
Cell proliferation of vector- and MKK7γ1-transfected cells was determined by 5-bromo-2-deoxyuridine (BrdU) incorporation assay. Both cell lines were kept under the same conditions. The data shown represent four separate experiments with ternairy ascertainment. ###, $p < 0.001$ for effect of transfection with MKK7γ1 vs. vector.

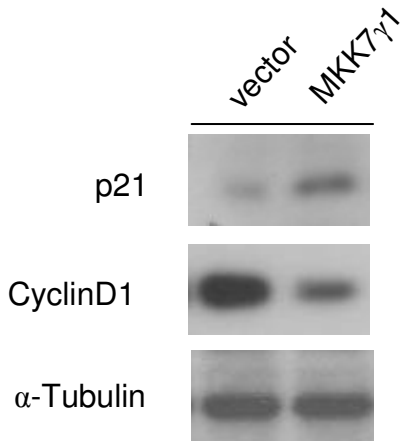

Fig. 12: Protein levels of the cell cycle regulators p21 and CyclinD1.
Whole cell lysates (20 µg) from vector- and MKK7γ1-transfected PC12 cells were immunoblotted against p21 and CyclinD1. α-Tubulin was used as a loading control. Western blots are representative for five independent experiments.

3.2.1.3 Apoptotic proteins

Due to the detection of more dead cells and cell debris in MKK7γ1 cells (Fig. 8) and the fact that JNKs serve as mediators of cell death (reviewed by (47)), molecules that are implicated in apoptotic JNK signalling were also analysed.

Western blots of whole cell extracts showed an up-regulation of Fas receptor protein in MKK7γ1-transfected PC12 cells under normal cell growth conditions, whereas the level of its ligand Fas-L was not altered (Fig. 13). Looking at the pro-apoptotic proteins, a distinct increase in Bim, but not Bax in MKK7γ1-transfected PC12 cells compared to vector-transfected cells was also observed. The functional counterparts of Bim and Bax in apoptosis are the anti-apoptotic proteins Bcl-2 and Bcl-xl. Their protein levels were clearly reduced in MKK7γ1-transfected cells.

The observed up-regulation of the death receptor Fas and pro-apoptotic proteins raised the question if spontaneous apoptosis of PC12 cells is induced by MKK7γ1 transfection. Therefore protein extracts from EGFP- and MKK7γ1-PC12 cells were blotted against cleaved (activated) effector Caspase-3 and total Caspase-3 (Fig. 13). Cleavage of Caspase-3 was increased by MKK7γ1 transfection, while the protein amount of Caspase-3 was unaffected.

Taken together, the observed changes in protein levels and phosphorylation of JNK targets demonstrate distinct alterations in the JNK signalling pathway, caused by transfection

with MKK7γ1. These changes promote sensitivity of MKK7γ1-transfected PC12 cells towards cell death and a repression of cell proliferation under normal cell growth conditions.

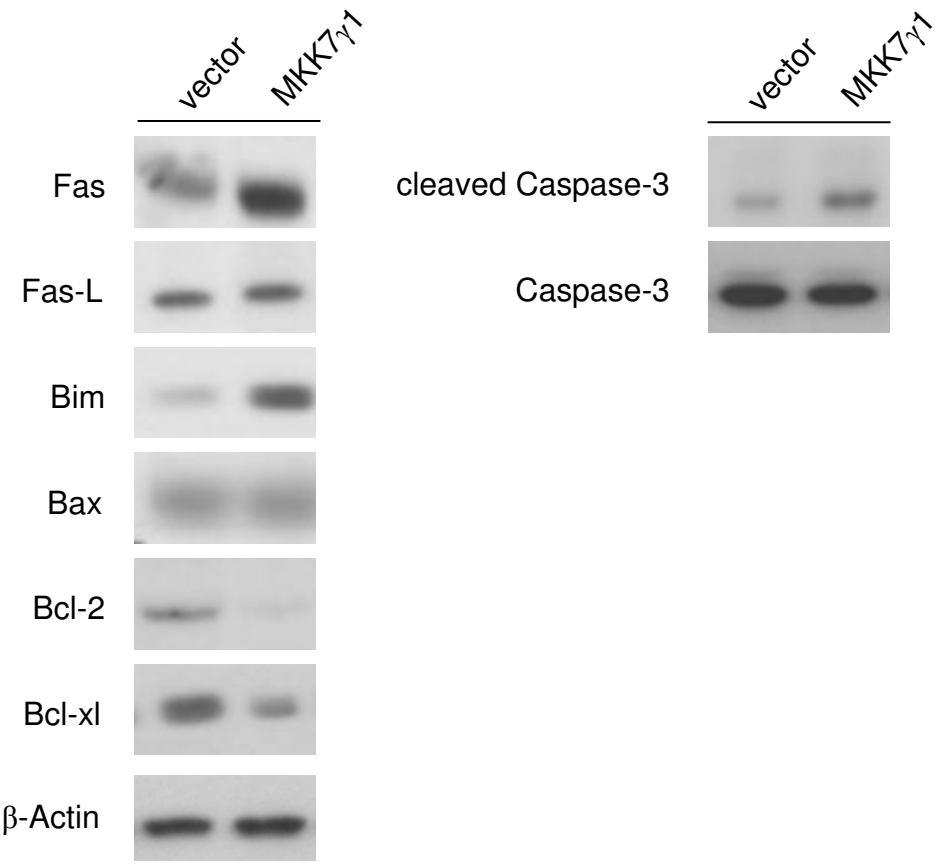

Fig. 13: Protein levels of JNK targets involved in apoptosis.
Whole cell lysates (20 µg) from vector- and MKK7γ1-transfected PC12 cells were immunoblotted against Fas, Fas-L, Bim, Bax, Bcl-2, Bcl-xl, cleaved Caspase-3 and Caspase-3. Both cell lines were kept under the same conditions. β-Actin was used as a control for equal loading. Western blots are representative for four independent experiments.

3.2.1.4 mRNA levels of targets

The observed MKK7γ1-mediated effects on activity and protein levels of JNK targets suggested changes in mRNA levels. Therefore, mRNA levels of some selected targets were determined by quantitative real time PCR in vector- and MKK7γ1-transfected PC12 cells.

Whereas the mRNA levels of the transcription factors c-Jun and p53 were increased by 37% and 8%, respectively, the c-Myc mRNA level was decreased by 50% in MKK7γ1-transfected cells compared to vector-transfected cells. The Fas receptor mRNA level was strongly enhanced (by 139%) following MKK7γ1 transfection of PC12 cells. Furthermore,

MKK7γ1 increased the mRNA amounts of pro-apoptotic Bim (by 116%) and Bax (by 11%), but decreased the mRNA level of anti-apoptotic Bcl-2 (by 88%).

Summarizing, transfection of MKK7γ1 did not only affect JNK targets on protein, but also on mRNA level. The relative tendency of the observed changes on mRNA levels did mostly correlate with the effects on protein amounts (Fig. 10 and Fig. 13).

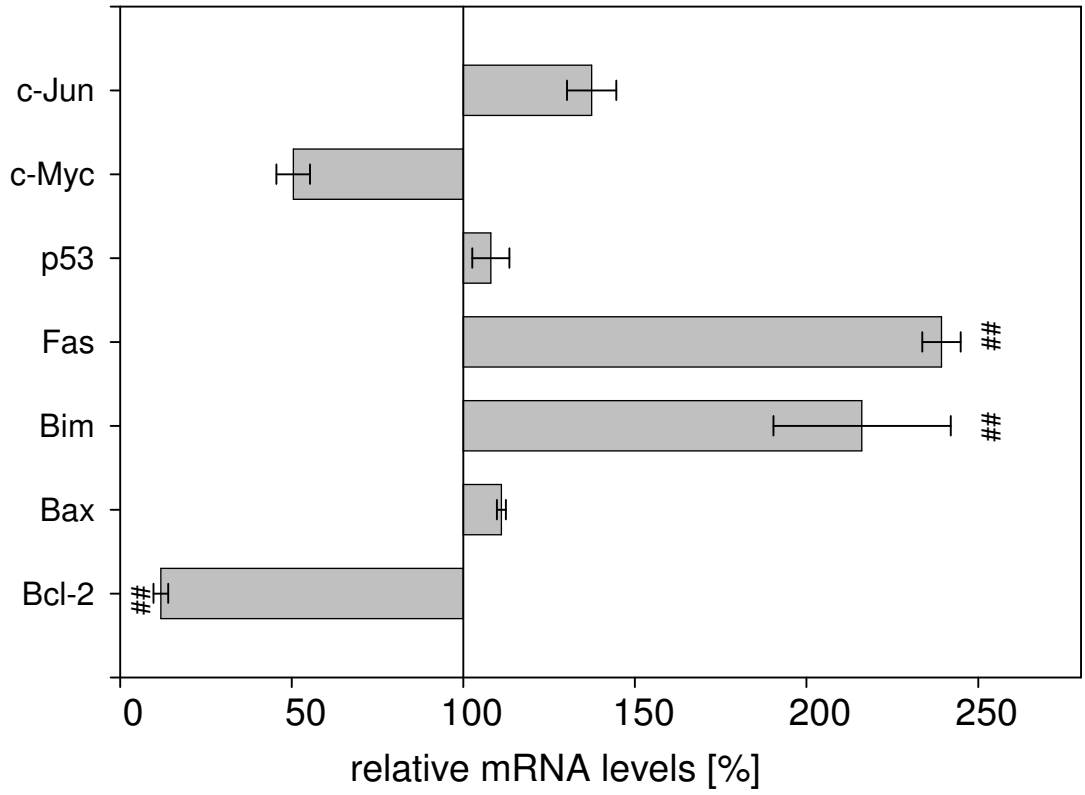

Fig. 14: Relative mRNA levels of JNK targets.
mRNA levels of *c-Jun*, *c-Myc*, *p53*, *Fas*, *Bim*, *Bax* and *Bcl-2* in vector- and MKK7γ1-transfected PC12 cells were quantified by real time PCR and normalized to the 18S mRNA level. Both cell lines were kept under the same culture conditions. The bars show the relative mRNA levels of targets in MKK7γ1-transfected cells compared to the mRNA levels in vector-transfected cells (set at 100%). The data shown represent three separate experiments with ternary ascertainment. ##, $p < 0.01$ for effect of transfection with MKK7γ1 vs. vector.

3.2.1.5 Summary I

The following table gives a simplified overview of the observed MKK7γ1-mediated changes in PC12 cells under normal cell growth conditions.

Tab. 12: MKK7γ1-mediated changes under normal cell growth conditions.

parameter			MKK7γ1
culture	cell number		▼
	proliferation		▼
MKK	MKK7	- protein - phosphorylation	– –
	MKK4	- protein - phosphorylation	▼ –
JNK	JNK1	- protein - phosphorylation	▲ ▲
	JNK2	- protein - phosphorylation	▲ ▲
transcription factors	c-Jun	- mRNA - protein - phosphorylation	▲ ▲ ▲
	c-Myc	- mRNA - protein - phosphorylation	▼ ▼ ▼
	p53	- mRNA - protein - phosphorylation	– ▲ ▲
cell cycle	p21	- protein	▲
	CyclinD1	- protein	▼
apoptosis	Fas	- mRNA - protein	▲ ▲
	Fas-L	- protein	–
	Bim	- mRNA - protein	▲ ▲
	Bax	- mRNA - protein	▲ –
	Caspase-3	- protein - cleavage	– ▲
	Bcl-2	- mRNA - protein	▼ ▼
	Bcl-xl	- protein	▼

Relative changes (▲, increase; ▬, no change; ▼, decrease) in naïve MKK7γ1-transfected PC12 cells compared to vector-transfected PC12 cells under normal cell growth conditions.

3.2.2 MKK7γ1 under stress conditions

Under normal cell growth conditions MKK7γ1 has an anti-proliferative and pro-apoptotic effect on PC12 cells (Fig. 11 and Fig. 13). This effect is accompanied by a high basal activity of JNK that leads to differences in the protein levels of transcription factors, cell cycle regulators and apoptotic proteins (Fig. 10, Fig. 12 and Fig. 13).

In light of these observations, one could expect that MKK7γ1-mediated changes affect the cellular reaction towards stress. Regarding the decrease of proliferation and increased protein levels of pro-apoptotic proteins, a higher stress sensitivity could be assumed, which was addressed in the next set of experiments. To exclude that these effects were mainly caused by a general increased availability of any MKK7 protein, PC12 cells transfected with the so far only known rat splice variant MKK7β1 were additionally analysed.

3.2.2.1 Cell death

TNF-α is a pro-inflammatory cytokine that induces cell death in PC12 cells (117). The chemotherapeutic agent taxol suppresses mitotic spindle assembly and chromosome movement. Thapsigargin induces endoplasmatic reticulum (ER) stress by inhibiting Ca^{2+}-ATPase, which maintains Ca^{2+} homeostasis in the ER. Tunicamycin is an antibiotic that disrupts the N-glycosylation of newly-synthesized proteins. It is known that all these types of stress result in a strong JNK and c-Jun activation (45, 56, 162, 191).

Vector-, MKK7γ1- and MKK7β1-transfected PC12 cells were synchronized and incubated with the stressors TNF-α (50 ng/ml), taxol (5 µM), thapsigargin (5 µM) or tunicamycin (1.4 µg/ml) for 24 h.

Electronic cell counts revealed that stimulation with TNF-α only slightly reduced the number of viable vector-transfected PC12 cells by 12%, whereas taxol significantly decreased the number of viable cells by 51% (Fig. 15). The two ER-stressors thapsigargin and tunicamycin also reduced the number of viable vector-transfected PC12 cells by 32% and 28%, respectively. MKK7β1-transfected cells showed no significant differences after 24 h incubation with TNF-α (11%), taxol (52%), thapsigargin (33%) and tunicamycin (24%) compared to vector-transfected cells. Interestingly, TNF-α, thapsigargin and tunicamycin evoked no significant change in the number of viable MKK7γ1-transfected cells, only incubation with taxol and thapsigargin significantly reduced the number of viable cells by 15% and 8% but not as strongly as in the other cell lines.

Contrary to the assumption of higher stress sensitivity from basal conditions, transfection with MKK7γ1 protected PC12 cells from thapsigargin-, tunicamycin- and taxol-induced cell death. This effect is exclusively triggered by MKK7γ1, but not by MKK7β1.

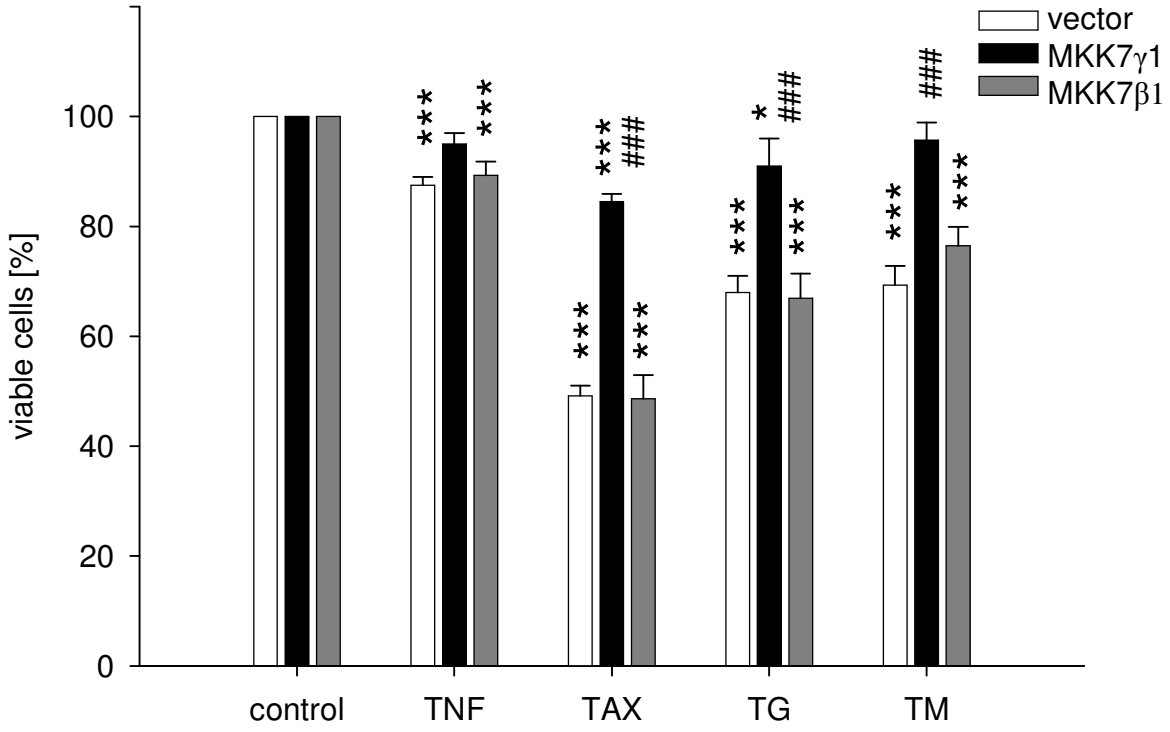

Fig. 15: Viability of vector-, MKK7γ1- and MKK7β1-transfected cells following stimulation with different stressors.
Electronic cell counts of vector-, MKK7γ1- and MKK7β1-transfected PC12 cells after 24 h treatment with different stressors: TNF, 50 ng/ml TNF-α; TAX, 5 µM taxol; TG, 5 µM thapsigargin; TM, 1.4 µg/ml tunicamycin. Control (unstimulated) = 100%. ∗, $p < 0.1$; ∗∗∗/###, $p < 0.001$ for effect of TNF, TAX, TG and TM/transfection with MKK7γ1 and MKK7β1 vs. vector. Data represent six independent experiments with ternary ascertainment.

3.2.2.2 JNK signalling pathway

Electronic cell counts showed, that MKK7γ1 transfection protected PC12 cells from cell death induced by different types of stressors (Fig. 15). As TNF-α only provoked a marginal cell death, it was excluded from further studies. From the two ER stressors, tunicamycin was further examined.

Following the line of previous experiments, the phosphorylation and protein levels of JNKs, their upstream kinases and substrates after 6 h incubation with tunicamycin in whole cell lysates were investigated. The levels of endogenous MKK7 and exogenous MKK7γ1 or

MKK7β1 proteins were not influenced by tunicamycin in vector- and MKK7γ1-transfected PC12 cells (Fig. 16). However, phosphorylation of endogenous MKK7 increased after 6 h stimulation with tunicamycin in both cell lines to a similar degree. The activation of transfected MKK7γ1 and MKK7β1 was unaffected. Activation levels of the second JNK activator MKK4, were only elevated by tunicamycin in vector- and MKK7β1-transfected PC12 cells. The MKK4 protein amount was unaffected by tunicamycin treatment but reduced by transfection with MKK7γ1. In whole cell extracts, phosphorylation of JNK1/2 increased after incubation with tunicamycin in all three cell lines. The level of JNK1/2 that was generally increased in MKK7γ1-transfected cells was not further elevated by tunicamycin.

After activation, JNKs either remain in the cytoplasm or translocate to the nucleus and activate transcription factors (reviewed by (12)). The phosphorylation and protein levels of the exclusive JNK substrate c-Jun were increased after stimulation with tunicamycin in vector-, MKK7γ1- and MKK7β1-transfected PC12 cells (Fig. 16). Whereas the amounts of activated and absolute c-Jun were comparable in vector- and MKK7β1-transfected PC12 cells, they were generally elevated in MKK7γ1-transfected PC12 cells. Tunicamycin had no impact on c-Myc phosphorylation and protein amount. Only transfection with MKK7γ1 caused a down-regulation of c-Myc and phospho-c-Myc under basal and pathophysiological conditions. After 6 h incubation with tunicamycin, p53 phosphorylation and protein level were enhanced in vector- and MKK7β1-transfected cells. In contrast, MKK7γ1-transfection mediated an increase of phospho-p53 and absolute p53 in PC12 cells under normal cell growth conditions that was abolished after stimulation with tunicamycin.

Taken together, both MKK7 splice variants increased phosphorylation of JNK1/2 following tunicamycin treatment. Whereas protein and phoyphorylation levels of the analysed transcription factors were mostly unaffected by transfection with MKK7β1, MKK7γ1 mediated distinct changes after stimulation with tunicamycin.

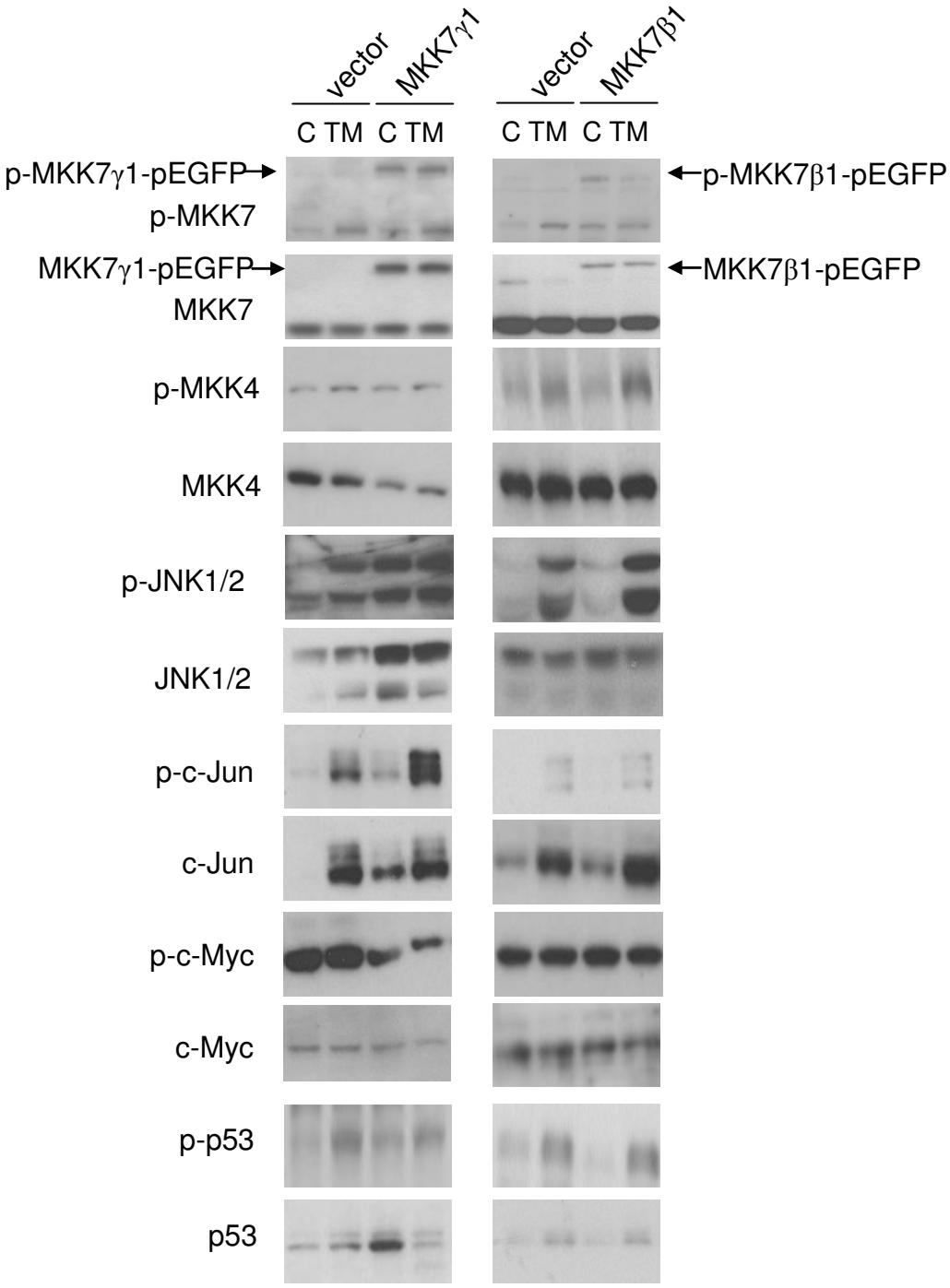

Fig. 16: Protein levels and phosphorylation of JNKs, upstream kinases and targets after stimulation with tunicamycin.
Whole cell extracts (20 µg) from unstimulated (C) and tunicamycin-stimulated (TM, 1.4 µg/ml tunicamycin for 6 h) vector-, MKK7γ1- and MKK7β1-transfected PC12 cells were immunoblotted against JNK1/2, their upstream kinases (MKK4 and MKK7) and some of their direct downstream targets (c-Jun, p53 and c-Myc). The Western blot membrane was first immunoblotted with phospho-specific antibodies (p-), than stripped and immunoblotted with an antibody directed against the total protein. Western blots are representative for five independent experiments.

3.2.2.3 Apoptotic proteins

Under normal growth conditions, a reduced cell number accompanied by an increase of pro-apoptotic and a decrease of anti-apoptotic proteins was observed in cultures from MKK7γ1-transfected PC12 cells compared to vector-transfected cells (Fig. 9 and Fig. 13). So far, the results obtained from experiments under stress conditions surprisingly indicated an anti-apoptotic JNK signalling mediated by MKK7γ1 transfection. Therefore, whole cell extracts were analysed by Western blots for pro- and anti-apoptotic JNK target proteins.

After stimulation with tunicamycin, Fas protein was increased in vector-transfected cells, while it was decreased in MKK7γ1-transfected cells (Fig. 17). The amount of Fas-L was unchanged in vector-transfected cells, but slightly decreased in MKK7γ1-transfected cells. The level of the pro-apoptotic protein Bim was also decreased in MKK7γ1-transfected cells after cellular stress, whereas it was increased in vector-transfected PC12 cells. Stimulation with tunicamycin did not change the protein levels of Bax, Bcl-2 and Bcl-xl in both cell lines.

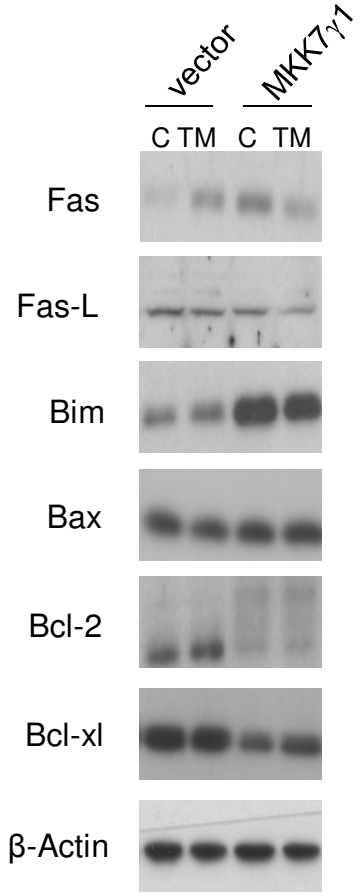

Fig. 17: Protein levels of pro- and anti-apoptotic proteins under stress conditions.
Whole cell extracts (20 µg) from unstimulated (C) and tunicamycin-stimulated (TM, 1.4 µg/ml tunicamycin for 6 h) vector- and MKK7γ1-transfected PC12 cells were blotted against different proteins involved in apoptosis. β-Actin was used as a loading control. Western blots are representative for five independent experiments.

Since MKK7γ1 seemed to reduce tunicamycin-mediated cell death (Fig. 15), Western blot analysis of the protein level and cleavage of effector Caspase-3 were performed. As expected, 18 h stimulation with tunicamycin strongly increased the cleavage of Caspase-3 in vector-transfected cells (Fig. 18). Indeed, transfection with MKK7γ1 decreased activation of Caspase-3 compared to vector-transfected cells. Surprisingly, cleavage of Caspase-3 was slightly reduced following tunicamycin stimulation in MKK7γ1-PC12 cells. In line with the observations above, Caspase-3 activation was increased in MKK7γ1-transfected cells compared to vector-transfected cells under normal cell growth conditions.

Summarizing, MKK7γ1 transfection protects PC12 cells from apoptosis induced by tunicamycin.

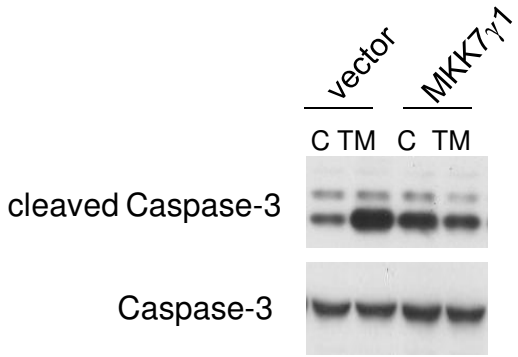

Fig. 18: Protein level and cleavage of Caspase-3 after tunicamycin stimulation.
Extracts (20 µg) from vector- and MKK7γ1-transfected PC12 cells after 18 h incubation with tunicamycin (TM; 1.4 µg/ml) were immunoblotted against Caspase-3 and cleaved Caspase-3. Western blots are representative for three independent experiments.

3.2.2.4 Cell proliferation

According to the observed changes in cell proliferation under normal cell growth conditions (Fig. 11), it was examined if the difference in cell survival is also caused by different cell division rates of the cell lines under stress conditions. Additionally to tunicamycin-stimulated cells, taxol-stimulated cells were analysed as this stressor interferes with the normal breakdown of microtubules during cell division.

Monitoring proliferation in 5-bromo-2-deoxyuridine (BrdU) incorporation assays with stimulated cells showed that tunicamycin and taxol reduced proliferation of vector-transfected cells by 29% and 26%, respectively (Fig. 19). Again, MKK7β1-transfected PC12 cells showed similarly reduced proliferation rates as vector-transfected cells after stimulation with tunicamycin (30%) and taxol (34%). In contrast, no changes after taxol stimulation in MKK7γ1-transfected cells were observed and even a significant proliferation increase following tunicamycin by 43%.

These findings indicate that only transfection with MKK7γ1, but not with MKK7β1, causes stress resistance in PC12 cells.

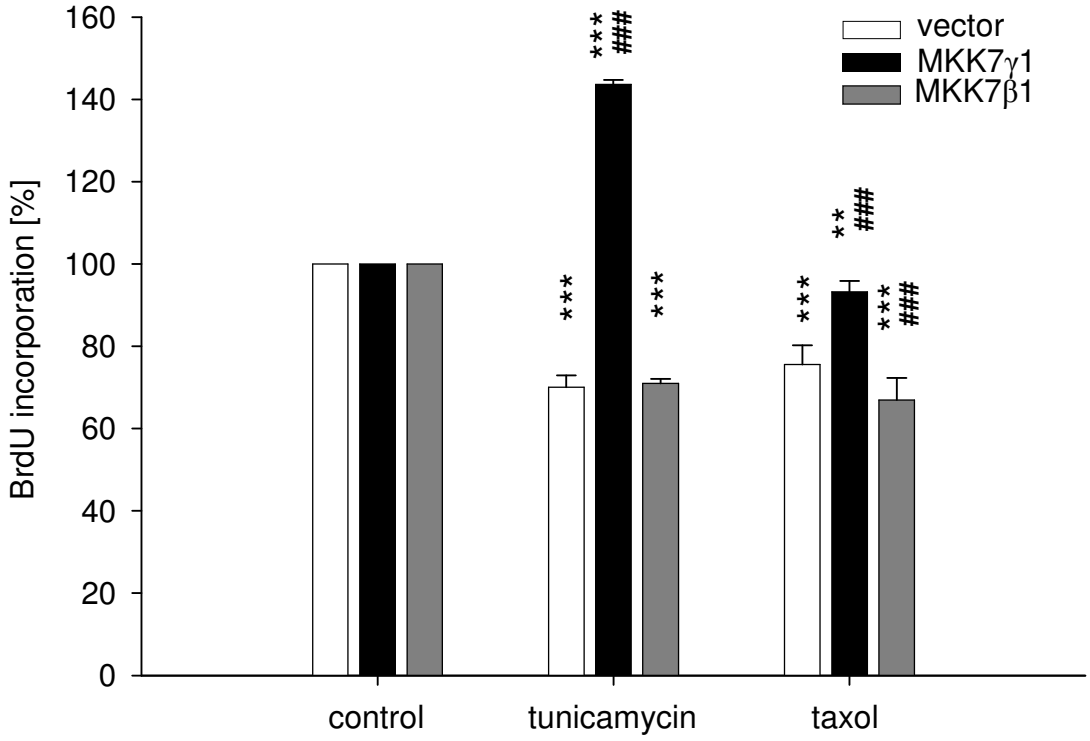

Fig. 19: Proliferation of vector-, MKK7γ1- and MKK7β1-transfected PC12 cells under stress conditions.
BrdU incorporation was measured after 24 h stimulation in the different cell lines. Control, unstimulated; tunicamycin [1.4 µg/ml]; taxol [5 µM]. Control = 100%. **, $p < 0.01$; ***/###, $p < 0.001$ for effect of tunicamycin and taxol/transfection with MKK7γ1 and MKK7β1 vs. vector. Data represent four independent experiments with ternary ascertainment.

3.2.2.5 Cell cycle regulators

To further characterise the changes in cell cycle regulation, p21 and CyclinD1 protein levels were monitored by Western blots. Twenty-four hours after stimulation with tunicamycin, the p21 amount of vector-transfected cells was increased, while it was decreased in MKK7γ1-transfected cells (Fig. 20A). CyclinD1 protein levels did not change in both cell lines after incubation with tunicamycin.

Afterwards the question came up, if the two cell cycle proteins are regulated on transcriptional or translational level. Therefore, RT-PCRs for *p21* and *CyclinD1* transcripts with cDNA isolated from both cell lines after 6 h incubation with tunicamycin were performed. Under normal cell growth conditions, MKK7γ1-transfection caused an up-regulation of *p21* mRNA (Fig. 20B). After stimulation with tunicamycin *p21* mRNA was increased in vector-transfected cells and decreased in MKK7γ1-transfected cells. No changes

in mRNA levels could be observed for *CyclinD1*. Correspondingly, the observed difference in p21 protein levels was caused by MKK7γ1-mediated transcriptional changes, whereas the basal decrease in CyclinD1 protein seemed to be regulated on a different level, such as protein stability.

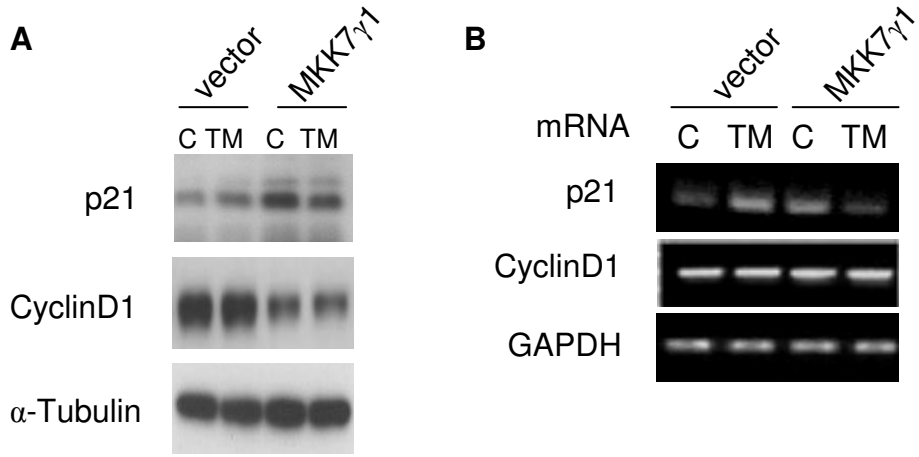

Fig. 20: Protein and mRNA levels of p21 and CyclinD1 after tunicamycin stimulation.
A, Whole cell extracts (20 µg) from unstimulated (C) and tunicamycin-stimulated (TM, 1,4 µg/ml for 6 h) vector and MKK7γ1-transfected PC12 cells was immunoblotted against p21 and CyclinD1. α-Tubulin was used as a loading control. Western blots are representative for five independent experiments.
B, RNA was isolated from unstimulated (C) and tunicamycin-stimulated (TM, 1.4 µg/ml for 6 h) vector and MKK7γ1-transfected PC12 cells. The *p21* and *CyclinD1* mRNAs were detected by semiquantitative RT-PCR (mRNA). GAPDH was used as a loading control. Data are representative for three independent experiments.

The transcription of *p21* is activated by the tumour suppressor and JNK substrate p53 (53). To further analyse the observed transcriptional changes in *p21* mRNA, chromatin immunoprecipitaions (ChIP) with lysates of unstimulated and with tunicamycin stimulated vector- and MKK7γ1-transfected cells were performed. Precipitation with a p53 antibody and a PCR with primers flanking a p53 binding-site in the *p21* promoter revealed that tunicamycin enhances p53 binding in vector-transfected cells. MKK7γ1-transfection caused a down-regulation of the generally increased p53-binding to the *p21* promoter after stimulation with tunicamycin (Fig. 21). This result shows that MKK7γ1 influences *p21* transcription by p53 binding to the *p21* promoter.

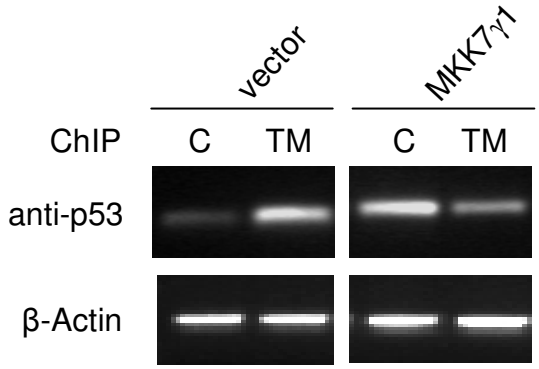

Fig. 21: p53 binding to the p21 promotor.
p53 binding to the *p21* promoter was analysed by chromatin immunoprecipitations (ChIP). Chromatin was isolated from unstimulated (C) and tunicamycin-stimulated (TM, 1.4 µg/ml for 6 h) vector- and MKK7γ1-transfected PC12 cells and immunoprecipitated with an antibody directed against p53 and β-Actin (internal control). PCR was done using β-Actin control primers and primers specific for a p53-binding site in the *p21* promoter. Data are representative for three independent experiments.

3.2.2.6 Inhibition of JNKs by SP600125

In the light of the observation that p53-binding to the *p21* promoter is affected by MKK7γ1 transfection (Fig. 21), it was investigated if this transcriptional regulation was JNK-dependent. One hour treatment with a low concentration (2 µM) of the ATP-competitive JNK inhibitor SP600125 slightly increased the p53 protein amount in vector-transfected cells (Fig. 22). Concurrently, the cell cycle inhibitor p21 protein was enhanced after incubation with SP600125.

As described above, MKK7γ1 mediates a strong increase in p53 and p21 protein levels under normal cell growth conditions compared to PC12-EGFP cells (Fig. 10 and Fig. 12). Indeed, incubation with SP600125 reversed these effects. Inhibition of JNKs in MKK7γ1-transfected cells reduced the amount of p53 and p21 proteins in MKK7γ1-transfected cells (Fig. 22).

Taken together, these results show that MKK7γ1 specifically up-regulates proliferation of PC12 cells via JNK, p53 and finally p21 under stress conditions.

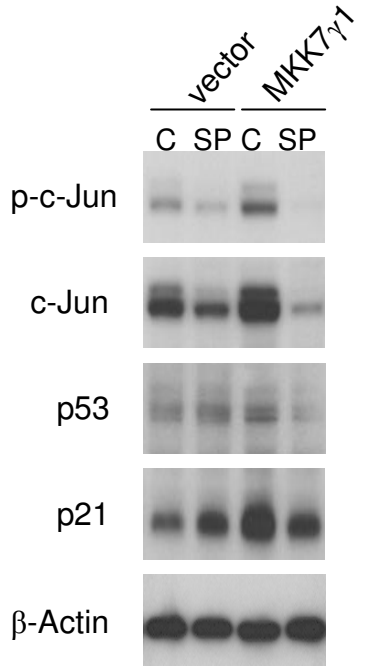

Fig. 22: JNK-dependent protein levels and phosphorylation of JNK targets in vector- and MKK7γ1-transfected PC12 cells.
Western blot analysis from whole cell extracts (20 µg) of vector- and MKK7γ1-transfected PC12 cells with antibodies directed against phosphorylated c-Jun (p-c-Jun), c-Jun, p53 and p21. Cells were unstimulated (C) or incubated for 24 h with SP600125 (SP; 2 µM). β-Actin was used as a loading control. Data are representative for three independent experiments.

3.2.2.7 Cell cycle distribution patterns

Based on the observed MKK7γ1-mediated changes in cell cycle regulators and cell proliferation (Fig. 19 and Fig. 20), further cell cycle analysis by flow cytometry were performed to elucidate cell cycle phase distribution of PC12 cells. The chemotherapeutic taxol provokes a G2/M-phase arrest of PC12 cells leading to cell death (191). As mentioned previously, MKK7γ1 transfection partially protects PC12 cells from taxol-induced apoptosis. Possibly, this protection is accompanied by a shift in cell cycle phases. Therefore, vector- and MKK7γ1-transfected PC12 cells were incubated with 1.4 µg/ml tunicamycin (TM) or 5 µM taxol for 6 h.

Under normal cell growth conditions, 55.2 ± 0.6% vector-transfected PC12 cells were in G1-, 19.6 ± 0.5% in S- and 25.2 ± 2% in G2-phase of the cell cycle (Fig. 23). Significantly more MKK7γ1-transfected cells were in G1-phase (61.4 ± 1.5%), whereas less cells were in G2-phase (18.7 ± 2.1%). Although after stimulation with taxol and tunicamycin, MKK7γ1 mediated differences in cell cycle distribution. Taxol caused a typical G2/M cell cycle arrest

of vector-transfected cells (55.8 ± 2.3%). In contrast, only 41.5 ± 0.9% MKK7γ1-transfected PC12 cells arrested in G2/M-phase and the number of cells in G1-phase was increased by 14.4%. Stimulation with tunicamycin caused a shift of vector-transfected cells, from G2/M (18.7 ± 1.6%) to G1-phase (60.2 ± 0.8%). MKK7γ1-transfected cells showed a contrary shift from G1- (56.5 ± 0.8%) to G2/M-phase (23.9 ± 2.3%). The number of cells in the S-phase of the cell cycle was nearly unaffected by stimulation and transfection.

Summing up, MKK7γ1-mediated changes in the expression of cell cycle regulators culminated in a shift of PC12 cell cycle distribution. This shift was already detectable under normal cell growth conditions and was enhanced by stimulation with taxol and tunicamycin.

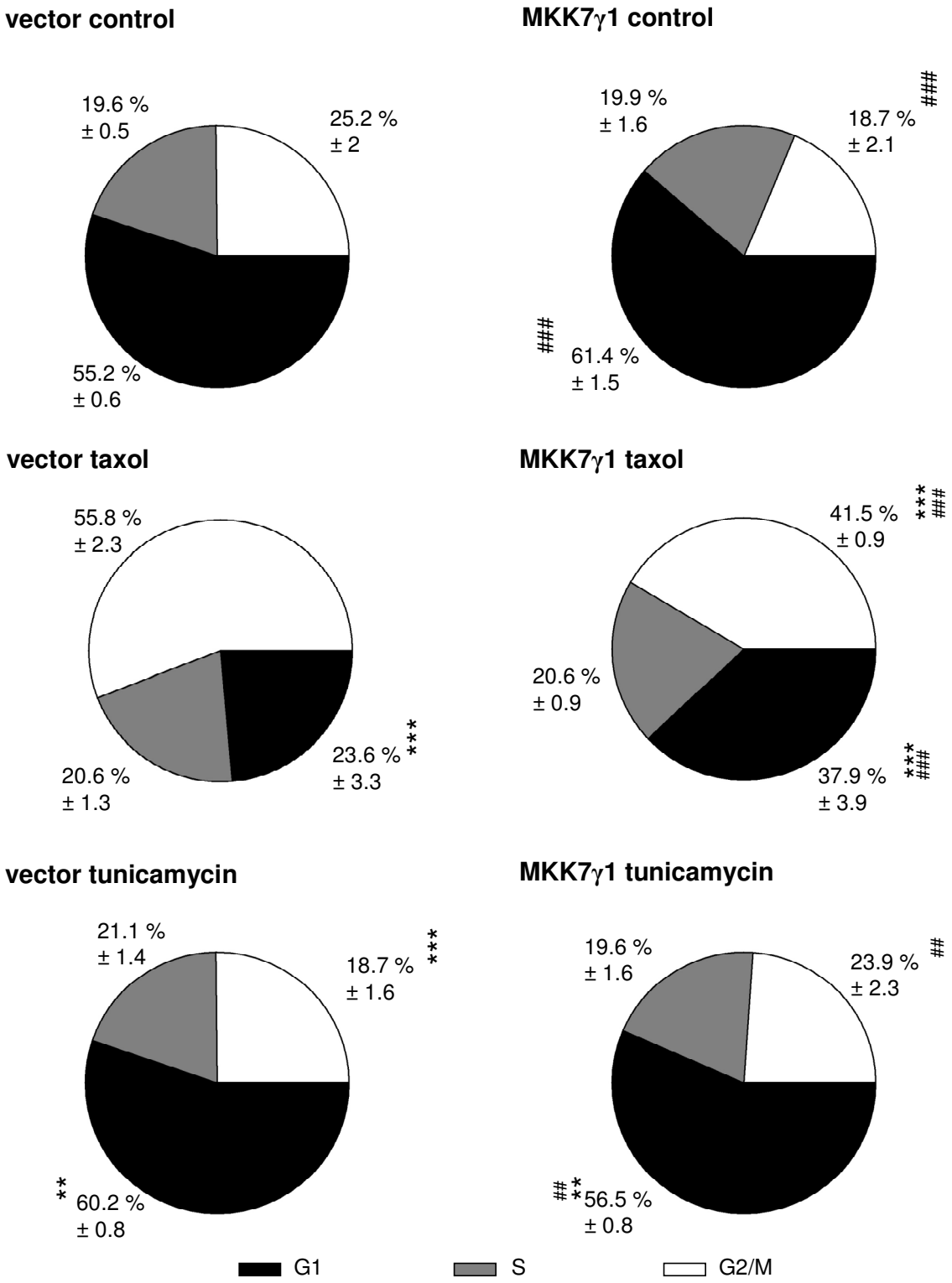

Fig. 23: Cell cycle distribution of vector- and MKK7γ1-transfected PC12 cells.
Cell cycle distribution of vector- and MKK7γ1-transfected PC12 cells under different growth conditions. The DNA of vector- and MKK7γ1-transfected cells was stained with propidium iodide and the content was measured by fluorescence-activated cell sorting. Control, unstimulated; taxol, 5 µM for 6 h; tunicamycin, 1.4 µg/ml for 6 h. Data represent the mean percentage of cells in G1, S, G2/M of 6 independent experiments with ternary ascertainments. **/##, $p < 0.01$; ***/###, $p < 0.001$ for effect of taxol and tunicamycin/transfection with MKK7γ1 vs. vector.

3.2.2.8 JNK protein levels, activation and localization

Overexpression of MKK7γ1 in PC12 cells caused a general increase in JNK activity (Fig. 10 and Fig. 23). As cellular localization is a determining factor in JNK functions (10), the distribution and phosphorylation levels of JNK isoforms in cytoplasmic and nuclear fractions were investigated.

In both cell lines, the major part of total JNK1/2 and active JNK1/2 was localized in the cytoplasmic cell fraction (Fig. 24). Stimulation with tunicamycin caused a typical increase of phosphorylated JNK1 and JNK2 in vector transfected cells. In MKK7γ1-transfected cells, phosphyorylation and amounts of JNK1 and 2 were generally increased, in particular in the nuclear fractions, but was only slightly affected by tunicamycin stimulation. The use of isoform-specific antibodies showed that the increase of total JNK protein as described above in MKK7γ1-transfected PC12 cells resulted from an increased JNK2 protein level .

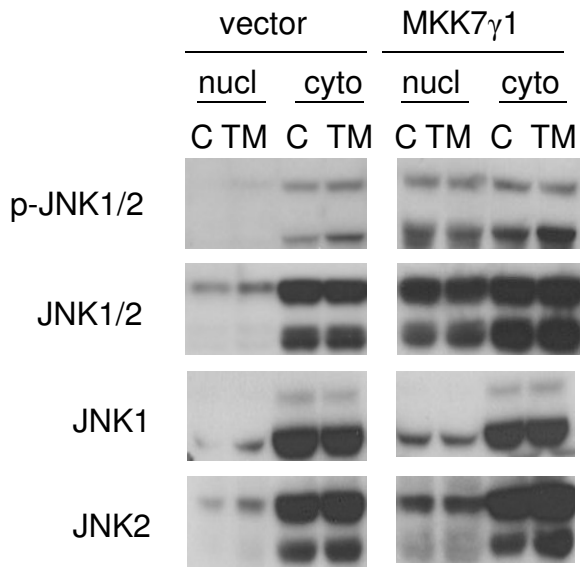

Fig. 24: Changes in protein levels, phosphorylation and localization of JNK isoforms after tunicamycin stimulation in MKK7γ1-transfected PC12 cells.
Western blots of nuclear (nucl) and cytoplasmic (cyto) extracts (each 20 µg) from vector- and MKK7γ1-transfected PC12 cells. Membranes were immunoblotted against phosphorylated (p-) and total JNK1/2 and single JNK isoforms. C, unstimulated control; TM, 1.4 µg/ml tunicamycin for 6 h). Western blots are representative for five independent experiments.

To determine if the MKK7γ1-mediated increase in JNK2 protein (Fig. 24) was based on the up-regulation of mRNA levels, RT-PCRs for *jnk1* and *jnk2* transcripts were performed. Accordingly, *jnk1* mRNA levels were not influenced by MKK7γ1 transfection or tunicamycin, but *jnk2* mRNA level was enhanced in MKK7γ1-transfected PC12 cells (Fig. 25). These results suggest an up-regulation of JNK2 in PC12 cells on both mRNA and protein level caused by transfection with MKK7γ1.

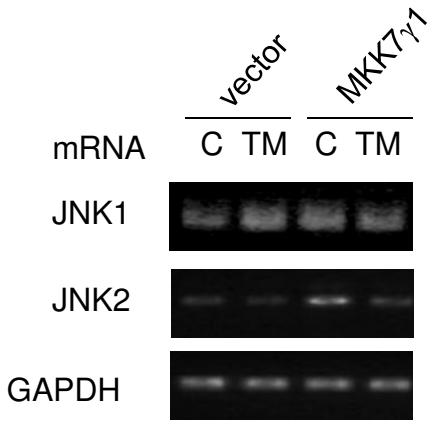

Fig. 25: JNK1 and JNK2 mRNA levels after tunicamycin stimulation.
RNA was isolated from unstimulated (C) and tunicamycin-stimulated (TM, 1.4 µg/ml for 6 h) vector and MKK7γ1-transfected PC12 cells. The *jnk1* and *jnk2* mRNAs were detected by semiquantitative RT-PCR (mRNA). GAPDH were used as a loading control. Data are representative for three independent experiments.

The increase of a single JNK isoform might not account for the observed changes in cellular reactions. More important is the activity status of the protein. For that reason, immunodepletions (IDs) of JNK1 or JNK2 in whole cell extracts from vector- and MKK7γ1-transfected PC12 cells were performed to dissect the activation of JNK1 and JNK2. The supernatants containing only one JNK isoform were subsequently analysed in Western blots with an antibody directed against phosphorylated JNK.

First of all, the IDs confirmed that the basal JNK activity was higher in MKK7γ1-transfected cells, mainly as a result of increased JNK2 phosphorylation (Fig. 26). It also became evident that JNK2 activation was more pronounced in MKK7γ1-transfected cells after stress. In contrast to unstimulated cells, transfection with MKK7γ1 resulted in an increase of phosphorylated JNK1 after stimulation with tunicamycin.

In summary, JNK activation and protein levels were increased in the cytoplasm and nucleus of MKK7γ1-transfected cells, which mainly consisted of up-regulated JNK2 under basal conditions and additionally up-regulated JNK1 after cellular stress.

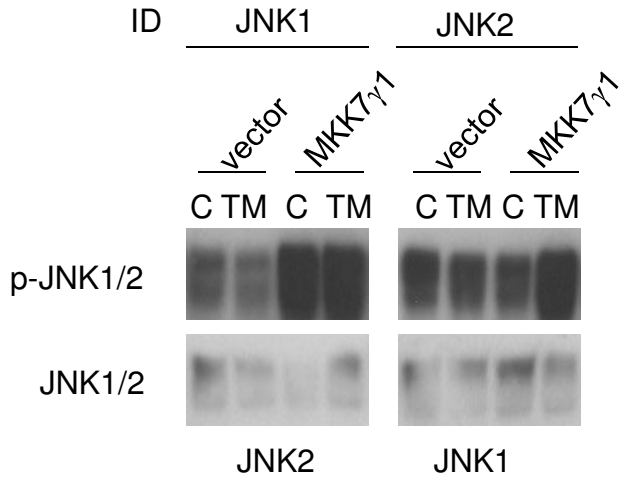

Fig. 26: MKK7γ1-mediated changes in phosphorylation of single JNK isoforms after tunicamycin stimulation.
Single JNK isoforms were immunodepleted (ID) in native protein extracts (100 µg) from unstimulated (C) and tunicamycin-stimulated (TM, 1.4 µg/ml for 6 h) EGFP- and MKK7γ1-transfected PC12 cells. The remaining extracts were first immunoblotted with an antibody against phosphoraylated JNK1/2, than stripped and incubated with and antibody against JNK1/2. Western blots are representative for three independent experiments.

3.2.2.9 JNK signalosomes

Presence and activation of JNK require the formation of signalosomes with their upstream kinases and scaffold proteins. The preferential activation of JNK2 (Fig. 26) raised the question for changes of JNK signalosomes. Therefore, whole cell extracts were immunoprecipitated with an antibody against MKK7 and blotted against JNK1, JNK2 and JIP-1.

As shown in Fig. 27A, JNK1:MKK7 complexes were hardly detectable under normal cell growth conditions in MKK7γ1-transfected cells. Six hours stimulation with tunicamycin had no effect on JNK1:MKK7 complex formation in MKK7γ1-transfected cells, while it reduced JNK1:MKK7 complexes in vector-transfected cells.

In contrast, JNK2:MKK7 complexes were present in MKK7γ1-transfected cells and decreased in both cell lines after incubation with tunicamycin (Fig. 27A). JIP-1 is one of the major scaffold proteins, which assembles MKK7 and JNK for activation. Transfection with MKK7γ1 substantially increased JIP-1:MKK7 complexes under normal growth conditions.

While JIP-1:MKK7 complex formation was slightly pronounced after tunicamycin stimulation in vector-transfected cells, it disappeared in MKK7γ1-transfected cells. JIP-1:JNK1 complexes were unaffected by tunicamycin and MKK7γ1 transfection. Precipitates with an antibody for JIP-1 blotted against JNK2 confirmed the hypothesis that the major signalosome occurring in MKK7γ1 cells is formed by JIP-1, MKK7 and JNK2 under normal cell growth conditions. This complex is disrupted following cellular stress such as tunicamycin.

The next step was to investigate if MKK7γ1 transfection has an impact on JNK2 binding to substrates. Immunoprecipitations with a c-Jun antibody blotted against JNK2 yielded no influence of MKK7γ1 transfection nor tunicamycin stimulation on JNK2:c-Jun complexes.

From non-neuronal cell types it is known that JNKs can bind to p21 and, thereby control p21 stability and activation (98). The results from immunoprecipitation demonstrate that JNK:p21 complexes are also present in neuronal cells (Fig. 27B). According to previous results, MKK7γ1-transfected PC12 cells showed an increased amount of JNK2:p21 complexes compared to vector-transfected cells. Stimulation with tunicamycin caused an increase of JNK2:p21 complexes in vector-transfected cells, while the amount was slightly attenuated in MKK7γ1-transfected cells. JNK1:p21 complexes were also observed but remained unchanged.

Taken together the results show profound changes in JNK signalosomes subject to MKK7γ1 transfection. An increase of JIP-1:MKK7, JIP-1:JNK2, MKK7:JNK2 and JNK2:p21 complexes under normal cell growth conditions was observed that almost disappeared after stimulation with tunicamycin. These findings indicate JIP-1:MKK7:JNK2 and JNK2:p21 as the major signalosomes regulating the switch between MKK7γ1-mediated anti-proliferation under normal and pro-proliferation under stress conditions.

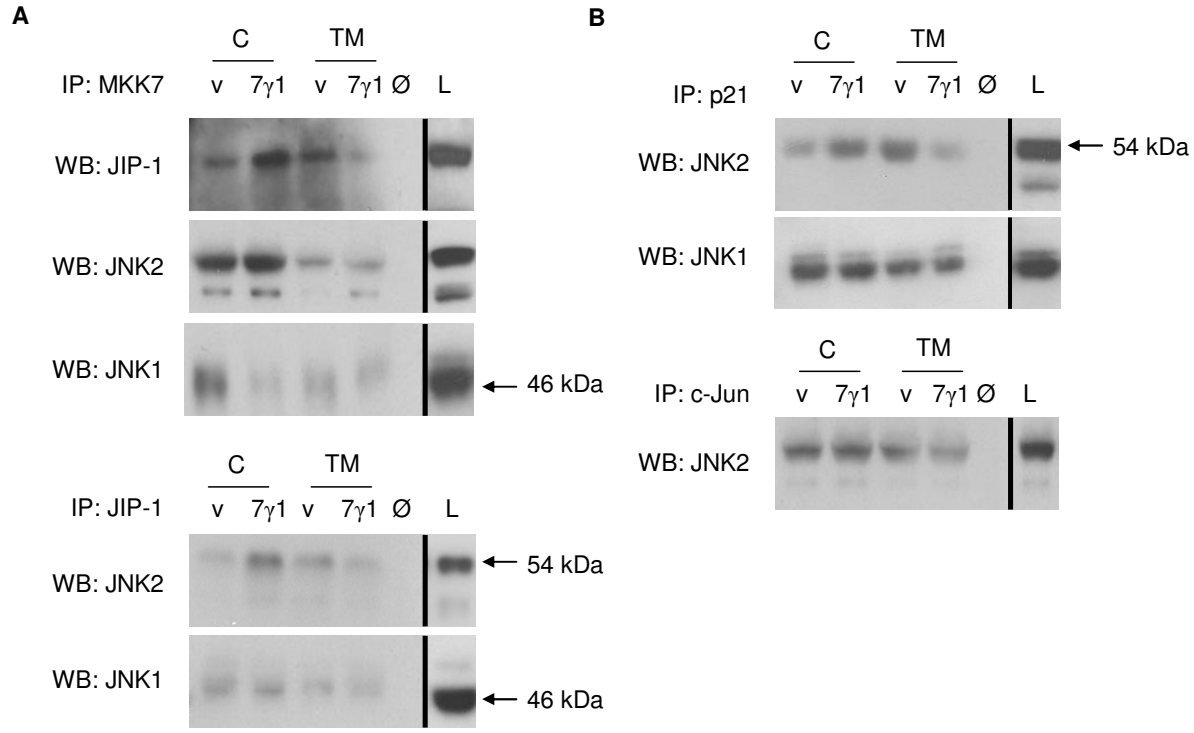

Fig. 27: MKK7γ1-mediated changes in protein-protein interactions.
Immunoprecipitations (IP) of native protein extracts (200 µg) from unstimulated (C) and tunicamycin-stimulated (TM; 1.4 µg/ml for 6 h) vector (v)- and MKK7γ1 (7γ1)-transfected PC12 cells. ∅, mock; L, lysate.
A, The native protein lysates were immunoprecipitated with antibodies raised against MKK7 or JIP-1 and immunoblotted with antibodies against JNK1, JNK2 and/or JIP-1.
B, The native protein lysates were immunoprecipitated with antibodies raised against p21 or c-Jun and immunoblotted with antibodies against JNK1 and/or JNK2.
The data shown represent four independent experiments.

3.2.2.10 Summary II

The following table gives a simplified overview of the MKK7γ1-mediated changes in PC12 cells following tunicamycin treatment.

Tab. 13: MKK7γ1-mediated changes following tunicamycin stimulation.

parameter			vector	MKK7γ1	MKK7γ1
			TM	TM	
culture	proliferation		↓	↑	▲
	apoptosis		↑	-	▼
MKK	MKK7	- protein	-	-	–
		- phosphorylation	↑	↑	–
	MKK4	- protein	-	-	▼
		- phosphorylation	↑	-	▼
JNK	JNK1	- mRNA	-	-	–
		- protein	-	-	▲
		- phosphorylation	-	↑	▲
		- complex JIP-1	-	-	–
		- complex MKK7	↓	-	▼
		- complex p21	-	-	–
	JNK2	- mRNA	-	↓	▲
		- protein	-	↑	▲
		- phosphorylation	↓	-	▲
		- complex JIP-1	↑	↓	▼
		- complex MKK7	↓	↓	▲
		- complex p21	↑	↓	–
		- complex c-Jun	-	-	–
transcription factors	c-Jun	- protein	↑	↑	▲
		- phosphorylation	↑	↑	▲
	c-Myc	- protein	-	-	▼
		- phosphorylation	-	-	▼
	p53	- protein	↑	-	–
		- phosphorylation	↑	-	–
		- p21 promoter	↑	↓	▼
cell cycle	p21	- mRNA	↑	↓	▼
		- protein	↑	↓	▲
	CyclinD1	- mRNA	-	-	–
		- protein	-	-	▼
apoptosis	Fas	- protein	↑	↓	▼
	Fas-L	- protein	-	↓	▼
	Bim	- protein	↑	↓	▲
	Bax	- protein	-	-	–
	Caspase-3	- protein	-	-	–
		- cleavage	↑	↓	▼
	Bcl-2	- protein	-	-	▼
	Bcl-xl	- protein	-	-	▼

Tunicamycin (TM)-mediated changes (↑, increase; -, no change; ↓, decrease) in vector- and MKK7γ1-transfected PC12 cells. Relative changes (▲, increase; —, no change;▼, decrease) in tunicamycin-treated MKK7γ1-transfected PC12 cells compared to vector-transfected PC12 cells.

3.3 Functional analysis of MKK7γ1 in differentiated PC12 cells

The next aim of this study was to characterise the effect of MKK7γ1 on NGF-induced neuronal differentiation of PC12 cells with regard to morphological changes, MAP kinase activity and the phosphorylation of central MAPK substrates.

3.3.1 Characterisation of NGF-treated MKK7γ1-transfected PC12 cells

Upon nerve growth factor (NGF) supplementation, PC12 cells cease to proliferate and start to differentiate into neuron-like cells with pronounced neurite formation (67). As described previously, MKK7γ1 has an anti-proliferative effect on PC12 cells under normal cell growth conditions (Fig. 11). For maintaining the MKK7γ1-specific effects during differentiation, 0.3 x 10^6 vector- or MKK7γ1-transfected PC12 cells were grown on collagen-coated 6-well plates for 2 days with serum-supplemented medium. The cell cycle was synchronized for 3 days by serum deprivation. Thereafter cells were treated for 5 days with 50 ng/ml NGF (called “NGF-treated” or “differentiated” below). Normally, this procedure results in almost 100% differentiated PC12 cells (189). The cell numbers in vector- and MKK7γ1-transfected PC12 cultures were determined by trypan blue staining to avoid misleading results from electronic cell counts caused by differences in cell sizes. Surprisingly, MKK7γ1-transfection significantly increased the number of viable cells by 110%, compared with vector-transfected PC12 cells after 5 days of differentiation (Fig. 28).

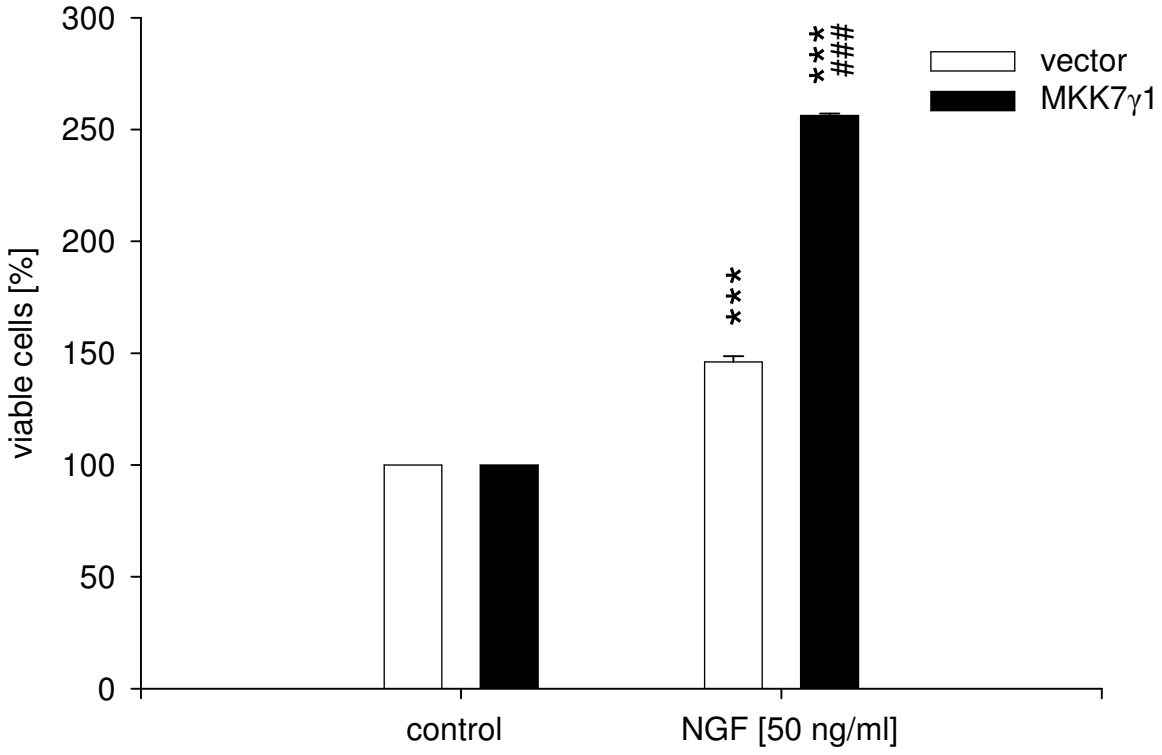

Fig. 28: Viability of NGF-treated vector- and MKK7γ1-transfected differentiated PC12 cells. Cell counts of trypan blue-stained vector- and MKK7γ1-transfected PC12 cells after 5 days treatment with NGF (50 ng/ml). The data represents six independent experiments with ternary ascertainment. Control = 100%. ***/###, $p < 0.001$ for effect of NGF/transfection with MKK7γ1 vs. vector.

3.3.2 Cell numbers

As previously described, the cell number of MKK7γ1-transfected PC12 cells is reduced compared to vector-transfected cells under normal cell growth conditions (Fig. 9). The increased number of MKK7γ1-transfected cells after 5 days of NGF treatment raised the question, when MKK7γ1 changed the phenotyp of PC12 cells from anti-proliferative to pro-proliferative. Again, 0,3 x 10^6 cells were grown on collagen-coated 6-well plates and counted before serum depletion, after serum depletion before NGF (50 ng/ml) was supplemented, and after 5 days of NGF (Fig. 29). Whereas the number of vector-PC12 cells increased by 1.34 x 10^6 cells (446%), the number of MKK7γ1-transfected cells only increased by 0.87 x 10^6 (389%) during 5 days with normal serum-supplemented medium. Serum depletion almost stopped the proliferation of both cell lines (0.17 x 10^6 (10%) for vector- and 0.1 x 10^6 (8%) for MKK7γ1-transfected PC12 cells). Following NGF supplementation, however, the number of EGFP-transfected PC12 cells was only elevated by 0.56 x 10^6 (41%). Interestingly,

the number of viable MKK7γ1-transfected cells further increased by 1.54 x 10^6 (178%). Therefore, proliferation of MKK7γ1-transfected cells occurred when least expected, namely during NGF supplementation.

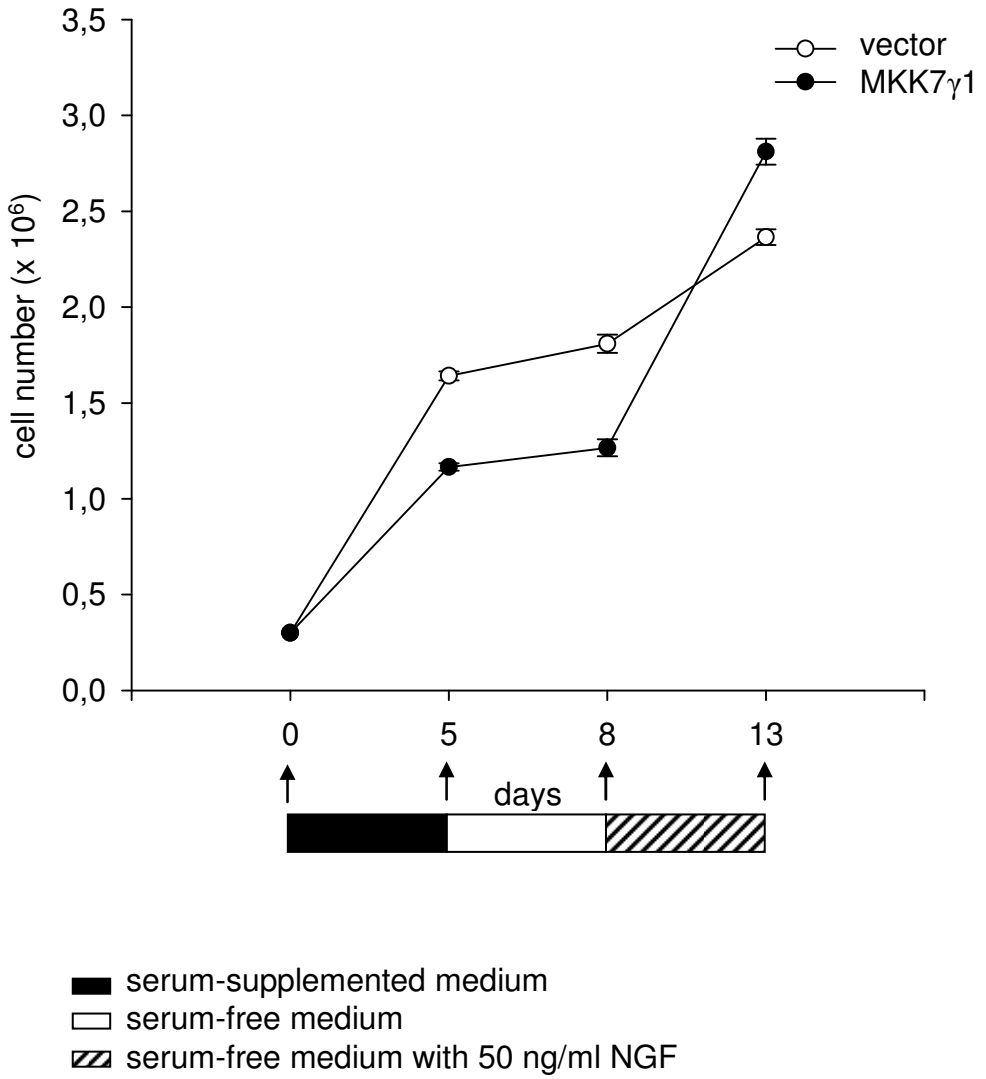

Fig. 29: Cell numbers of vector- and MKK7γ1-transfected PC12 cells during differentiation. Cell counts of trypan blue stained vector- and MKK7γ1-transfected cells after 5 days with serum-supplemeted medium (5), 3 days with serum-free medium (8) and 5 days with NGF-supplemented medium (50 ng/ml; 13). The data represents five independent experiments with ternary ascertainment.

3.3.3 Sprouting

Normally, NGF treatment induces the extension of neurites in PC12 cells. The observed proliferative effect of MKK7γ1 during NGF supplementation raised the question if neurites formation is blocked. Microscopical analysis revealed that NGF-differentiated vector- and

MKK7γ1-transfected PC12 cells showed a polygonal form and developed neurites (Fig. 30). Typically, both cell lines generated a monolayer of enlarged cell bodies with branched neurites on collagen-coated dishes. However, on top of the substrate-adhering MKK7γ1-transfected PC12 cells were small round cells without processes.

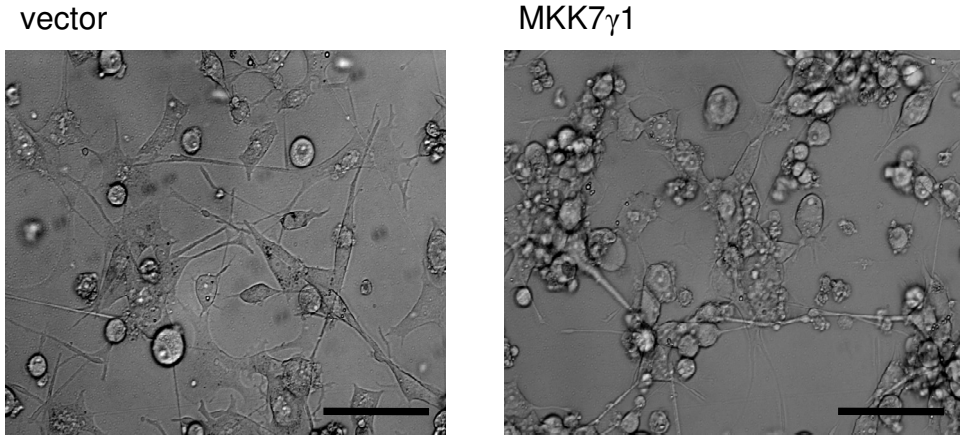

Fig. 30: Cell morphology of NGF-treated vector- and MKK7γ1-transfected PC12 cells.
Light microscopic images of vector- and MKK7γ1-transfected PC12 cells after 5 days treatment with NGF (50 ng/ml). Bars, 50 µM.

To assess the extent of neuronal differentiation, neurite outgrowth (sprouting) was examined in both cell lines. Therefore, 1x 10^5 vector- and MKK7γ1-transfected PC12 cells were grown on an object slide and differentiated for 5 days with 50 ng/ml NGF. The percentage of cells with neurites longer than 1.5 diameters of the cell body were counted with the ImageJ software. As expected, 98% of vector-transfected cells had developed neurites after 5 days of differentiation. In contrast, only 70.6% of MKK7γ1-transfected cells were sprouting (Fig. 31).

Summing up, MKK7γ1 prevented complete sprouting of PC12 cells during NGF supplementation. Indeed, a minor part of MKK7γ1 transfected cells remained naïve and exhibited no differentiation features.

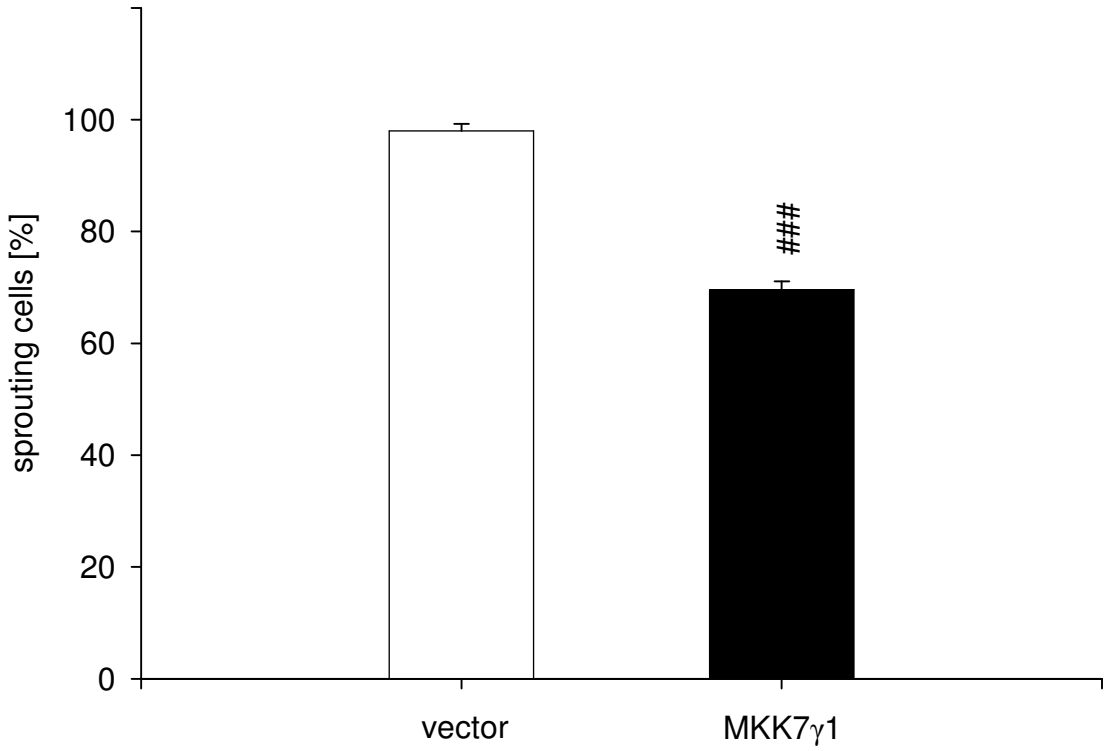

Fig. 31: Sprouting of NGF-treated vector- and MKK7γ1-transfected PC12 cells.
Cell counts of sprouting vector- and MKK7γ1-transfected cells after 5 days treatment with 50 ng/ml NGF. ###, $p < 0.001$ for effect of transfection with MKK7γ1 vs. vector.

3.3.4 Activation of AKT, ERK1/2 and JNK pathways

How does MKK7γ1 affect NGF-mediated PC12 cell differentiation? Normally, NGF supplementation enhances the expression of its high-affinity receptor TrkA and the low-affinity receptor p75 in PC12 cells (146, 192). These increases in TrkA and p75 protein amount could only be observed in vector-transfected cells after 5 days of differentiation with 50 ng/ml NGF (Fig. 32A). MKK7γ1-transfected cells, however, showed a general decrease in TrkA protein under naïve and differentiated conditions. NGF treatment mediated only a slight increase in TrkA protein amount compared to vector-transfected cells. Under normal cell growth conditions, p75 levels of vector- and MKK7γ1-transfected cells were equal. Again, NGF only mediated a slight elevation in p75 protein in MKK7γ1-transfected cells compared to vector-transfected cells.

TrkA can activate the ERK1/2 pathway in PC12 cells, which is linked to differentiation (21, 144). While the levels of the ERK1/2 activator MEK-1 (mitogen-activated

protein kinase/extracellular signal-regulated protein kinase kinase 1) were comparable in vector- and MKK7γ1-transfected PC12 cells (Fig. 32B), MEK-1 phosphorylation was decreased after 5 days of differentiation in MKK7γ1-transfected cells compared to controls. Similar observations were made for the protein and activation levels of ERK1/2 in both cell lines.

Phosphatidylinositol-3-kinase (PI3K), another kinase activated by TrkA, phosphorylates the serine/threonine-kinase protein kinase B (AKT) (3). Differentiation slightly reduced the protein level and activation of AKT in vector-transfected PC12 cells (Fig. 32B). In MKK7γ1-transfected PC12 cells the amount AKT was unchanged, but phosphorylation of AKT was generally decreased and unaffected by differentiation.

Finally, JNKs are also activated after NGF-binding to the TrkA receptor (90). This pathway includes mitogen-activated protein kinase/ERK kinase kinase-1 (MEKK-1) that in turn phosphorylates the MAP2Ks MKK4 and MKK7, which finally leads to JNK activation. The protein level of MEKK-1 was elevated in NGF-treated PC12 cells following MKK7γ1-transfection (Fig. 32C). No differences could be observed for the amount of MKK4, only phosphorylation of MKK4 was slightly reduced by MKK7γ1-transfection, with subsequent reduction of p38 protein level in MKK7γ1-transfected cells. Activation of MKK4 was decreased in naïve and differentiated MKK7γ1-transfected PC12 cells compared to vector-transfected cells. For MKK7 protein, no differences could be observed exempt an additional expression of exogenous MKK7γ1 in transfected PC12 cells. NGF mediated a slightly increased activity of endogenous MKK7 in both PC12 cell lines. As under normal cell growth conditions, phosphorylation of JNKs was increased by MKK7γ1 transfection and NGF treatment. The amount of JNK1/2 was also elevated by transfection with MKK7γ1, but seemed to be decreased after 5 days of differentiation. For JNK1 the amount was comparable in MKK7γ1-transfected PC12 cells after differentiation. However, JNK2 levels were slightly decreased after differentiation of MKK7γ1-transfected PC12 cells.

Taken together, MKK7γ1 mediated a down-regulation of the two NGF receptors TrkA and p75 during differentiation, which attenuated the activation of MEK-1, ERK1/2 and AKT, all of them critical for differentiation of PC12 cells. In contrast, JNK signalling is strongly up-regulated following NGF exposure in MKK7γ1-transfected PC12 cells.

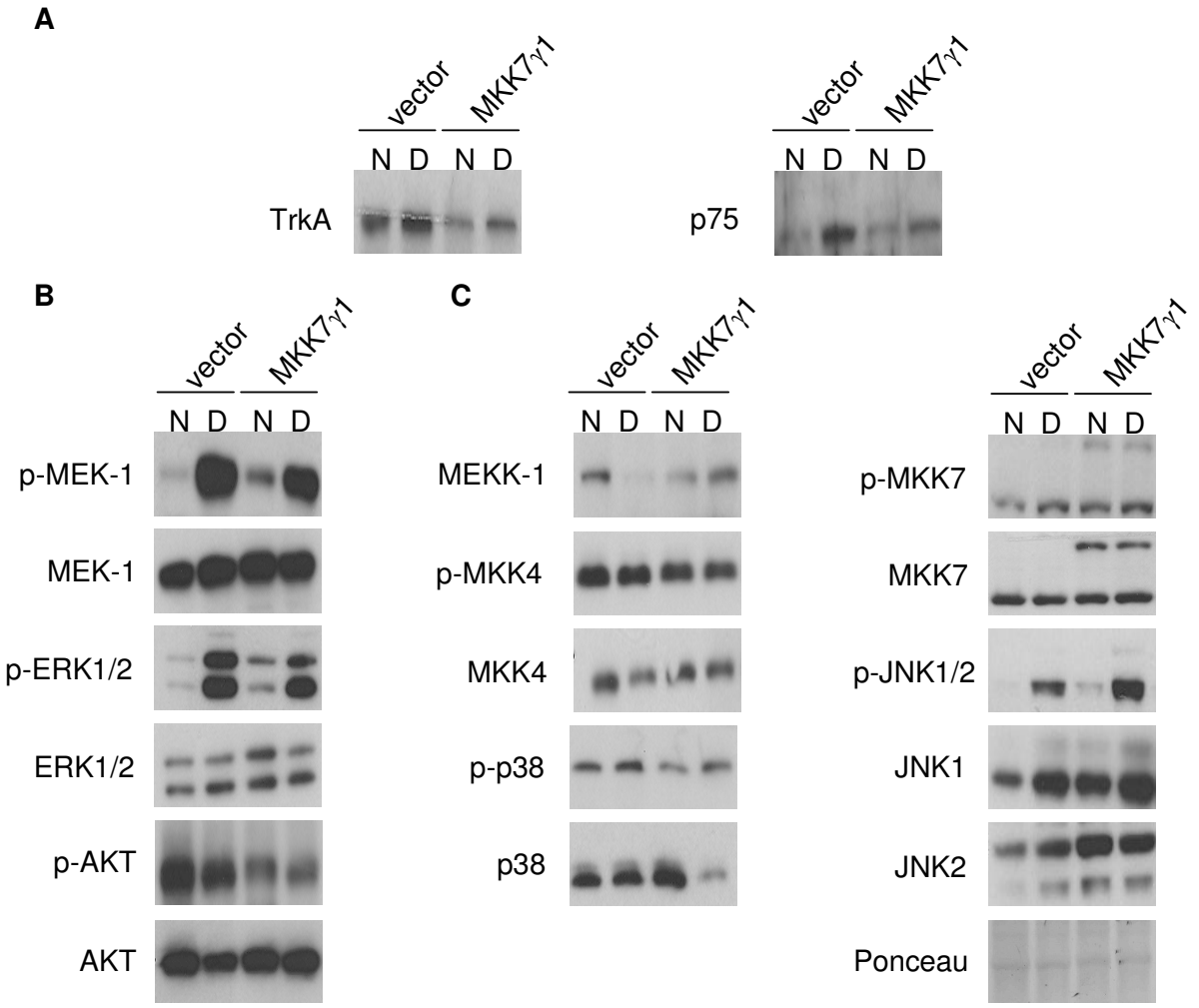

Fig. 32: Protein and phosphorylation levels of NGF receptors and downstream pathways.
Western blot analysis of whole cell extracts (20 µg) of naïve (N) and NGF-treated (D) vector- and MKK7γ1-transfected PC12 cells. Membranes were first immunoblotted against phosphorylated (p-) kinases or receptors of the NGF-pathway, then stripped and incubated with antibodies against the total protein. Equal loading was checked by Ponceau S staining of the membranes. Data are representative for three independent experiments.

3.3.4.1 JNK protein levels, activation and localization

The enhanced JNK activation in NGF-treated MKK7γ1-transfected PC12 cells brought up the question of isoform- and compartment-specific differences. Therefore, activated JNKs were detected in nuclear and cytoplasmic extracts from naïve and differentiated (5 days 50 ng/ml NGF) vector- and MKK7γ1-transfected PC12 cells by a phospho-specific antibody and membranes were stripped and re-hybridized with an antibody against total JNK.

After NGF treatment MKK7γ1-transfected cells showed phosphorylation of JNK1/2 in both cellular fractions, with a marked activity in the nucleus. Total JNK protein levels were also increased in both fractions of MKK7γ1-transfected cells compared to vector-transfected

cells. Interestingly, the amount of 46 and 54 kDa JNK splice variants was enhanced in the nucleus of MKK7γ1-PC12 cells. Studies with isoform-specific antibodies directed against JNK1 and JNK2 revealed that this increase was due to high levels of JNK2 54 kDa splice variants in the nuclear fraction of MKK7γ1-transfected cells. In cytoplasmic fractions of MKK7γ1-tarnsfected cells, also 54 kDa splice variants of JNK2 were predominant. In contrast to JNK2, distribution and amount of JNK1 was comparable in vector- and MKK7γ1-transfected PC12 cells. JNK1 only contributed to the 46 kDa JNK fraction.

Summing up, MKK7γ1 mediated an increase in activation and protein levels of JNK1 and JNK2 in the nucleus and cytoplasm of NGF-stimulated PC12 cells. Especially the 54 kDa splice variants of JNK2 (JNK2α2 and JNK2β2) showed a high level in MKK7γ1-transfected PC12 cells compared to control cells.

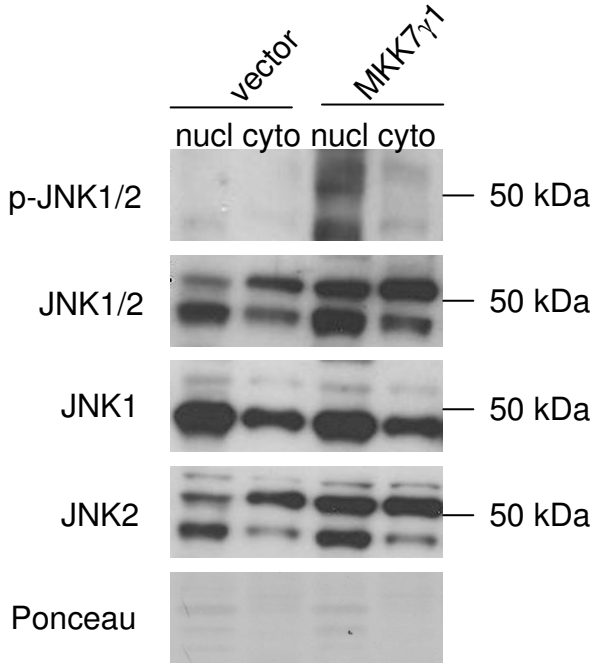

Fig. 33: Changes in amount, phosphorylation and localization of JNK isoforms after NGF treatment in MKK7γ1-transfected PC12 cells.
Immunoblots of nuclear (nucl) and cytoplasmic (cyto) extracts (each 20 µg) from NGF-treated vector- and MKK7γ1-transfected PC12 cells. Membranes were immunoblotted against phosphorylated (p-) and total JNK1/2 and single JNK isoforms. Equal loading was checked by Ponceau S staining of the membranes. Western blots are representative for four independent experiments.

3.3.4.2 JNK targets

The results so far and especially the strong nuclear JNK signal in MKK7γ1-transfected cells suggested an analysis of JNK substrates (Fig. 33). Therefore, the protein levels and phosphorylation of JNK targets involved in transcription, proliferation and apoptosis were investigated in naïve and differentiated (5 days 50 ng/ml NGF) vector- and MKK7γ1-transfected PC12 cells by Western Blot analysis.

c-Jun is known to be induced by NGF and to be involved in differentiation of PC12 cells (52, 201). Similarly, the tumour suppressor p53 plays an important role in neuronal sprouting (4, 48, 140). NGF mediated an increase of c-Jun and p53 activation and amounts that were strongly pronounced in MKK7γ1-transfected cells compared to vector-transfected cells (Fig. 34). The transcription factor c-Myc and its targets can regulate the switch from proliferation to differentiation (32, 82, 186). Here, protein level and phosphorylation of c-Myc were differentially regulated in both cell lines dependent on NGF exposure. Differentiation caused an induction of c-Myc and its phosphorylation in vector-transfected PC12 cells. In naïve MKK7γ1-transfeceted PC12 cells c-Myc protein and phosphorylation were already down-regulated. NGF had no impact on the level and phosphorylation of c-Myc in MKK7γ1-transfected cells.

Due to the prolonged proliferation after NGF supplementation, the cell cycle regulators p21 and CyclinD1 were examined. NGF mediated an increase of the cell cycle inhibitor p21 in vector- and MKK7γ1-transfected PC12 cells (Fig. 34). However, the p21 protein amount was more pronounced in vector-transfected cells compared to MKK7γ1-transfected cells after differentiation. Inversely, the level of CyclinD1 was almost unaffected by NGF in vector-transfected cells but strongly increased in MKK7γ1-transfected cells.

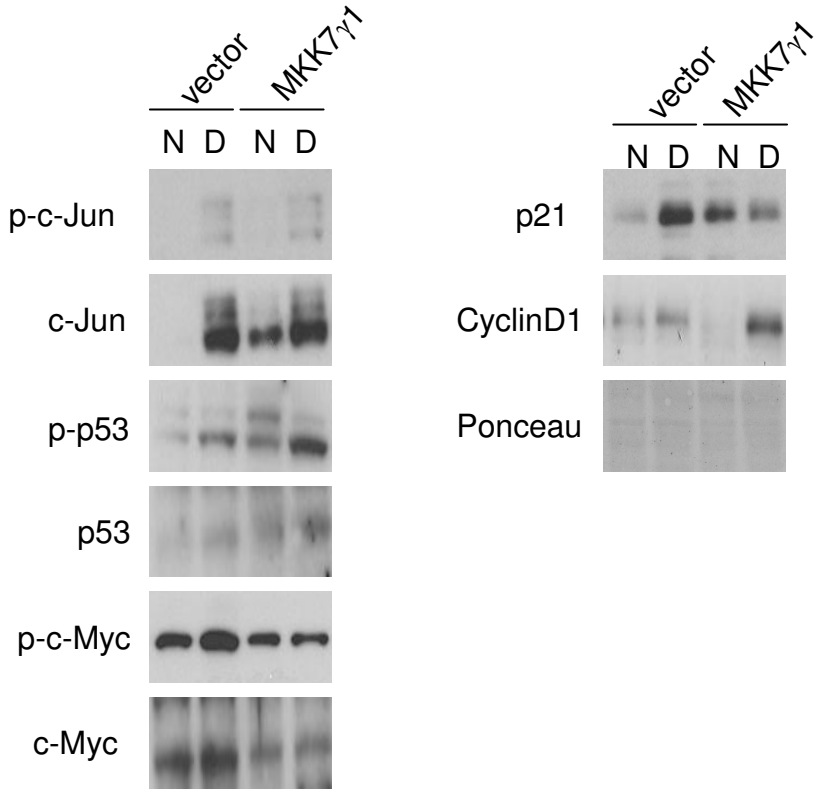

Fig. 34: Protein amounts and phosphorylation of JNK targets in vector- and MKK7γ1-transfected PC12 cells following NGF treatment.
Whole cell extracts (20 µg) from naïve (N) and NGF-treated (D) vector- and MKK7γ1-transfected PC12 cells were analysed by Western blot. Membranes were first immunoblotted against phosphorylated (p-) transcription factors, then stripped and blotted against the total protein. Equal loading was checked by Ponceau S staining of the membranes. Data are representative for four independent experiments.

3.3.4.3 Inhibition of JNKs

To investigate the influence of JNKs on different substrates during NGF supplementation, two specific inhibitors were used. SP600125 is a small molecular weight, potent, cell-permeable, reversible inhibitor that competes with ATP for binding to kinases and has a high specificity toward JNKs (7).

Inhibition of JNKs after 24 h incubation with SP600125 (2 µM) reduced the protein amounts and phosphorylation of the eponymous target c-Jun in vector- and MKK7γ1-transfected PC12 cells (Fig. 35). Whereas the JNK-inhibitor increased activation and protein levels of p53 in vector-transfected cells contrary effects were observed in MKK7γ1-

transfected PC12 cells. p53 induction was reflected in the protein level of the cell cycle inhibitor p21. CyclinD1 was increased in both cell lines due to JNK inhibition.

These results demonstrate that MKK7γ1 increased the NGF-mediated increase of c-Jun and p53 protein levels and activation via JNKs.

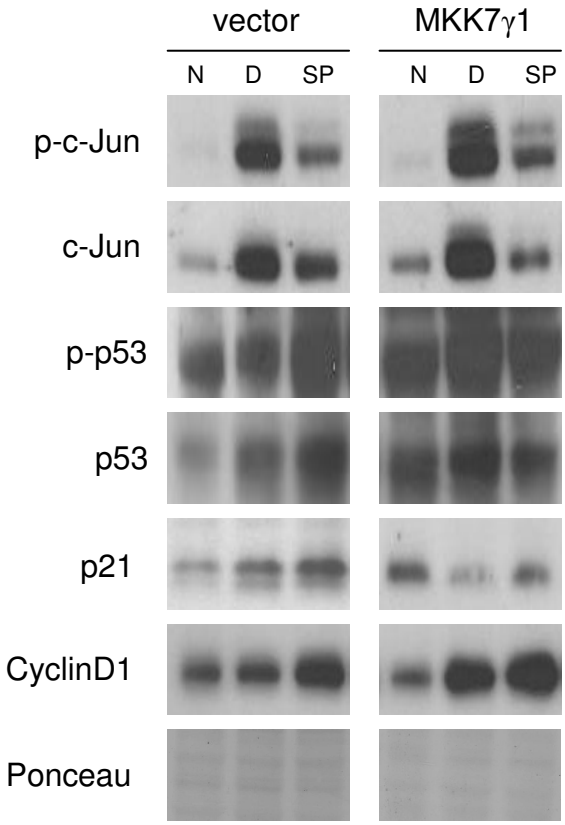

Fig. 35: JNK-dependent protein levels and phosphorylation of transcription factors and cell cycle regulators in NGF-treated vector- and MKK7γ1-transfected PC12 cells.
Western blot analysis from whole cell extracts (20 µg) of vector- and MKK7γ1-transfected PC12 cells with antibodies directed against phosphorylated (p-) c-Jun (p-c-Jun), c-Jun, p-p53, p53, p21 and CyclinD1. Cells were naïve (N) or NGF-treated and unstimulated (D) or incubated for 24 h with SP600125 (SP; 2 µM). Equal loading was checked by Ponceau S staining of the membranes. Blots are representative of three independent experiments.

3.3.4.4 p53 actions

The proto-oncogene p53 is a transcriptional activator of *p21*. Furthermore, p53 was shown to be important for PC12 cell differentiation. As shown above, NGF-treatment increased activation of p53 and the protein level of p21 in vector-transfected cells, while transfection with MKK7γ1 enhanced p53 phosphorylation but decreased p21 protein levels. Both processes are JNK-dependent. This brought up the questions, (i) if p53 regulates p21 levels

during NGF-treatment and (ii) how MKK7γ1 and JNKs affects both proteins.

Pifithrin-α is a potent inhibitor of p53 actions (103). The mechanism, how Pifithrin-α blocks p53 is not identified yet. To investigate the effect of p53 on p21, vector- and MKK7γ1-transfected PC12 cells were treated with NGF and incubated with Pifithrin-α for 24 h. Afterwards whole cell extracts from treated PC12 cells were immunoblotted against p21. As shown in Fig. 36A, inhibition of p53 reduced p21 protein levels in vector-transfected PC12 cells. In contrast, stimulation with Pifihrin-α slightly enhanced the amount of p21 in MKK7γ1-transfected PC12 cells. Thus, p53 positively regulates p21 in control cells but negatively regulates p21 following overexpression of MKK7γ1.

Apart from phosphorylation, JNKs bind to p53 (2, 84). To analyse JNK:p53 complexes, whole cell extracts from naïve and NGF-treated vector- and MKK7γ1-transfected PC12 cells were immunoprecipitated with an antibody against p53 and immunoblotted with isoform-specific JNK1 and JNK2 antibodies. Transfection with MKK7γ1 mediated an increase in JNK1:p53 complexes (Fig. 36B). However, JNK1:p53 complexes were unaffected by NGF treatment. In contrast, JNK2:p53 complexes were enhanced in differentiated vector-transfected PC12 cells and reduced in MKK7γ1-PC12 cells following NGF-treatment.

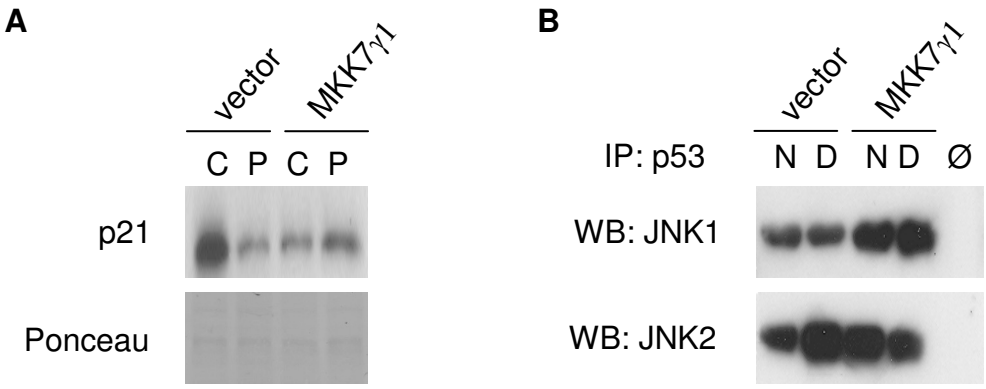

Fig. 36: Influence of MKK7γ1 on p53 actions in NGF-treated PC12 cells.
A, Western blot against p21 of whole cell extracts (20 µg) from NGF-treated or vector- and MKK7γ1-transfected PC12 cells. C, unstimulated control; P, 2 µM Pifithrin-α for 24 h.
B, Immunoprecipitation (IP) of native protein extracts (200 µg) from naïve (N) and NGF-treated (D) vector- and MKK7γ1-transfected PC12 cells. The native protein lysates were immunoprecipitated with an antibody against p53 and immunoblotted with antibodies against JNK1 and JNK2. ∅, mock.

3.3.5 MKK7γ1 under stress conditions in NGF-treated PC12 cells

As MKK7γ1 mediated stress resistance in naïve PC12 cells (see section 3.2.2), the next set of experiments addressed the influence of MKK7γ1 on the reaction of NGF-trated PC12 cells

towards stress conditions. Therefore, experiments were carried out with taxol as a differentiation-dependent stimuli and tunicamycin that causes cell death in naïve and differentiated PC12 cells. The anticancer agent taxol binds to microtubules and provokes a cell cycle arrest during mitosis that leads to apoptosis. Thus, only proliferating cells, but not differentiated cells are susceptible for taxol. The observed proliferation of MKK7γ1-transfected cells during NGF supplementation could maintain their responsiveness towards taxol. The ER stressor tunicamycin, however, should have a stronger apoptotic effect on vector-transfected cells, than MKK7γ1 cells.

3.3.5.1 Cell death

Vector- and MKK7γ1-transfected PC12 cells were differentiated for 5 days with 50 ng/ml NGF. Afterwards, the cells were incubated for 24 h with two different concentrations of taxol (2.5 or 5 µM) and counted by trypan blue staining. Stimulation with taxol did not affect the viability of vector-transfected PC12 cells (2.5 µM taxol; 103%) or even increased it (5 µM taxol; 127%) as shown in Fig. 37. In contrast, survival of NGF-treated MKK7γ1-transfected PC12 cells was decreased by 26% (2.5 µM taxol) and 24% (5 µM taxol).

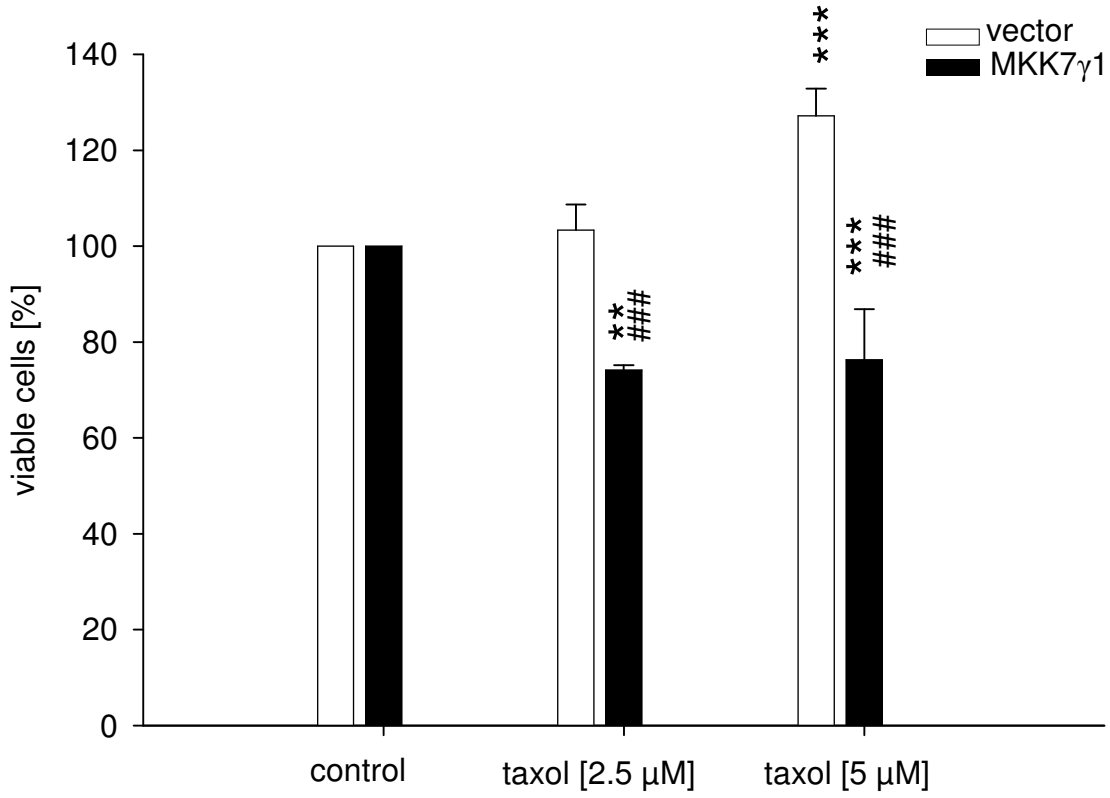

Fig. 37: Viability of NGF-treated vector- and MKK7γ1-transfected cells following stimulation with taxol.
Cell counts of trypane blue stained NGF-treated vector- and MKK7γ1-transfected PC12 cells. The cells were unstimulated (control) or stimulated with two different concentrations (2.5 or 5 µM) of taxol for 24 h. Stimulation with 2.5 or 5 µM taxol. Control = 100%. **, $p < 0.01$; ***/###, $p < 0.001$ for effect of taxol/transfection with MKK7γ1 vs. vector. Data represent four independent experiments with ternary ascertainment.

As a marker for apoptosis, cell extracts from both cell lines were blotted against cleaved and total effector Caspase-3. Differentiated vector- and MKK7γ1-transfected PC12 cells were stimulated with taxol (5 µM), the JNK inhibitor SP600125 (2 µM) or both for 18 h and proteins were extracted. Protein amount and cleavage of Caspase-3 were unaffected by taxol as well as SP600125 in vector-transfected cells (Fig. 38). Even in MKK7γ1-transfected PC12 cells, the level of Caspase-3 did not change. However, differentiated MKK7γ1-transfected cells showed an increase of activated Caspase-3 following taxol treatment. Pretreatment with SP600125 reduced Caspase-3 activity to basal levels, which means that transfection with MKK7γ1 caused a JNK-dependent increase of Caspase-3 cleavage in differentiated PC12 cells.

Taken together, the chemotherapeutic taxol has no effect on differentiated vector-transfected PC12 cells. The fact that MKK7γ1 did not stop proliferation during NGF treatment of PC12 cells promoted JNK-induced apoptosis of PC12 cells following taxol stimulation.

Stimulation with 1.4 µg/ml tunicamycin for 18 h reduced the number of viable vector-transfected PC12 cells by 27% (Fig. 39). Survival of MKK7γ1-transfected cells was only decreased by 9%.

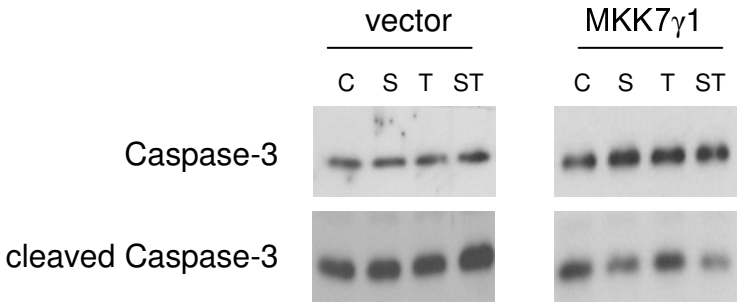

Fig. 38: Cleavage and protein levels of Caspase-3 in NGF-treated vector- and MKK7γ1-transfected PC12 cells following stimulation with taxol and SP600125.
Whole cell extracts (20 µg) from NGF-treated vector- and MKK7γ1-transfected PC12 cells were analysed by Western blot. Membranes were first incubated with an antibody directed against cleaved Caspase-3, then stripped and immunoblotted with a Caspase-3 antibody. C, unstimulated control, S, 2 µM SP600125 for 18 h; T, 5 µM taxol for 18 h and ST, 2 µM SP600125 30 min before 18 h treatment with 5 µM taxol. Equal loading was checked by Ponceau S staining of the membranes. Western blots are representative for three independent experiments.

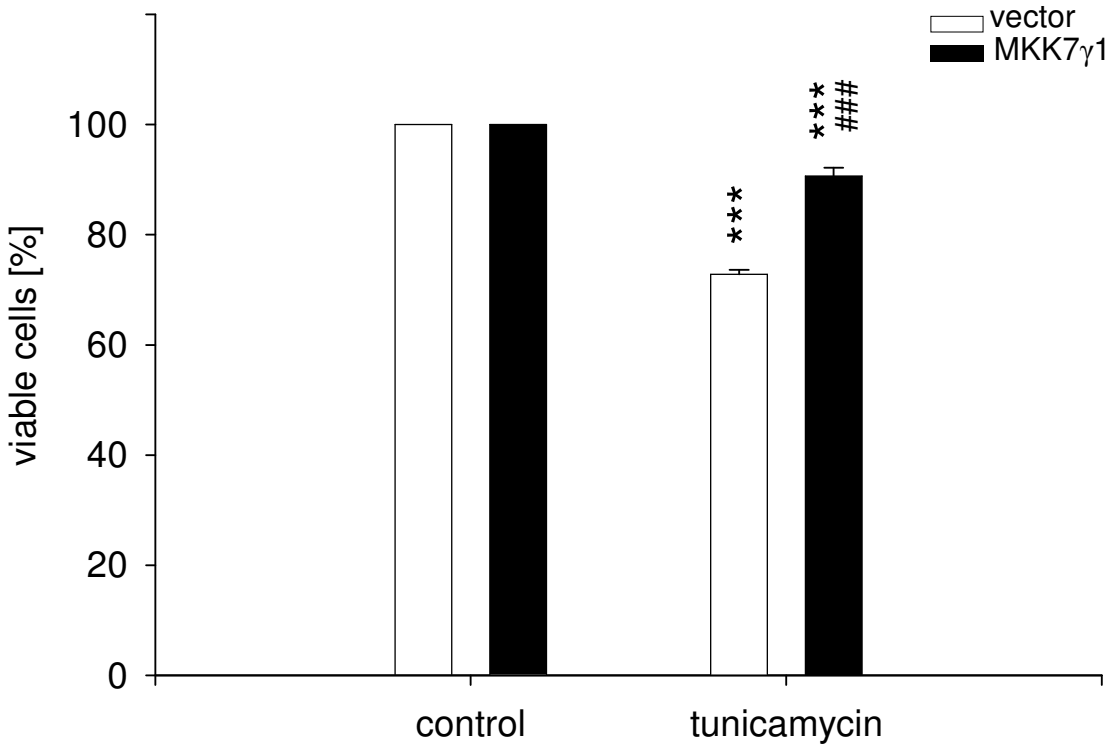

Fig. 39: Viability of NGF-treated vector- and MKK7γ1-transfected cells following stimulation with tunicamycin.
Cell counts of NGF-treated vector- and MKK7γ1-transfected PC12 cells after 24 h stimulation with 1.4 µg/ml tunicamycin. The cells were counted after trypane blue staining. Control = 100%. ***/###, $p < 0.001$ for effect of tunicamycin/transfection with MKK7γ1 vs. vector. Data represent four independent experiments with ternary ascertainment.

Also cleavage of Caspase-3 was increased in vector-transfected PC12 cells compared to MKK7γ1-transfected cells (Fig. 40). Inhibition of JNKs by incubation with SP600125 decreased activation of Caspase-3 in both cell lines. Caspase-3 protein levels were unaffected by tunicamycin as well as SP600125.

Taken together, taxol has no apoptotic effect on differentiated vector-transfected PC12 cells. MKK7γ1 did not stop proliferation during differentiation of PC12 cells, and accordingly promoted JNK-induced apoptosis of PC12 cells following taxol stimulation. As in naïve PC12 cells, MKK7γ1 mediated protection of NGF-treated cells against tunicamycin-induced apoptosis.

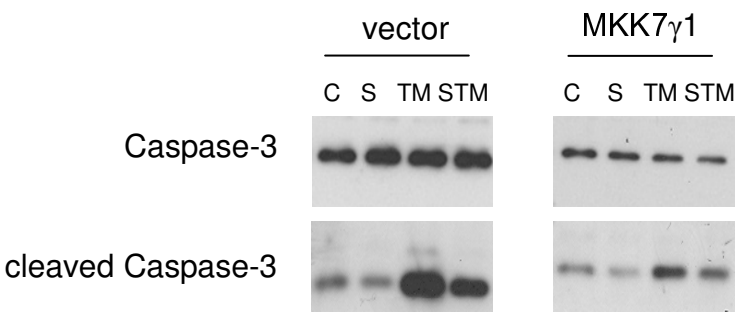

Fig. 40: Cleavage and protein levels of Caspase-3 in NGF-treated vector- and MKK7γ1-transfected PC12 cells following stimulation with tunicamycin and SP600125.
Whole cell extracts (20 µg) from NGF-treated vector- and MKK7γ1-transfected PC12 cells were analysed by Western blot. Membranes were first incubated with an antibody directed against cleaved Caspase-3, then stripped and immunoblotted with a Caspase-3 antibody. C, unstimulated control, S, 2 µM SP600125 for 18 h; TM, 1.4 µg/ml tunicamycin for 18 h and STM, 2 µM SP600125 30 min before 18 h treatment with 1.4 µg/ml tunicamycin. Equal loading was checked by Ponceau S staining of the membranes. Western blots are representative for three independent experiments.

3.3.5.2 JNKs and their targets

To further characterise the MKK7γ1-mediated susceptibility of NGF-treated PC12 cells to taxol, Western blots with antibodies directed against JNKs and their targets were performed.

Taxol caused an increase of activated JNK1/2 in NGF-treated vector- and MKK7γ1-transfected PC12 cells, which was more pronounced in MKK7γ1-transfected cells (Fig. 41). JNK1/2 protein levels were unaffected by taxol stimulation but slightly elevated by transfection with MKK7γ1. Similar to JNK activation, taxol increased c-Jun phosphorylation in both cell lines. Interestingly, the c-Jun protein level was down-regulated in MKK7γ1-transfected cells after stimulation with taxol, whereas it was increased in vector-transfected cells. Furthermore, taxol evoked a strong activation of p53 in differentiated vector- and MKK7γ1-transfected cells. No change in p53 levels could be observed in vector-transfected cells. However, stimulation with taxol decreased the amount of p53 in MKK7γ1-transfected cells. Phospho-c-Myc and c-Myc levels were not affected by stimulation with taxol, but down-regulated by MKK7γ1 transfection. After application of taxol, changes in p21 and CyclinD1 protein levels were detected. In vector-transfected cells, taxol had only a slight effect on p21, whereas it was up-regulated in MKK7γ1-transfected PC12 cells. Taxol induced a down-regulation of CyclinD1 protein in both cell lines.

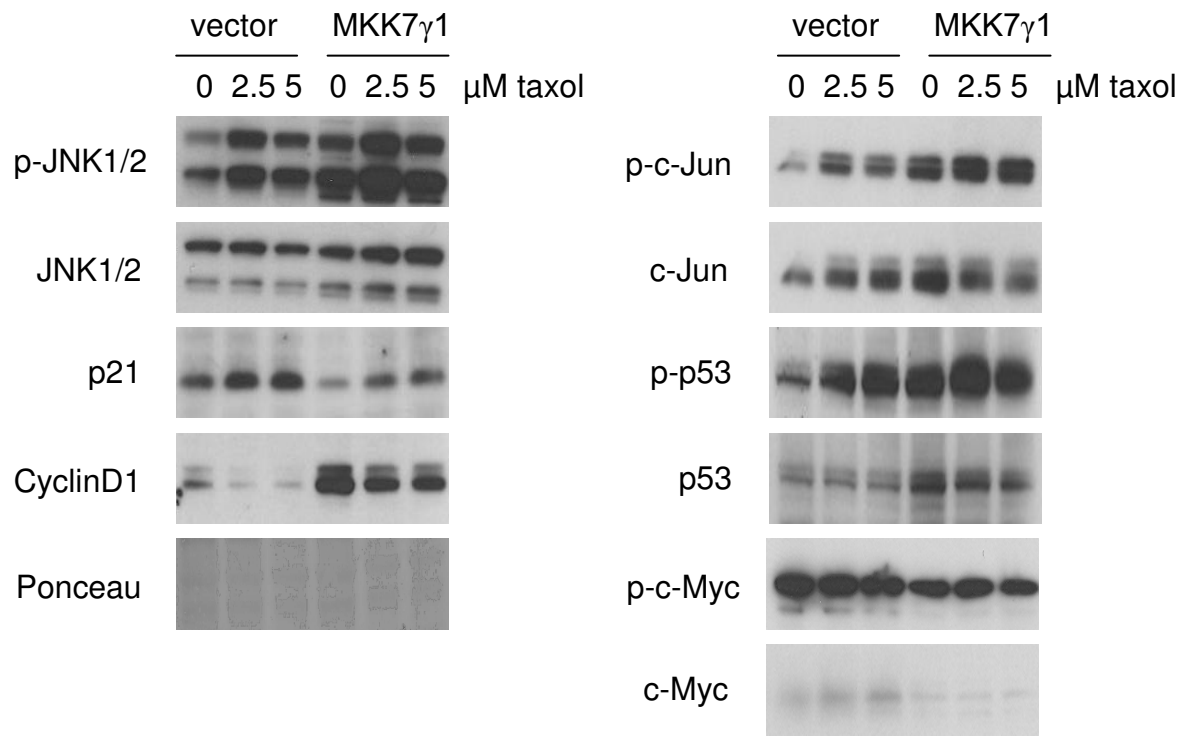

Fig. 41: Protein levels and phosphorylation of JNKs and their targets after taxol stimulation in NGF-treated PC12 cells.
Western blot analysis from whole cell extracts (20 µg) of vector- and MKK7γ1-transfected PC12 cells with antibodies directed against phosphorylated (p-) JNK1/2, JNK1/2, p-c-Jun, c-Jun, p-p53, p53, p21, p-c-Myc, c-Myc and CyclinD1. Taxol-stimulated (24 h) differentiated PC12 cells. Equal loading was checked by Ponceau S staining of membranes. Western blots are representative of four independent experiments.

3.3.5.3 Summary III

The following table gives a simplified overview of the MKK7γ1-mediated changes in PC12 cells following NGF treatment.

Tab. 14: MKK7γ1-mediated changes following NGF treatment.

parameter			vector	MKK7γ1	MKK7γ1
			NGF	NGF	
culture	cell number		↑	↑	▲
	sprouting		↑	↑	▼
NGF receptors	TrkA	- protein	↑	↑	▼
	p75	- protein	↑	↑	▼
	AKT	- protein - phosphorylation	↓ ↓	- ↓	– ▼
MKKK	MEKK-1	- protein	↓	↑	▲
MKK	MEK-1	- protein - phosphorylation	- ↑	- ↑	– ▼
	MKK4	- protein - phosphorylation	↓ -	↓ -	– ▼
	MKK7	- protein - phosphorylation	- ↑	- ↑	– –
MAPK	ERK1/2	- protein - phosphorylation	- ↑	- ↑	– ▼
	p38	- protein - phosphorylation	- -	↓ -	▼ ▼
	JNK1/2	- protein - phosphorylation	↑ ↑	↑ ↑	▲ ▲
transcription factors	c-Jun	- protein - phosphorylation	↑ ↑	↑ ↑	– ▲
	c-Myc	- protein - phosphorylation	↑ ↑	- -	▼ ▼
	p53	- protein - phosphorylation - complex JNK1 - complex JNK2	↑ ↑ - ↑	↑ ↑ - ↓	▲ ▲ ▲ ▼
cell cycle	p21	- protein	↑	↓	▼
	CyclinD1	- protein	↑	↑	▲

NGF- mediated changes (↑, increase; -, no change; ↓, decrease) in vector- and MKK7γ1-transfected PC12 cells. Relative changes (▲, increase; ▬, no change;▼, decrease) in NGF-treated MKK7γ1-transfected PC12 cells compared to vector-transfected PC12 cells.

3.4 Characterisation of MKK4 and MKK4Δ in naïve PC12 cells

For characterisation of MKK4 and MKK4Δ, electronic cell counts were carried out. Therefore, 0.3 x 10^6 cells were grown on collagen-coated 6-well plates for 5 days. Transfection with the established MKK4 splice variant decreased the number of viable PC12 cells by 35% (Fig. 42). In contrast, transfection with the so far unknown MKK4Δ splice variant mediated an increase of viable PC12 cells by 40% compared to vector transfection.

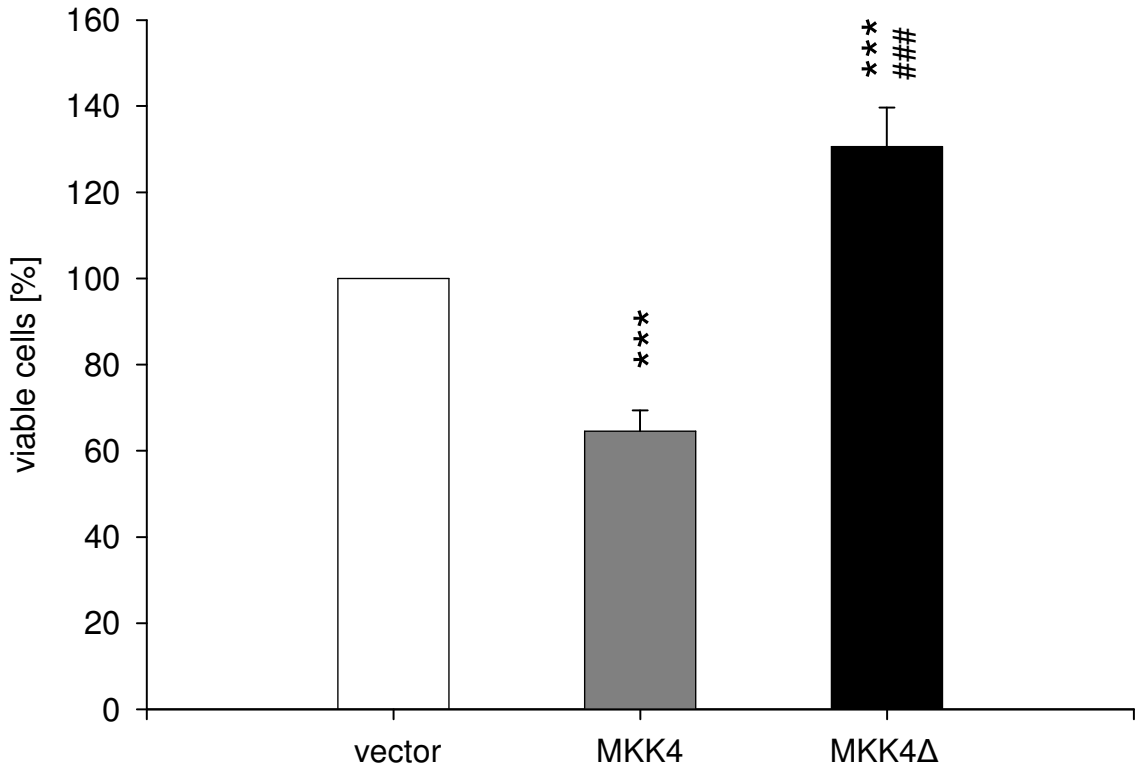

Fig. 42: Electronic cell counts of vector-, MKK4- and MKK4Δ-transfected PC12 cells.
The three cultures were kept under the same conditions. The data represent six independent experiments with ternary ascertainment. ***/###, $p < 0.001$ for vector- vs. MKK4-/MKK4Δ-transfected cells/ transfection with MKK4Δ vs. MKK4.

Afterwards, stable cell clones were screened for the protein level and activation of MKK4, their counterpart MKK7, their substrates p38 and JNKs and other downstream targets. Transfection of PC12 cells with the pEGFP vector, MKK4-pEGFP or MKK4Δ-pEGFP did not change the amount and phosphorylation of endogenous MKK4 (Fig. 43). The protein levels and phosphorylation of exogenous MKK4 and MKK4Δ was slightly reduced compared to endogenous MKK4. Transfection with both MKK4 splice variants had no impact on the MKK7 protein levels. However, activation of MKK7 was reduced in MKK4-

transfected cells and further decreased by transfection with MKK4Δ compared to transfection with the empty pEGFP vector. All three cell clones showed similar levels of JNK1/2 proteins. Activation of JNK1/2, especially the 54 kDa splice variants, was slightly elevated by transfection with MKK4 and MKK4Δ. No changes could be observed in the amount and phosphorylation of the second direct MKK4 substrate p38.

The transcription factor p53 can be phosphorylated by p38 or JNKs, respectively (84, 138). Whereas the protein amount of p53 was comparable in MKK4- and vector-transfected PC12 cells, transfection with MKK4Δ strongly induced p53. Activation of p53 was also increased in MKK4Δ-transfected cells, while it was slightly decreased following MKK4 transfection compared to vector-transfected PC12 cells. Protein amounts and phosphorylation of the transcription factor c-Jun were unaffected by transfection with MKK4 but decreased by transfection with MKK4Δ.

The two cell cycle regulators p21 and CyclinD1 are targets of p38 and JNK signalling. The p21 protein level was unaffected by transfection with MKK4Δ, whereas it was increased by transfection with MKK4 compared to vector-transfected cells. Furthermore the amounts of CyclinD1 were oppositely affected by MKK4 and MKK4Δ transfection. MKK4 transfection reduced and MKK4Δ transfection increased CyclinD1 levels.

Transfection with both MKK4 splice variants increased the levels of the anti-apoptotic BH3-only protein Bcl-2. However, the amounts of pro-apoptotic Bim were decreased by the transfection with MKK4Δ and further reduced by exogenous MKK4.

In summary, though the novel MKK4Δ only includes an additional exon compared to MKK4, overexpression of both MKK4 splice variants provoked different effects in PC12 cells. Transfection with MKK4 slightly reduced the number of viable PC12 cells and the phosphorylation of p53. Furthermore, p21 levels were increased but CyclinD1 and Bim protein amounts were decreased. In contrast, MKK4Δ enhanced the number of viable PC12 cells and the protein level and phosphorylation of p53. c-Jun and Bim were down-regulated and CyclinD1 protein increased following MKK4Δ transfection.

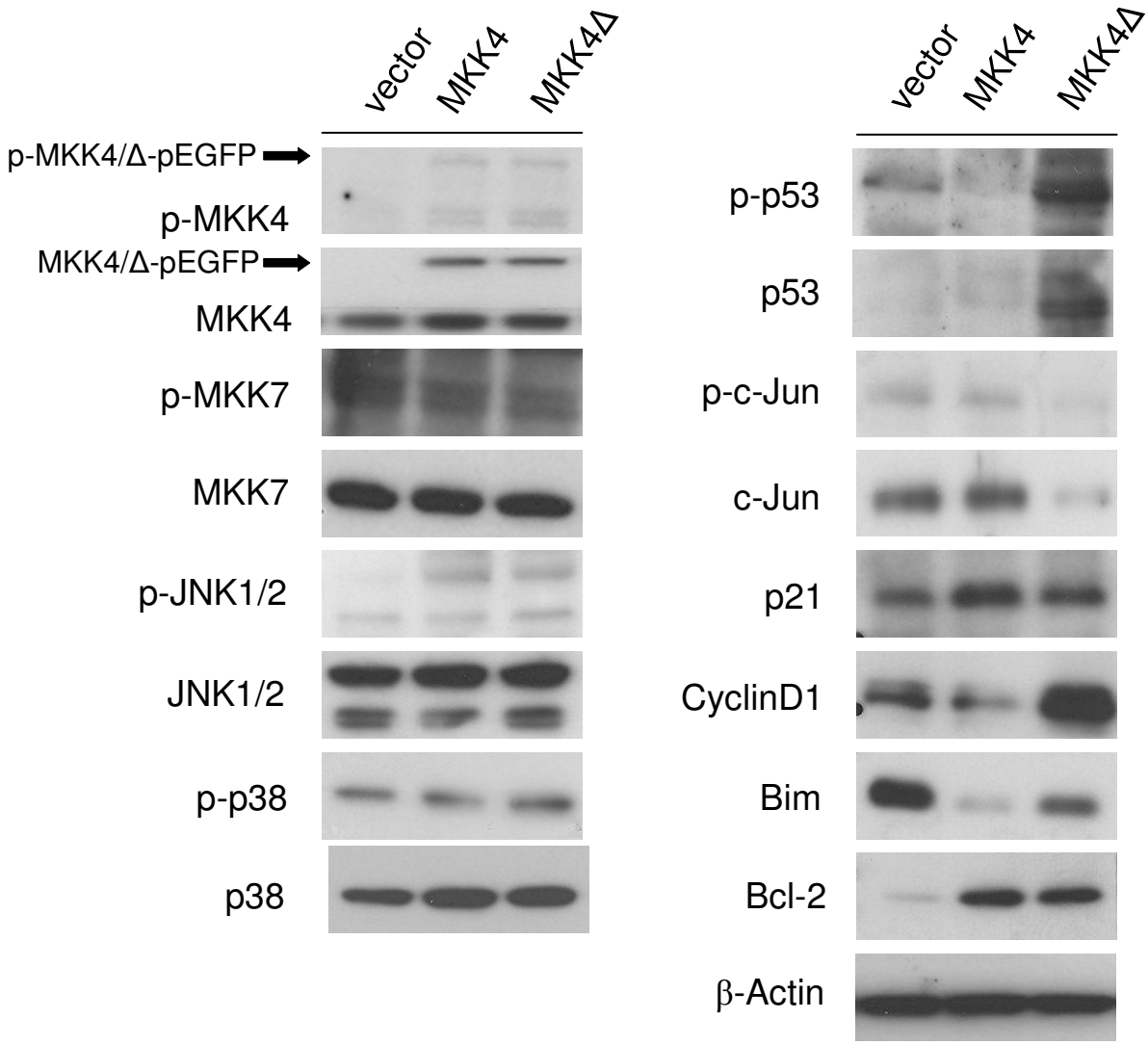

Fig. 43: Protein levels and phosphorylation of JNKs, upstream kinases and targets.
Whole cell extracts (20 µg) from vector-, MKK4 and MKK4Δ-transfected PC12 cells were immunoblotted against JNK1/2, their upstream kinases (MKK4 and MKK7) and some of their direct downstream targets (c-Jun, p53 and c-Myc). All three cell lines were kept under the same conditions. The Western blot membrane was first immunoblotted with phospho-specific antibodies (p-), then stripped and immunoblotted with an antibody directed against the total protein. β-Actin was used as a loading control. Western blots are representative for five independent experiments.

The next experiment addressed the question, if overexpression of MKK4 and MKK4Δ affects the survival of PC12 cells under cellular stress conditions. Vector-, MKK4- and MKK4Δ-transfected PC12 cells were synchronized and incubated with the chemotherapeutic taxol (5 µM) for 24 hours. Electronic cell counting revealed that transfection with MKK4 significantly increased the viability of PC12 cells by 15% following taxol stimulation (Fig. 44). However, survival of taxol-stimulated MKK4Δ-transfected PC12 cells was reduced by 6% compared to vector-transfected PC12 cells.

Taken together, the observed differences between MKK4- and MKK4Δ-transfected cells alter the cellular reaction following stimulation with the stressor taxol.

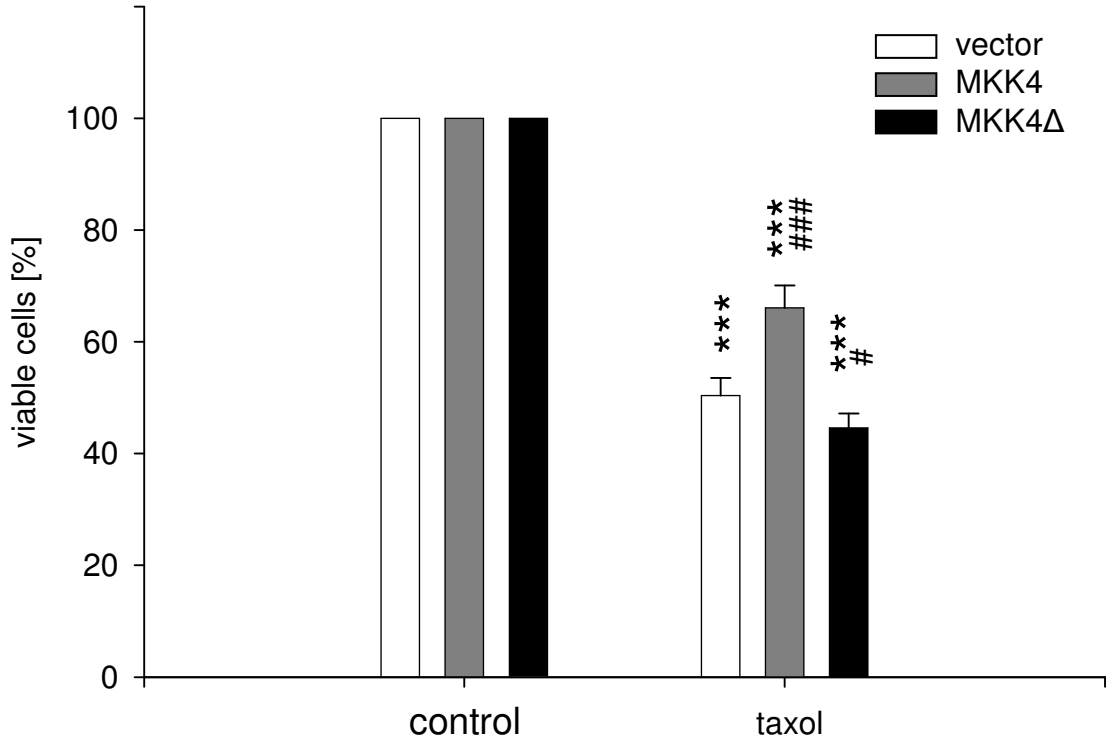

Fig. 44: Viability of vector-, MKK4- and MKK4Δ-transfected PC12 cells following stimulation with taxol.
Electronic cell counts of unstimulated (control) and taxol-stimulated (taxol, 5 µM for 24 h) vector-, MKK4- and MKK4Δ-transfected PC12 cells. Control = 100%. #, $p < 0.1$; ***/###, $p < 0.001$ for effect of taxol/transfection with MKK4 and MKK4Δ vs. vector. Data represent four independent experiments with ternary ascertainment.

3.4.1.1 Summary IV

Table 15 gives a simplified overview of MKK4- and MKK4Δ-mediated changes in naïve PC12 cells.

Tab. 15: MKK4- and MKK4Δ-mediated changes in naïve PC12 cells.

parameter			MKK4	MKK4 Δ
culture	cell number		▼	▲
	apoptosis	- taxol	▼	▲
MKK	MKK7	- protein	–	–
		- phosphorylation	▼	▼
	MKK4	- protein	–	–
		- phosphorylation	–	–
MAPK	p38	- protein	–	–
		- phosphorylation	–	–
	JNK1/2	- protein	–	–
		- phosphorylation	▲	▲
transcription factors	c-Jun	- protein	–	▼
		- phosphorylation	–	▼
	p53	- protein	–	▲
		- phosphorylation	▼	▲
cell cycle	p21	- protein	▲	–
	CyclinD1	- protein	▼	▲
apoptosis	Bim	- protein	▼	▼
	Bcl-2	- protein	▲	▲

Relative changes (▲, increase; ▬, no change; ▼, decrease) in naïve MKK4-/MKK4Δ-transfected PC12 cells compared to vector-transfected PC12 cells.

4 Discussion

The aim of this study was to investigate the functions of single MKK4 and MKK7 splice variants in proliferating and differentiated neuronal cells under physiological and pathological conditions. Their effect on activation and protein levels of JNKs and downstream targets was to be examined and the resulting consequences for basic cellular processes like proliferation and apoptosis.

4.1 The cellular system

PC12 cells were used for the functional characterization of MKK4 and MKK7 splice variants. The aim of this study was the evaluation of a stable neuronal model system, which could be used for determining the potential of MKK4 and MKK7 splice variants under different conditions, like cellular stress or neuronal differentiation. The physiological effects of overexpression approaches are rather moderate. Therefore, it was necessary to use a reliable system with a very low susceptibility to experimental interferences. The use of primary cultures of mice or rat sympathetic neurons would, of course, have come closer to the *in vivo* situation. However, not only the preparation and the varying physiological conditions of the animals, but also contaminations with other cell types (*e.g.*, glia cells), influence the reproducibility of the experiments (13). Another disadvantage of primary neurons is their susceptibility to gene transfer. They are difficult to transfect with a maximal efficiency of 30%, moreover, the majority of cells already die during the transfection procedure (39).

It was not the aim of this study to examine the *in vivo* situation but rather to come closer to the understanding of signal transduction triggered by MKK4 and MKK7 splice variants. By characterizing such basic processes, it will be possible plan experiments for *in vivo* situations more accurately. In addition, a large amount of cell culture experiments was conducted in the present thesis. To carry out a comparable set of experiments with primary neurons would have been quite delicate from an ethical point of view, since numerous animals would have been sacrificed for addressing basic questions of signal transduction.

Apart from PC12 cells, other neuronal permanent cell lines, human or mouse neuroblastoma cells, for example, can also be differentiated by treatment with retinoic acid, but do not display the extent of neuritogenesis as PC12 cells (149). Furthermore, a loss of neuronal characteristics with increasing passage number has been described for permanent

neuroblastoma cells. In contrast, no major changes in cell growth characteristics or growth factor sensitivity were detected in PC12 cells even after 70 generations (68).

An important feature of PC12 cells is that their biochemical properties have fairly well been characterized and their sets of MAPKs has been determined (124, 168, 170, 177, 189). Apoptotic processes and differentiation of PC12 cells have been extensively examined over several years. All these qualities render PC12 cells a well-defined cell culture system for the analysis of MAPK pathways under various environmental conditions.

4.2 Methodology

Functional analysis of proteins can be done by different methods. The most obvious one is to characterize and investigate knockout animals or primary cells from those animals. Unfortuntely, *mkk7*$^{-/-}$ mice are embryonic lethal and only embryonic fibroblasts of these animals can serve as a research object. However, splice variant-specific studies are impossible as gene deletion affects all transcripts. Another option is using RNA interference approaches. Efficient gene silencing without side effects can provide unequivocal information of protein functions. For a strong reduction of target mRNA levels a cocktail of 2 to 4 siRNAs (each ~21 nucleotides) is necessary (37). Furthermore, more than 16 to 17 contiguous base pairs of homology to other coding sequences should be excluded. MKK4 and MKK4Δ, or MKK7β1 and MKK7γ1 splice variants only differ in a single exon of 30 or 48 base pairs, respectively. After extensive studies of gene and transcript sequences and consulting of siRNA manufacturers, RNA interference approaches had to be ruled out. Thus, overexpression was the method of choice for this thesis. Stable transfection, continuous validation of construct expression via microscope (GFP-Tag) or Western blot analysis enabled constant and reliable results. In addition, most experiments were done with several cell clones in parallel and multiple independent repetitions were performed of every experiment shown in this study.

All protein analyses of this thesis were done with specificity-evaluated mono- or polyclonal antibodies. Fortunately, most backround signals of individual antibodies, mainly the phospho-specific antibodies, could be prevented by using optimized dilutions and concentrations of blocking solution. The JNK antibodies used for immunoprecipitations and immunodepletions were tested on tissues from knockout mice (216). With negative controls and the ExactaCruz reagents, artefacts originated from the heavy chains of immunoprecipitation antibodies could be eliminated.

4.3 MKK7γ1 as a regulator of cell proliferation in PC12 cells

4.3.1 Naïve PC12 cells

Normal cell growth conditions- The results of the present study show that MKK7γ1 is a negative regulator of neuronal cell proliferation under normal cell growth conditions. The decrease in proliferation is accompanied by a high JNK activity, a reduced amount of CyclinD1 protein and a JNK-dependent increase in the cyclin-kinase inhibitor p21 on mRNA and protein level. CyclinD1 forms complexes with cyclin-dependent kinase (CDK) 4 and 6 which promote the cell cycle transition from G1- to S-phase (195). p21 inhibits CDK2 and CDK4 and thereby stops cell cycle progression in late G1-phase (116, 122). The observed changes on the level of both cell cycle regulators and the increase of PC12 cells in G1 present a mechanism how MKK7γ1 can block cell cycle progression and decrease proliferation. Previous studies on the proliferative impact of total MKK7 revealed contradictory results and the effect of MKK7γ1 has not been addressed so far. Consistent with the results of this study, MKK7 was shown to be a negative regulator of haematopoietic cell proliferation, assumably via induction of the cell cycle inhibitor p16INK4a and down-regulation of CyclinD1 levels (50, 155). In contrast, studies on *mkk7*$^{-/-}$ MEFs revealed that MKK7 has no impact on proliferation in passages 1 to 3, but is a positive regulator of proliferation and an antagonist of senescence beginning with passage 4 to 5 (187). The expression of CyclinD1 and p21 was not altered in *mkk7*$^{-/-}$ MEFs. Thus, the effect of MKK7 on proliferation is dependent on the cell type, the age or number of passage. Furthermore, there is a difference between MKK7 splice variants. Expression of constitutive active MKK7β1 in the human embryonal kidney carcinoma cell line HEK293 demonstrated that MKK7β1 suppresses proliferation (200).

Stress conditions- The chemotherapeutic agent taxol suppresses mitotic spindle assembly which leads to dysfunction of the cytoskeleton (118). Tunicamycin is an antibiotic that disrupts the N-glycosylation of newly-synthesized proteins (158). Cellular stress response to both stimuli involves JNK signalling in PC12 cells (162, 191). Stimulation with taxol and tunicamycin reduced proliferation of vector- and MKK7β1-transfected PC12 cells. Only transfection with MKK7γ1 increased proliferation of PC12 cells in response to tunicamycin. Treatment with taxol induces a G2-phase cell cycle arrest with an decrease of G1-phase cell population (41). Both, vector and MKK7β1 transfection showed this effect, whereas MKKγ1 reduced G2 cell population. To a lesser extent tunicamycin shifts cells from G2- in G1-phase (119), as described for control and MKK7β1-transfected PC12 cells in this study. Again,

MKK7γ1-transfected cells showed an opposite reaction. The percentages of cells was decreased in G1- and increased in G2-phase and the distribution of tunicamycin-stimulated MKK7γ1-PC12 cells nearly reached that of unstimulated control cells.

mRNA and protein levels of p21 confirm the observations from proliferation and cell cycle assays. Transfected MKK7γ1 selectively decreased the amount of p21 after stimulation with tunicamycin. In vector- and MKK7β1-transfected cells tunicamycin stimulation increased p21 levels. Results from chromatin immunoprecipitations show that p53, which is known to be an inducer of *p21* transcription under various conditions (53), is involved in the transcriptional regulation of *p21* in the used PC12 cell model. Additionally, MKK7γ1 influences *p21* promoter-binding of the transcription factor p53. The data from JNK inhibition experiments with SP600125 show that this regulation is triggered by JNKs. So far no other publication investigated the influence of single MKK7 splice variants on cellular growth behavior under conditions of stress. The results of this thesis demonstrate that MKK7γ1 positively regulates neuronal proliferation by modulation of cell cycle regulators on mRNA and protein levels under stress conditions.

4.3.2 NGF-treated PC12 cells

In the presence of NGF, PC12 cells cease to proliferate and differentiate into a near-neuronal phenotype with neurite outgrowth and dramatic changes in mRNA and protein levels (176). Concerning the cell cycle, NGF induces the expression of the cell cycle inhibitor p21 and the G1-phase CyclinD1 (16, 207).

During serum deprivation, vector-transfected PC12 cells stopped proliferation, but after 5 days of NGF supplementation a small increase in cell numbers was observed. Western blot analysis revealed a strong increase in p21 levels, which is required for the mitotic arrest mediated by NGF (64). The experiment with the p53 inhibitor Pifithrin-α showed that the NGF-mediated increase in p21 is p53-dependent. The increase of CyclinD1 confirmed several findings on mitogenic effects of NGF during early stages of differentiation in PC12 cells (17) and it also explains the slightly increased cell number of vector-transfected cells.

The first part of this thesis on naïve PC12 cells showed that MKK7γ1 attenuates proliferation under normal cell growth conditions, increases p21 and suppresses CyclinD1 levels. Therefore, I expected that overexpression of MKK7γ1 accelerate PC12 cell differentiation, too. Surprisingly, 5 days of NGF treatment strongly increased the number of MKK7γ1-transfected cells, reduced p21 protein levels and drastically enhanced CyclinD1

levels. NGF-mediated cell cycle arrest is blocked and proliferation is sustained. In contrast to vector-transfected cells, inhibition of p53 slightly enhanced p21 protein in MKK7γ1-transfected PC12 cells. Thus, MKK7γ1 interferes with the central process of neuronal differentiation by antagonising cell cycle arrest.

4.4 MKK7γ1 is a negative regulator of neuritogenesis in PC12 cells

NGF signalling through the receptor tyrosine kinase TrkA induces differentiation (92). NGF-binding to the TrkA and p75 receptors activates several signalling pathways underlying the formation of neurites (reviewed by (85, 93)). Five days of NGF supplementation (50 ng/ml) following serum deprivation caused a pronounced differentiation of all vector-transfected PC12 cells. However, NGF treatment failed to induce sprouting of all MKK7γ1-transfected cells. Furthermore, differentiated cells were overgrown by naïve, proliferating PC12 cells. This non-physiological phenotype is accompanied by alterations in molecular signalling. In vector-transfected cells, NGF strongly enhanced TrkA and p75 levels and the activation of ERK1/2. In contrast, MKK7γ1 transfection attenuated a substantially lesser increase of TrkA, p75 and activated ERK1/2 levels, which explains the partially defective neurite formation (33, 144, 148).

The activation and protein levels of AKT, a co-effector of neuritogenesis (108, 120, 131), were also examined in this study. As for TrkA, p75 and ERK1/2, AKT phosphorylation was markedly attenuated in MKK7γ1-transfected cells, which might further contribute to decreased neurite formation.

Beyond stress response and cell death (31, 42), JNKs exert important functions in response to growth factors and regulation of neurite outgrowth (101, 190). ERK1/2 and JNKs interact to induce neurite formation and both are crucial for regeneration of damaged neurites in PC12 cells (189, 190). This study shows that MKK7γ1 potentiates JNK signalling by increased levels of MEKK-1 as well as activation of MKK7 and JNK1/2. Simultaneously, phosphorylation and amounts of MKK4 were down-regulated. Only in MKK7γ1-transfected cells, this decrease was reflected by reduction of active p38. What cellular consequences could that have? In cerebral granule neurons MKK4 was mostly associated with JNK-mediated stress reactions and MKK7 with JNK-induced neuritogenesis (30). Furthermore, MKK7 activity is increased during neuroregeneration of injured PC12 cells, whereas phoshorylation of MKK4 is unaffected (190). In MKK7γ1-transfected PC12 cells, however,

the strong activation of the JNK pathway might not be sufficient for differentiation, especially when the activation of ERK1/2 and AKT are decreased.

4.5 MKK7γ1 as regulator of PC12 cell stress response

4.5.1 Naïve PC12 cells

Normal cell growth conditions- Transfection with MKK7γ1 increased the mRNA and protein levels of the death receptor Fas and the pro-apoptotic BH3-only protein Bim. Furthermore, the cleavage of the effector Caspase-3 was enhanced under basal conditions. Concurrently, the amount of anti-apoptotic proteins Bcl-2 and Bcl-xl were decreased compared to vector-transfected PC12 cells. JNKs activate Bim and Bcl-2 and thereby promote apoptosis in neurons (113, 142). Therefore the reduced number of viable cells in response to transfection with MKK7γ1 could partially be caused by an increase of spontaneous apoptotic cell death via the JNK-Bcl-axis and a decrease in cellular proliferation, respectively.

Stress conditions- In contrast to vector- and MKK7β1-transfected PC12 cells, transfection with MKK7γ1 significantly reduced cell death after stimulation with taxol, tunicamycin and thapsigargin. Interestingly, overexpression of MKK7γ1 prevented PC12 cells from death usually induced by TNF-α and tunicamycin. According to the results from vector- and MKK7β1-transfected cells, all tested stressors induce apoptotic cell death in PC12 cells (162, 172, 191). Thus, the observed neuronal death resistance is splice variant-specific for MKK7γ1.

With regard to signal transduction, tunicamycin-triggered activation of the effector Caspase-3 was reduced in MKK7γ1-transfected PC12 cells. Additionally, the protein amounts of the death receptor Fas and its ligand Fas-L were decreased in MKK7γ1-cells. In vector-transfected cells stimulation with tunicamycin caused an increase of Fas, while Fas-L was unaffected. Stress is known to increase the expression of Fas in PC12 cells and activation of Fas turns on a pathway leding to Caspase-3 cleavage (26, 58). Studies on Fas-deficient mice showed reduced apoptosis in neurons (1, 19). Interestingly, treatment with the Fas inhibitor protein Fas-Fc decreased neuronal regeneration of PC12 cells following injury (192). The results of this study suggest that the MKK7γ1-mediated down-regulation of the Fas-receptor is a relevant factor in promoting stress-resistance of PC12 cells.

4.5.2 NGF-treated PC12 cells

The preceding section has shown that overexpression of MKK7γ1 protects PC12 cells against different types of stress, including taxol and tunicamycin. Normally, NGF also promotes cell survival in response to taxol, by with-drawl from mitosis (34). However, MKK7γ1 transfection caused cell death of NGF-treated PC12 cells. This effect resulted from an incomplete differentiation caused by MKK7γ1. MKK7γ1-transfected PC12 cells still proliferated in spite of NGF supplementation, which rendered them susceptible to taxol, which blocks mitosis.

Interestingly, reactions of MKK7γ1-transfected cells towards the ER-stressor tunicamycin were unaffected by NGF treatment. Whereas tunicamycin stimulation induced apoptosis in differentiated control cells, MKK7γ1 could antagonise cell death. Presumably, the observed resistance of NGF-treated PC12 cells is caused by a MKK7γ1-mediated down-regulation of death receptor Fas as in naïve MKK7γ1-transfected cells. However, further analysis of apoptotic proteins will be necessary.

4.6 MKK7γ1 activates a distinct JNK signalling pathway in PC12 cells

4.6.1 Naïve PC12 cells

Normal cell growth conditions- Comparable to the results from vector-transfected cells, naïve PC12 cells possess a low basal level of JNK, c-Jun and p53 activity (15, 124). Overexpression of MKK7γ1 strongly enhances the amount and phosphorylation of JNKs and their targets c-Jun and p53. Based on the high activation of JNK, it is conceivable that the observed changes are controlled by JNK. Apart from phosphorylation of c-Jun, JNKs activate a number of transcription factors in neurons that contribute to the *c-Jun* promoter activity, including c-Jun itself and ATF-2 (31). The results from experiments with the JNK inhibitor SP600125 confirm that both transcription factors and the cell cycle inhibitor p21 are JNK-dependent up-regulated in PC12 cells following transfection with MKK7γ1. In contrast, the p53 protein level is slightly down-regulated via JNKs in control PC12 cells. p53 is suppressed by JNK1 in primary human fibroblasts (171). However, immunodepletions clearly showed that phosphorylated JNK2 forms the majority of activated JNK in MKK7γ1-transfected PC12 cells. Interestingly, JNK2 deficiency leads to increased cell numbers of primary MEFs and immortalized 3T3 cells, due to enhanced proliferation (151). In addition to the ability of p53 phosphorylation, activated JNK2 is a positive regulator of p53 (2, 171). The results of this

thesis show that regulation of p53 rather occurs on protein, than on mRNA level. On the one hand, p53 can mediate cell cycle arrest through p21 (53) and, on the other hand, p53 regulates apoptosis through the Bcl-2/Bax balance in neurons (184). Indeed, p53 is rather linked to anti-proliferation than to differentiation and apoptosis in neuronal precursor cells (183).

Overexpression of MKK7γ1 decreased c-Myc mRNA, protein and phosphorylation levels. A rapid down-regulation of c-Myc is often triggered by anti-proliferative signals (18, 43). In *jnk1*$^{-/-}$ liver cancers, c-Myc and CyclinD1 expression are strongly reduced, while p21 expression is increased (86, 153). Mechanistically c-Myc is a repressor of *p21* transcription via binding to the *p21* promoter (165). Furthermore, increased p21 protein levels negatively regulate CyclinD1 expression in liver cell proliferation following partial hepatectomy (166, 203). Assumably, MKK7γ1 preferentially activates JNK2, thereby increases p53 and decreases c-Myc and CyclinD1 levels, which in turn positively regulates p21.

JNKs are also involved in regulation of apoptotic proteins (reviewed by (47)). They can activate pro-apoptotic mediators such as Bax, Bad, and Bim (51, 74, 126, 142, 179) and de-activate anti-apoptotic proteins like Bcl-2 (96, 142, 156). Transfection with MKK7γ1 caused an up-regulation of Bim and cleaved Caspase-3 and a down-regulation of Bcl-2 and Bcl-xl. As shown by previous studies, JNK2 positively regulates *bim* transcription in PC12 cells (55). This mechanism involves nuclear activation of the transcription factor c-Jun (197). The regulation of cell survival by Bcl-2 is tightly linked to activated JNK1, which phosphorylates Bcl-2 (44). In contrast, JNK1, but not JNK2 knockdown via siRNA, leads to reduced Bcl-2 levels in human leukemic CEM cells (36).

Summarizing, MKK7γ1 triggers a distinct JNK signalling pathway in PC12 cells by modulation of JNK isoform acitivities. Thereby, MKK7γ1 mediates changes on mRNA (Fas, Bim and Bcl-2), protein (c-Jun, c-Myc, p53, Fas, Bim, Bcl-2 and Bcl-xl) and activity levels (c-Jun, p53, c-Myc) of JNK targets which alters the normal PC12 cell phenotype to an anti-proliferative and pro-apoptotic one.

Tunicamycin stimulation- Cellular stress induced by tunicamycin is known to cause cell death by activation JNK and c-Jun in PC12 cells (213). Additionally, tunicamycin mediates a cell cycle arrest of neuronal cells (81). In MKK7γ1-transfected PC12 cells, tunicamycin hardly induces cell death, but stimulates proliferation. The changes in cellular JNK signalling might provide an explanation for these individual splice-variant-specific actions. Stimulation with tunicamycin generally increased phosphorylation of endogenous and exogenous MKK7 and JNK1/2. The cellular pool of activated JNK was located in nucleus and

cytoplasm and increased after transfection with MKK7γ1. Immunodepletion experiments revealed a strong increase of activated JNK1 in MKK7γ1-transfected cells. This shift in isoform-specific JNK activity could be a reason for changes in cellular proliferation and apoptosis. Several studies observed a positive function of JNK1 in proliferation (86, 137, 196), putatively by JNK1-dependent down-regulation of p21 (86). Here, MKK7γ1 offers an explanation for the observed contrary effects of tunicamycin by activation of a distinct downstream signalling.

4.6.2 NGF-treated PC12 cells

Basal conditions- The multiplicity of pathophysiological and physiological JNK functions in neurons are dependent on different factors, such as isoform specificity and cellular localization (reviewed by (11, 12, 36, 72). Looking at the cellular distribution of activated JNKs after differentiation, transfection with MKK7γ1 strongly increased the nuclear JNK pool. Western blots with isoform-specific antibodies revealed that this increase could be ascribed to JNK2α2 and JNK2β2, whereas JNK1 only contributes to the 46 kDa JNK fraction. This suggests that MKK7γ1 mediates its effects through JNK2 splice-variants in NGF-treated PC12 cells. The described functions of JNK2 cover a wide spectrum such as induction of apoptosis and tumour growth and promotion of proliferation and neurite regrowth (31, 49, 54, 190). In human neuroblastoma cells, nuclear JNK2 is involved in both promotion of apoptosis and proliferation (193). Only little is known about splice-variant specific effects of JNK2α2 and JNK2β2, which are unique among JNKs in their ability of autophosphorylation (182). JNK2α2 was found to be the major isoform in human brain glioblastoma (35). Therefore, MKK7γ1 might be the upstream component underlying the activation of JNK2 isoforms in the cellular transition of pro-proliferation during NGF supplementation.

Several studies using inhibitors or siRNA approaches have suggested that the transcription factor c-Jun acts as a JNK substrate during neuronal differentiation (114, 189, 215). In this study c-Jun is strongly induced and phosphorylated after differentiation of PC12 cells. The fact that MKK7γ1 further increased c-Jun levels implies that c-Jun not only contributes to differentiation, but also to proliferation as reported previously (6).

It is known that neurite outgrowth is a p53-dependent process in PC12 cells (4, 48). Mutant p53 protein, which lost its transcriptional activity, inhibits neurite extensions (48, 57, 202). Opposite findings, however, report that a lack of functional p53 does not prevent terminal differentiation of PC12 cells (185) and p53 is rather linked to down-regulation of

proliferation than to differentiation in murine neuronal precursors (183). This thesis shows that p53 phosphorylation is enhanced during differentiation of PC12 cells. Whereas its phosphorylation is increased after JNK inhibition in vector-transfected cells, it is decreased in MKK7γ1-transfected cells. Therefore, transfection with MKK7γ1 leads to an enhanced JNK-dependent phosphorylation of p53 during differentiation of PC12 cells. Assumably, p53 is normally phosphorylated by other kinases (*e.g.*, ERK1/2 or p38) during PC12 cell differentiation. MKK7γ1 down-regulates those pathways and concurrently triggers p53 phosphorylation by JNK. As all three MAPK have distinct p53 phosphorylation sites this MKK7γ1-mediated changes could influence p53 transcriptional activities. JNKs regulate p53 not only by phosphoryation but also by direct interaction (2). This interaction is not linked to p53 activation, but to p53 stability (2, 61). This thesis shows that p53 binds to JNK1 and JNK2 in NGF-treated PC12 cells. Furthermore, MKK7γ1 reduced p53:JNK2 complexes and increased p53:JNK1 complexes, which implies contrary isoform-specific JNK functions and partially explains the differential effects in MKK7γ1- and vector-transfected cells. Whereas increased levels of phosphorylated JNK1 cause a decrease in p53, enhanced phosphorylated JNK2 levels increase p53 amounts in primary human fibroblasts (171).

The JNK target c-Myc is supposed to regulate around 15% of all genes of the genome (66). These genes are involved in apoptosis, cell cycle, adhesion and differentiation (32, 40). MKK7γ1-transfected PC12 cells showed decreased c-Myc levels that were not affected by differentiation. The constant down-regulation of c-Myc in naïve and differentiated MKK7γ1-transfected cells could be an important mechanism of MKK7γ1-mediated effects.

Two important JNK-dependent cell cycle regulators are p21 and CyclinD1. The results of the present study show that p21 regulation during NGF-mediated PC12 cell differentiation is JNK-dependent. JNKs modulate p21 on various levels, like transcription, activation or stability (59, 65, 98). Therefore, some studies describe JNK as a negative regulator of p21 or in contrast as an positive regulator of p21 (71, 83, 136, 141). This study shows that active JNK represses p21 in naïve and differentiated PC12 cells. Interestingly, MKK7γ1 caused a reversion of the JNK effects on p21. Thus, MKK7 splice-variants constitute a further level upstream of JNKs in p21 regulation. Additionally, a JNK-mediated repression of CyclinD1 in differentiated PC12 cells has been observed. MKK7γ1 transfection further enhanced CyclinD1 induction following NGF treatment.

In summary, NGF activates or induces specific JNK signalling modules in PC12 cells, such as of c-Jun, p21 and CyclinD1 that promote differentiation. MKK7γ1 partially enhanced JNK signalling (c-Jun activation and induction; CyclinD1 induction) but also triggered

additional JNK-dependent activities (p53 activation, induction and binding) or even inverted JNK effects (c-Myc and p21 repression), which all might help to reverse the NGF-mediated PC12 cell phenotype.

Taxol stimulation- This thesis shows that MKK7γ1-transfected PC12 cells still proliferated in spite of NGF supplementation, which rendered them susceptible to taxol that blocks mitosis. On a molecular level, taxol repressed c-Jun and p53 and induced p21 in NGF-treated MKK7γ1-transfected cells. This is contrary to stress reactions in naïve PC12 cells, where MKK7γ1 even increased c-Jun and p53 and repressed p21 under stress conditions.

4.7 Conditional changes in MKK7-JNK complex formation in naïve PC12 cells

The composition of JNK signalosomes has been investigated for several years (reviewed by (12)). However, the link between defined signalosomes and their cellular function is often missing. This study strongly suggest an anti-proliferative and pro-apoptotic function for JIP-1:MKK7:JNK2 signalosome (Fig. 45). Kukekov and colleagues already found a complex consisting of POSH, JIP-1, MLK, MKK7 and JNK and assumed a function in PC12 cell death for this signalosome (105). Complexes between MKK7 and JNK1 only revealed a strong signal in unstimulated vector-transfected PC12 cells. After stimulation with tunicamycin and transfection with MKK7γ1, the complex almost completely disappeared. Furthermore, binding of JIP-1 and JNK1 was absolutely unaffected by transfection and stimulation with tunicamycin.

JNK1 is known to interact with p21 in T-lymphocytes (137). This study demonstrates the presence of JNK:p21 complexes in neuronal cells for the first time. The amount of complexes between JNK2 and p21 correlated with the amount of p21 protein in PC12 cells, whereas JNK1:p21 complexes did not change. The results suggest different functions for JNK1 and JNK2 in the regulation of the cyclin-dependent kinase inhibitor p21. As JNKs phosphorylate, bind and stabilize p21, it is conceivable that individual JNK isoforms contribute to distinct functions (98, 137, 161). Binding between JNK and p21 is a further mechanism for JNK-mediated cell cycle regulation.

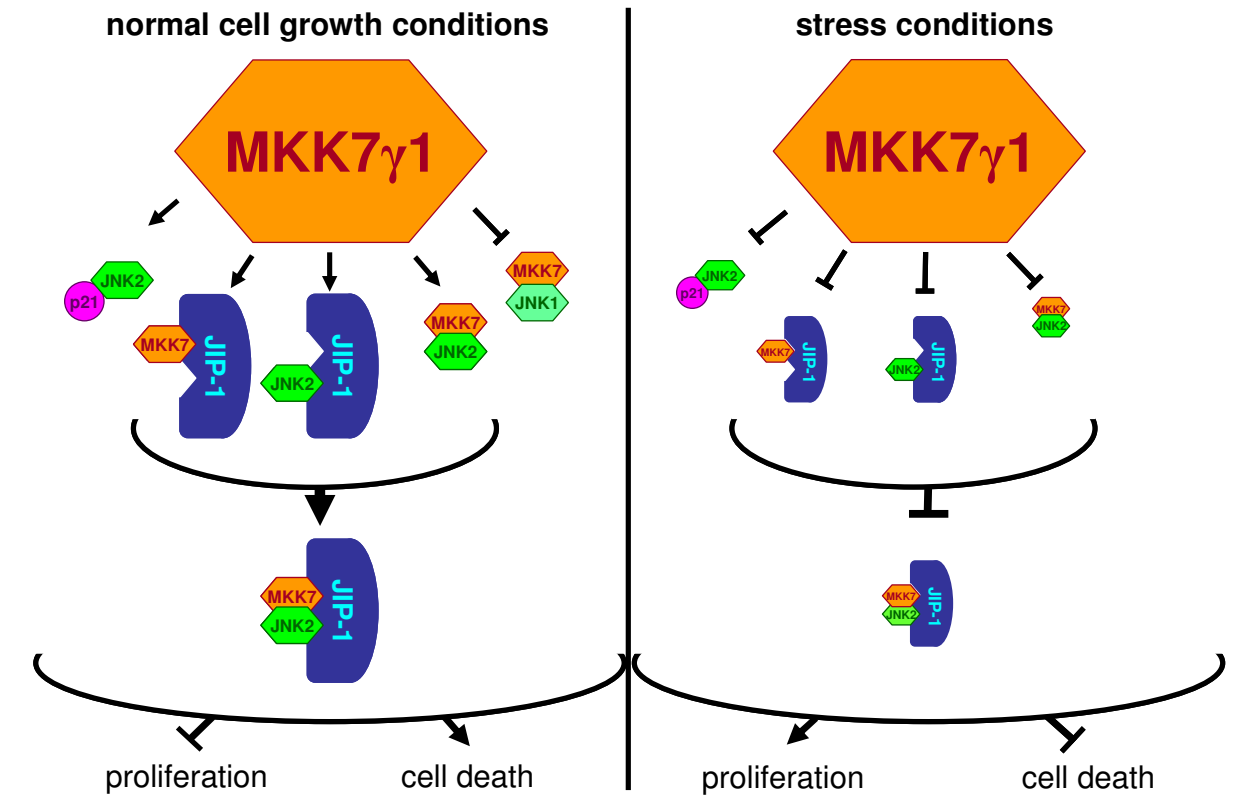

Fig. 45: Schematic model of MKK7γ1-mediated protein interactions.
Differential impact of MKK7γ1 on protein interactions under normal cell growth conditions and after stimulation with tunicamycin (stress conditions). The JIP-1:MKK7:JNK2 signalosome is involved in regulation of proliferation and death in PC12 cells.

4.8 MKK4 and MKK4Δ differently affect naïve PC12 cells

This thesis presents a novel splice variant of MKK4, called MKK4Δ. So far, only one gene product of mammalian *mkk4* genes has been described. MKK4Δ contains an additional exon of 30 bp. This exon is located directly in front of the region encoding the JNK-binding domain. Therefore, a functional relevance was assumable.

The preliminary results from overexpression of both MKK4 splice variants in naïve PC12 cells, revealed different results. Whereas MKK4 transfection decreased the number of viable PC12 cells under basal conditions MKK4Δ transfection increased it. Those changes in cell numbers can be caused by altered proliferation or cell death. Indeed, MKK4 mediated an increase in p21 protein levels whereas CyclinD1 levels were down-regulated compared to vector transfection, which could reduce proliferation of PC12 cells (59, 65, 98). Transfection with MKK4Δ, however, strongly increased CyclinD1 levels compared to control PC12 cells and did not affect the p21 protein amount. The increased levels of anti-apoptotic Bcl-2 and

decreased levels of Bim following MKK4- and MKK4Δ-transfection could also attenuate spontaneous apoptosis of MKK4Δ-PC12 cells (143), but do not explain the observed decrease in cell number of MKK4-PC12 cells.

MKK4 is unique among all MKKs in its ability to phosphorylate two different MAPKs, p38 and JNKs. Nevertheless, some studies revealed that the MKK4 activity towards p38 is less pronounced than towards JNKs (38). For example, knockout of *mkk4* in MEFs causes a decrease in phospho-JNK levels but not in phospho-p38 levels under basal and stress conditions (188). Indeed, overexpression of the MKK4 splice variants only enhanced JNK1/2 phosphorylation, whereas phophorylated p38 was unaffected. Concurrently, the activity levels of MKK7 was decreased in MKK4- and MKK4Δ-transfected PC12 cells which indicates that the increase of activated JNK1/2 was due to MKK4 and the observed changes are mediated by JNKs.

Surprisingly, phosphorylation of c-Jun was unaffected by MKK4 transfection and even reduced following MKK4Δ transfection. Studies on the distribution of MKK4, JNKs and c-Jun in primary neurons have shown that MKK4 and JNKs are mainly located in the cytoplasm, whereas c-Jun and MKK7 are mainly located in the nucleus under basal conditions (30).

In response to taxol treatment, MKK4- and MKK4Δ-transfected PC12 cells showed dramatically opposite reactions. MKK4 caused an increase of viable cells, whereas MKK4Δ transfection mediated a reduced cell survival. To understand these MKK4/Δ-triggered differences in cell survival under stress conditions, further analysis needs to be done.

Summarizing, MKK4 and MKK4Δ have different effects on naïve PC12 cells even though their coding mRNAs only differ in 30 bp. Some of the investigated effects are contrary (*e.g.*, cell numbers, taxol-induced cell death, p21 and CyclinD1 protein levels) and others are comparable for both MKK4 splice variants and only differ from control PC12 cells (*e.g.*, activation and protein levels of MKK7, JNKs, p38).

4.9 Perspectives

The results of the present thesis have provided a basis for further research. It is of interest to investigate the observed MKK7γ1-mediated effects *in vivo*. Viral gene transfer enables the expression of single splice variants linked to a cell type-specific promoter in mice. This could be an adequate approach to check if the *in vitro* findings can be applied to primary neurons. Apart from physiological conditions, mouse models for different pathologies provide a system

to investigate a putative impact of MKK7γ1 based on the results of this study. On the one hand, MKK7γ1 could be an important player in neurological diseases as it blocks neuritogenesis. On the other hand, its opposing effects on cell proliferation and apoptosis following taxol indicate a role of MKK7γ1 in tumourigenesis.

With regard to the functional characterization of MKK4 and MKK7 splice variants, the effects of the so far unknown MKK4Δ should be examined and compared to MKK4. PC12 cells have proved a useful model system for the analysis of parallel MAPK signalling, which will be necessary for MKK4 functions since they can activate JNKs and p38. Therefore, not only different substrates will be analysed, but also specific inhibitors for JNK (SP600125) and p38 (SB239063) will be used to distinguish between the different MAPK pathways.

The only structural difference between MKK4 and MKK4Δ is an additional protein fragment of 30 amino acids in MKK4Δ in front of the JNK binding domain. It is conceivable that this domain has an impact on the binding properties of MKK4 towards JNKs. Therefore, protein interactions of MKK4 and single JNK isoforms will be investigated by immunopreciptitations.

5 Summary

The mitogen-activated protein kinase (MAPK) pathways are ubiquitious and highly expressed in all eukaryotic cells. Diverse stimuli activate MAPKs, whose intracellular network translates and integrates those signals into complex cytoplasmatic and nuclear processes which lead to organized cellular responses, like proliferation, differentiation or apoptosis. The c-Jun N-terminale kinases (JNKs), one subfamily of MAPKs, are considered as essential signalling molecules for the differentiation, regeneration and programmed cell death of neurons. Apart from those physiological functions, JNKs mediate neurodegeneration and are involved in a number of pathologies such as Alzheimer's or Parkinson's disease. In answering the question, how JNKs regulate this functional dichotomy, their upstream activators, mitogen-activated protein kinase kinase (MKK) 4 and MKK7 are largely underestimated. The aim of this thesis was to use stable overexpression of MKK4 and MKK7 to investigate their effects on JNK functions in the rat adrenal pheochromocytoma cell line PC12. During cloning of both known JNK activators in the rat, MKK4 and MKK7β1, two so far unknown splice variants, MKK4Δ and MKK7γ1, were identified. Overexpression of MKK7γ1 in PC12 cells mediated distinct changes in activation and protein levels of JNK isoforms. Consequently, JNK signalling was changed at mRNA, protein and phosphorylation levels of JNK targets, such as transcription factors (c-Jun, p53, c-Myc), cell cycle regulators ($p21^{WAF-1/CIP-1}$, CyclinD1) and apoptotic proteins (Fas, Bim, Bcl-2, Bcl-xl). Additionally, the assembly of JNK signalosomes was affected. These alterations promoted the sensitivity of PC12 cells towards cell death and repressed proliferation under normal cell growth conditions. After stimulation with taxol and tunicamycin, MKK7γ1 but not MKK7β1 transfection, reduced cell death and even increased cell proliferation.

Furthermore, MKK7γ1 partially blocked nerve growth factor (NGF)-induced differentiation of PC12 cells via additional down-regulation of the NGF receptors TrkA and p75 as well as of the differentiation-promoting extracellular signal-regulated kinase 1/2 (ERK1/2) and phosphatidylinositol-3-kinase (PI3K) pathways. These MKK7γ1-triggered effects induced an escape from cell cycle arrest and rendered PC12 cells sensitive to taxol-mediated cell death.

Overexpression of MKK4 and MKK4Δ caused opposite effects in PC12 cells. MKK4 decreased the viability of cells under basal conditions and enhanced cell survival following taxol stimulation. In contrast, MKK4Δ increased the number of viable cells under basal

conditions, but reduced the viability of taxol-treated cells. Thus, single MKK4 and MKK7 splice variants are powerful inductors of distinct and contrasting JNK actions depending on the cellular context and are at least partially responsible for the dichotomy of JNK signalling.

6 Zusammenfassung

Die Mitogen-aktivierten Proteinkinasen (MAPK) sind zentrale Elemente der Signaltransduktion bei allen Eukaryoten. MAPK werden von einer Vielzahl verschiedenster Stimuli aktiviert. In der Zelle bilden sie ein Enzymnetzwerk, dass die Signale aufnimmt und in zytoplasmatische und nukleäre Vorgänge übersetzt, die schließlich zu organisierten zellulären Reaktionen, wie Proliferation, Differenzierung oder Apoptose führen. Eine wichtige Unterfamilie der MAPK sind die c-Jun N-terminalen Kinasen (JNK), die eine entscheidende Rolle bei der Differenzierung, Regeneration und beim programmierten Zelltod von Neuronen spielen. Abgesehen von diesen physiologischen Funktionen, vermitteln JNK auch Neurodegeneration und sind an einer Vielzahl von Krankheitsbildern wie Morbus Alzheimer oder Morbus Parkinson beteiligt. Bei der Beantwortung der Frage, wie JNK diese funktionelle Dichotomie bewirken, hat man der Bedeutung ihrer Aktivatoren, der Mitogen-aktivierten Proteinkinasekinase (MKK) 4 und MKK7, bisher zu wenig Aufmerksamkeit geschenkt. Das Ziel dieser Arbeit war es, den Effekt von MKK4 und MKK7 auf JNK-vermittelte Funktionen zu untersuchen. Dazu wurden sie in Phäochromozytom (PC12)-Zellen aus der Ratte stabil überexprimiert. Bei der Klonierung der beiden JNK-Aktivatoren, MKK4 und MKK7β1, wurden zwei bisher unbekannte Spleißvarianten, MKK4Δ und MKK7γ1, in PC12 Zellen identifiziert. Überexpression von MKK7γ1 in PC12-Zellen veränderte die Phosphorylierung und die Proteinmenge von JNK-Isoformen. Infolgedessen war die Wirkung der JNK auf ihre Substrate verändert. Effekte konnten auf mRNA-, Protein- und Aktivitätsebene von Transkriptionsfaktoren (c-Jun, p53, c-Myc), Zellzyklusregulatoren ($p21^{WAF1/CIP1}$, CyclinD1) und Regulatoren der Apoptose (Fas, Bim, Bcl-2 und Bcl-xl) beobachtet werden. Zusätzlich war die Zusammensetzung von JNK-Signalosomen verändert. All diese Veränderungen erhöhten die basale Apoptoserate der Zellen und verringerten ihre Proliferation unter normalen Wachstumsbedingungen. Nach Stimulation der Zellen mit Taxol oder Tunicamycin, verringerte MKK7γ1, aber nicht MKK7β1, den Zelltod und verstärkte gleichzeitig die Proliferation.

Des Weiteren wurde die durch den Nervenwachstumsfaktor (*nerve growth factor*, NGF) eingeleitete Differenzierung von PC12-Zellen durch MKK7γ1 blockiert. Überexpression von MKK7γ1 verringerte die Proteinmengen und Phosphorylierung der NGF-Rezeptoren (TrkA und p75) und einzelner Komponenten differenzierungsfördernder Signaltransduktionswege, wie den Extrazellulären Signal-regulierten Kinase 1/2 (ERK1/2)

und Phosphatidyl-Inositol-3-Kinase (PI3K). Außerdem verhinderte MKK7γ1 den Zelllzyklusarrest und machte die Zellen so anfällig gegenüber Taxol.

Die Überexpression von MKK4 und MKK4Δ in PC12-Zellen bewirkte gegensätzliche Effekte. MKK4 verringerte die Viabilität der Zellen unter basalen Bedingungen und erhöhte die Überlebensrate der Zellen nach Taxol-Stimulation. Im Gegensatz dazu, erhöhte MKK4Δ die Anzahl lebender Zellen unter basalen Bedingungen, verstärkte jedoch den Taxol-induzierten Zelltod. Somit sind einzelne MKK4 und MKK7 Spleißvarianten entscheidende Regulatoren von unterschiedlichen, teils auch gegensätzlichen JNK-Wirkungen in Abhängigkeit von der zellulären Umgebung.

7 References

1. **Ackery, A., S. Robins, and M. G. Fehlings.** 2006. Inhibition of Fas-mediated apoptosis through administration of soluble Fas receptor improves functional outcome and reduces posttraumatic axonal degeneration after acute spinal cord injury. J Neurotrauma **23:**604-16.
2. **Adler, V., M. R. Pincus, T. Minamoto, S. Y. Fuchs, M. J. Bluth, P. W. Brandt-Rauf, F. K. Friedman, R. C. Robinson, J. M. Chen, X. W. Wang, C. C. Harris, and Z. Ronai.** 1997. Conformation-dependent phosphorylation of p53. Proc Natl Acad Sci U S A **94:**1686-91.
3. **Andjelkovic, M., H. S. Suidan, R. Meier, M. Frech, D. R. Alessi, and B. A. Hemmings.** 1998. Nerve growth factor promotes activation of the alpha, beta and gamma isoforms of protein kinase B in PC12 pheochromocytoma cells. Eur J Biochem **251:**195-200.
4. **Bacsi, A., G. J. Stanton, T. K. Hughes, M. Kruze, and I. Boldogh.** 2005. Colostrinin-driven neurite outgrowth requires p53 activation in PC12 cells. Cell Mol Neurobiol **25:**1123-39.
5. **Bardwell, A. J., E. Frankson, and L. Bardwell.** 2009. Selectivity of docking sites in MAPK kinases. J Biol Chem **284:**13165-73.
6. **Behrens, A., M. Sibilia, and E. F. Wagner.** 1999. Amino-terminal phosphorylation of c-Jun regulates stress-induced apoptosis and cellular proliferation. Nat Genet **21:**326-9.
7. **Bennett, B. L., D. T. Sasaki, B. W. Murray, E. C. O'Leary, S. T. Sakata, W. Xu, J. C. Leisten, A. Motiwala, S. Pierce, Y. Satoh, S. S. Bhagwat, A. M. Manning, and D. W. Anderson.** 2001. SP600125, an anthrapyrazolone inhibitor of Jun N-terminal kinase. Proc Natl Acad Sci U S A **98:**13681-6.
8. **Berg, M. M., D. W. Sternberg, B. L. Hempstead, and M. V. Chao.** 1991. The low-affinity p75 nerve growth factor (NGF) receptor mediates NGF-induced tyrosine phosphorylation. Proc Natl Acad Sci U S A **88:**7106-10.
9. **Birnboim, H. C., and J. Doly.** 1979. A rapid alkaline extraction procedure for screening recombinant plasmid DNA. Nucleic Acids Res **7:**1513-23.
10. **Bjorkblom, B., J. C. Vainio, V. Hongisto, T. Herdegen, M. J. Courtney, and E. T. Coffey.** 2008. All JNKs can kill, but nuclear localization is critical for neuronal death. J Biol Chem **283:**19704-13.
11. **Bogoyevitch, M. A.** 2006. The isoform-specific functions of the c-Jun N-terminal Kinases (JNKs): differences revealed by gene targeting. Bioessays **28:**923-34.
12. **Bogoyevitch, M. A., and B. Kobe.** 2006. Uses for JNK: the many and varied substrates of the c-Jun N-terminal kinases. Microbiol Mol Biol Rev **70:**1061-95.
13. **Brewer, G. J., and C. W. Cotman.** 1989. Survival and growth of hippocampal neurons in defined medium at low density: advantages of a sandwich culture technique or low oxygen. Brain Res **494:**65-74.
14. **Bruckner, S. R., and S. Estus.** 2002. JNK3 contributes to c-jun induction and apoptosis in 4-hydroxynonenal-treated sympathetic neurons. J Neurosci Res **70:**665-70.
15. **Brynczka, C., and B. A. Merrick.** 2008. The p53 transcriptional target gene wnt7b contributes to NGF-inducible neurite outgrowth in neuronal PC12 cells. Differentiation **76:**795-808.

16. **Buchkovich, K. J., and E. B. Ziff.** 1994. Nerve growth factor regulates the expression and activity of p33cdk2 and p34cdc2 kinases in PC12 pheochromocytoma cells. Mol Biol Cell **5:**1225-41.
17. **Burstein, D. E., and L. A. Greene.** 1982. Nerve growth factor has both mitogenic and antimitogenic activity. Dev Biol **94:**477-82.
18. **Campisi, J., H. E. Gray, A. B. Pardee, M. Dean, and G. E. Sonenshein.** 1984. Cell-cycle control of c-myc but not c-ras expression is lost following chemical transformation. Cell **36:**241-7.
19. **Casha, S., W. R. Yu, and M. G. Fehlings.** 2005. FAS deficiency reduces apoptosis, spares axons and improves function after spinal cord injury. Exp Neurol **196:**390-400.
20. **Chang, L., Y. Jones, M. H. Ellisman, L. S. Goldstein, and M. Karin.** 2003. JNK1 is required for maintenance of neuronal microtubules and controls phosphorylation of microtubule-associated proteins. Dev Cell **4:**521-33.
21. **Chao, M. V.** 2003. Neurotrophins and their receptors: a convergence point for many signalling pathways. Nat Rev Neurosci **4:**299-309.
22. **Chen, J. T., D. H. Lu, C. P. Chia, D. Y. Ruan, K. Sabapathy, and Z. C. Xiao.** 2005. Impaired long-term potentiation in c-Jun N-terminal kinase 2-deficient mice. J Neurochem **93:**463-73.
23. **Chen, L., and X. Gao.** 2002. Neuronal apoptosis induced by endoplasmic reticulum stress. Neurochem Res **27:**891-8.
24. **Chen, N., M. Nomura, Q. B. She, W. Y. Ma, A. M. Bode, L. Wang, R. A. Flavell, and Z. Dong.** 2001. Suppression of skin tumorigenesis in c-Jun NH(2)-terminal kinase-2-deficient mice. Cancer Res **61:**3908-12.
25. **Chen, P., J. F. O'Neal, N. D. Ebelt, M. A. Cantrell, S. Mitra, A. Nasrazadani, T. L. Vandenbroek, L. E. Heasley, and C. L. Van Den Berg.** 2010. Jnk2 effects on tumor development, genetic instability and replicative stress in an oncogene-driven mouse mammary tumor model. PLoS One **5:**e10443.
26. **Chen, Y. R., X. Wang, D. Templeton, R. J. Davis, and T. H. Tan.** 1996. The role of c-Jun N-terminal kinase (JNK) in apoptosis induced by ultraviolet C and gamma radiation. Duration of JNK activation may determine cell death and proliferation. J Biol Chem **271:**31929-36.
27. **Chi, H., M. R. Sarkisian, P. Rakic, and R. A. Flavell.** 2005. Loss of mitogen-activated protein kinase kinase kinase 4 (MEKK4) results in enhanced apoptosis and defective neural tube development. Proc Natl Acad Sci U S A **102:**3846-51.
28. **Choukroun, G., R. Hajjar, S. Fry, F. del Monte, S. Haq, J. L. Guerrero, M. Picard, A. Rosenzweig, and T. Force.** 1999. Regulation of cardiac hypertrophy in vivo by the stress-activated protein kinases/c-Jun NH(2)-terminal kinases. J Clin Invest **104:**391-8.
29. **Chu, R., M. Upreti, W. X. Ding, X. M. Yin, and T. C. Chambers.** 2009. Regulation of Bax by c-Jun NH2-terminal kinase and Bcl-xL in vinblastine-induced apoptosis. Biochem Pharmacol **78:**241-8.
30. **Coffey, E. T., V. Hongisto, M. Dickens, R. J. Davis, and M. J. Courtney.** 2000. Dual roles for c-Jun N-terminal kinase in developmental and stress responses in cerebellar granule neurons. J Neurosci **20:**7602-13.
31. **Coffey, E. T., G. Smiciene, V. Hongisto, J. Cao, S. Brecht, T. Herdegen, and M. J. Courtney.** 2002. c-Jun N-terminal protein kinase (JNK) 2/3 is specifically activated by stress, mediating c-Jun activation, in the presence of constitutive JNK1 activity in cerebellar neurons. J Neurosci **22:**4335-45.
32. **Coller, H. A., C. Grandori, P. Tamayo, T. Colbert, E. S. Lander, R. N. Eisenman, and T. R. Golub.** 2000. Expression analysis with oligonucleotide microarrays reveals

that MYC regulates genes involved in growth, cell cycle, signaling, and adhesion. Proc Natl Acad Sci U S A **97:**3260-5.

33. **Colucci-D'Amato, G. L., A. D'Alessio, D. Califano, G. Cali, C. Rizzo, L. Nitsch, G. Santelli, and V. de Franciscis.** 2000. Abrogation of nerve growth factor-induced terminal differentiation by ret oncogene involves perturbation of nuclear translocation of ERK. J Biol Chem **275:**19306-14.
34. **Corvaja, N., A. Di Luzio, S. Biocca, A. Cattaneo, and P. Calissano.** 1982. Morphological and ultrastructural changes in PC12 pheochromocytoma cells induced by a combined treatment with NGF and taxol. Exp Cell Res **142:**385-95.
35. **Cui, J., S. Y. Han, C. Wang, W. Su, L. Harshyne, M. Holgado-Madruga, and A. J. Wong.** 2006. c-Jun NH(2)-terminal kinase 2alpha2 promotes the tumorigenicity of human glioblastoma cells. Cancer Res **66:**10024-31.
36. **Cui, J., Q. Wang, J. Wang, M. Lv, N. Zhu, Y. Li, J. Feng, B. Shen, and J. Zhang.** 2009. Basal c-Jun NH2-terminal protein kinase activity is essential for survival and proliferation of T-cell acute lymphoblastic leukemia cells. Mol Cancer Ther **8:**3214-22.
37. **Cullen, B. R.** 2006. Induction of stable RNA interference in mammalian cells. Gene Ther **13:**503-8.
38. **Cunningham, S. C., E. Gallmeier, T. Hucl, D. A. Dezentje, E. S. Calhoun, G. Falco, K. Abdelmohsen, M. Gorospe, and S. E. Kern.** 2006. Targeted deletion of MKK4 in cancer cells: a detrimental phenotype manifests as decreased experimental metastasis and suggests a counterweight to the evolution of tumor-suppressor loss. Cancer Res **66:**5560-4.
39. **Dalby, B., S. Cates, A. Harris, E. C. Ohki, M. L. Tilkins, P. J. Price, and V. C. Ciccarone.** 2004. Advanced transfection with Lipofectamine 2000 reagent: primary neurons, siRNA, and high-throughput applications. Methods **33:**95-103.
40. **Dang, C. V., K. A. O'Donnell, K. I. Zeller, T. Nguyen, R. C. Osthus, and F. Li.** 2006. The c-Myc target gene network. Semin Cancer Biol **16:**253-64.
41. **Das, G. C., D. Holiday, R. Gallardo, and C. Haas.** 2001. Taxol-induced cell cycle arrest and apoptosis: dose-response relationship in lung cancer cells of different wild-type p53 status and under isogenic condition. Cancer Lett **165:**147-53.
42. **Davis, R. J.** 1999. Signal transduction by the c-Jun N-terminal kinase. Biochem Soc Symp **64:**1-12.
43. **Dean, M., R. A. Levine, and J. Campisi.** 1986. c-myc regulation during retinoic acid-induced differentiation of F9 cells is posttranscriptional and associated with growth arrest. Mol Cell Biol **6:**518-24.
44. **Deng, X., L. Xiao, W. Lang, F. Gao, P. Ruvolo, and W. S. May, Jr.** 2001. Novel role for JNK as a stress-activated Bcl2 kinase. J Biol Chem **276:**23681-8.
45. **Deng, Y., X. Ren, L. Yang, Y. Lin, and X. Wu.** 2003. A JNK-dependent pathway is required for TNFalpha-induced apoptosis. Cell **115:**61-70.
46. **Derijard, B., J. Raingeaud, T. Barrett, I. H. Wu, J. Han, R. J. Ulevitch, and R. J. Davis.** 1995. Independent human MAP-kinase signal transduction pathways defined by MEK and MKK isoforms. Science **267:**682-5.
47. **Dhanasekaran, D. N., and E. P. Reddy.** 2008. JNK signaling in apoptosis. Oncogene **27:**6245-51.
48. **Di Giovanni, S., C. D. Knights, M. Rao, A. Yakovlev, J. Beers, J. Catania, M. L. Avantaggiati, and A. I. Faden.** 2006. The tumor suppressor protein p53 is required for neurite outgrowth and axon regeneration. Embo J **25:**4084-96.
49. **Dietrich, N., J. Thastrup, C. Holmberg, M. Gyrd-Hansen, N. Fehrenbacher, U. Lademann, M. Lerdrup, T. Herdegen, M. Jaattela, and T. Kallunki.** 2004. JNK2

mediates TNF-induced cell death in mouse embryonic fibroblasts via regulation of both caspase and cathepsin protease pathways. Cell Death Differ **11:**301-13.

50. **Dong, C., D. D. Yang, C. Tournier, A. J. Whitmarsh, J. Xu, R. J. Davis, and R. A. Flavell.** 2000. JNK is required for effector T-cell function but not for T-cell activation. Nature **405:**91-4.
51. **Donovan, N., E. B. Becker, Y. Konishi, and A. Bonni.** 2002. JNK phosphorylation and activation of BAD couples the stress-activated signaling pathway to the cell death machinery. J Biol Chem **277:**40944-9.
52. **Dragunow, M., R. Xu, M. Walton, A. Woodgate, P. Lawlor, G. A. MacGibbon, D. Young, H. Gibbons, J. Lipski, A. Muravlev, A. Pearson, and M. During.** 2000. c-Jun promotes neurite outgrowth and survival in PC12 cells. Brain Res Mol Brain Res **83:**20-33.
53. **el-Deiry, W. S., T. Tokino, V. E. Velculescu, D. B. Levy, R. Parsons, J. M. Trent, D. Lin, W. E. Mercer, K. W. Kinzler, and B. Vogelstein.** 1993. WAF1, a potential mediator of p53 tumor suppression. Cell **75:**817-25.
54. **Eminel, S., A. Klettner, L. Roemer, T. Herdegen, and V. Waetzig.** 2004. JNK2 translocates to the mitochondria and mediates cytochrome c release in PC12 cells in response to 6-hydroxydopamine. J Biol Chem **279:**55385-92.
55. **Eminel, S., L. Roemer, V. Waetzig, and T. Herdegen.** 2008. c-Jun N-terminal kinases trigger both degeneration and neurite outgrowth in primary hippocampal and cortical neurons. J Neurochem **104:**957-69.
56. **Engedal, N., C. G. Korkmaz, and F. Saatcioglu.** 2002. C-Jun N-terminal kinase is required for phorbol ester- and thapsigargin-induced apoptosis in the androgen responsive prostate cancer cell line LNCaP. Oncogene **21:**1017-27.
57. **Fabian, Z., M. Vecsernyes, M. Pap, and J. Szeberenyi.** 2006. The effects of a mutant p53 protein on the proliferation and differentiation of PC12 rat phaeochromocytoma cells. J Cell Biochem **99:**1431-41.
58. **Facchinetti, F., S. Furegato, S. Terrazzino, and A. Leon.** 2002. H(2)O(2) induces upregulation of Fas and Fas ligand expression in NGF-differentiated PC12 cells: modulation by cAMP. J Neurosci Res **69:**178-88.
59. **Fan, Y., H. Chen, B. Qiao, Z. Liu, L. Luo, Y. Wu, and Z. Yin.** 2007. c-Jun NH2-terminal kinase decreases ubiquitination and promotes stabilization of p21(WAF1/CIP1) in K562 cell. Biochem Biophys Res Commun **355:**263-8.
60. **Foltz, I. N., R. E. Gerl, J. S. Wieler, M. Luckach, R. A. Salmon, and J. W. Schrader.** 1998. Human mitogen-activated protein kinase kinase 7 (MKK7) is a highly conserved c-Jun N-terminal kinase/stress-activated protein kinase (JNK/SAPK) activated by environmental stresses and physiological stimuli. J Biol Chem **273:**9344-51.
61. **Fuchs, S. Y., V. Adler, M. R. Pincus, and Z. Ronai.** 1998. MEKK1/JNK signaling stabilizes and activates p53. Proc Natl Acad Sci U S A **95:**10541-6.
62. **Ganiatsas, S., L. Kwee, Y. Fujiwara, A. Perkins, T. Ikeda, M. A. Labow, and L. I. Zon.** 1998. SEK1 deficiency reveals mitogen-activated protein kinase cascade crossregulation and leads to abnormal hepatogenesis. Proc Natl Acad Sci U S A **95:**6881-6.
63. **Gao, M., T. Labuda, Y. Xia, E. Gallagher, D. Fang, Y. C. Liu, and M. Karin.** 2004. Jun turnover is controlled through JNK-dependent phosphorylation of the E3 ligase Itch. Science **306:**271-5.
64. **Gollapudi, L., and K. E. Neet.** 1997. Different mechanisms for inhibition of cell proliferation via cell cycle proteins in PC12 cells by nerve growth factor and staurosporine. J Neurosci Res **49:**461-74.

65. **Gong, Y., H. Sohn, L. Xue, G. L. Firestone, and L. F. Bjeldanes.** 2006. 3,3'-Diindolylmethane is a novel mitochondrial H(+)-ATP synthase inhibitor that can induce p21(Cip1/Waf1) expression by induction of oxidative stress in human breast cancer cells. Cancer Res **66:**4880-7.
66. **Grandori, C., S. M. Cowley, L. P. James, and R. N. Eisenman.** 2000. The Myc/Max/Mad network and the transcriptional control of cell behavior. Annu Rev Cell Dev Biol **16:**653-99.
67. **Greene, L. A.** 1978. Nerve growth factor prevents the death and stimulates the neuronal differentiation of clonal PC12 pheochromocytoma cells in serum-free medium. J Cell Biol **78:**747-55.
68. **Greene, L. A., and A. S. Tischler.** 1976. Establishment of a noradrenergic clonal line of rat adrenal pheochromocytoma cells which respond to nerve growth factor. Proc Natl Acad Sci U S A **73:**2424-8.
69. **Guo, C., and A. J. Whitmarsh.** 2008. The beta-arrestin-2 scaffold protein promotes c-Jun N-terminal kinase-3 activation by binding to its nonconserved N terminus. J Biol Chem **283:**15903-11.
70. **Gupta, S., D. Campbell, B. Derijard, and R. J. Davis.** 1995. Transcription factor ATF2 regulation by the JNK signal transduction pathway. Science **267:**389-93.
71. **Gurzov, E. N., L. Bakiri, J. M. Alfaro, E. F. Wagner, and M. Izquierdo.** 2008. Targeting c-Jun and JunB proteins as potential anticancer cell therapy. Oncogene **27:**641-52.
72. **Haeusgen, W., R. Boehm, Y. Zhao, T. Herdegen, and V. Waetzig.** 2009. Specific activities of individual c-Jun N-terminal kinases in the brain. Neuroscience **161:**951-9.
73. **Han, Z. S., H. Enslen, X. Hu, X. Meng, I. H. Wu, T. Barrett, R. J. Davis, and Y. T. Ip.** 1998. A conserved p38 mitogen-activated protein kinase pathway regulates Drosophila immunity gene expression. Mol Cell Biol **18:**3527-39.
74. **Harris, C. A., and E. M. Johnson, Jr.** 2001. BH3-only Bcl-2 family members are coordinately regulated by the JNK pathway and require Bax to induce apoptosis in neurons. J Biol Chem **276:**37754-60.
75. **Harwood, F. G., S. Kasibhatla, I. Petak, R. Vernes, D. R. Green, and J. A. Houghton.** 2000. Regulation of FasL by NF-kappaB and AP-1 in Fas-dependent thymineless death of human colon carcinoma cells. J Biol Chem **275:**10023-9.
76. **Hibi, M., A. Lin, T. Smeal, A. Minden, and M. Karin.** 1993. Identification of an oncoprotein- and UV-responsive protein kinase that binds and potentiates the c-Jun activation domain. Genes Dev **7:**2135-48.
77. **Hirosumi, J., G. Tuncman, L. Chang, C. Z. Gorgun, K. T. Uysal, K. Maeda, M. Karin, and G. S. Hotamisligil.** 2002. A central role for JNK in obesity and insulin resistance. Nature **420:**333-6.
78. **Ho, D. T., A. J. Bardwell, M. Abdollahi, and L. Bardwell.** 2003. A docking site in MKK4 mediates high affinity binding to JNK MAPKs and competes with similar docking sites in JNK substrates. J Biol Chem **278:**32662-72.
79. **Ho, D. T., A. J. Bardwell, S. Grewal, C. Iverson, and L. Bardwell.** 2006. Interacting JNK-docking sites in MKK7 promote binding and activation of JNK mitogen-activated protein kinases. J Biol Chem **281:**13169-79.
80. **Holland, P. M., M. Suzanne, J. S. Campbell, S. Noselli, and J. A. Cooper.** 1997. MKK7 is a stress-activated mitogen-activated protein kinase kinase functionally related to hemipterous. J Biol Chem **272:**24994-8.
81. **Hoozemans, J. J., J. Stieler, E. S. van Haastert, R. Veerhuis, A. J. Rozemuller, F. Baas, P. Eikelenboom, T. Arendt, and W. Scheper.** 2006. The unfolded protein

response affects neuronal cell cycle protein expression: implications for Alzheimer's disease pathogenesis. Exp Gerontol **41:**380-6.

82. **Hopewell, R., L. Li, D. MacGregor, C. Nerlov, and E. B. Ziff.** 1995. Regulation of cell proliferation and differentiation by Myc. J Cell Sci Suppl **19:**85-9.
83. **Hsu, S. P., P. Y. Ho, Y. C. Liang, Y. S. Ho, and W. S. Lee.** 2009. Involvement of the JNK activation in terbinafine-induced p21 up-regulation and DNA synthesis inhibition in human vascular endothelial cells. J Cell Biochem **108:**860-6.
84. **Hu, M. C., W. R. Qiu, and Y. P. Wang.** 1997. JNK1, JNK2 and JNK3 are p53 N-terminal serine 34 kinases. Oncogene **15:**2277-87.
85. **Huang, E. J., and L. F. Reichardt.** 2003. Trk receptors: roles in neuronal signal transduction. Annu Rev Biochem **72:**609-42.
86. **Hui, L., K. Zatloukal, H. Scheuch, E. Stepniak, and E. F. Wagner.** 2008. Proliferation of human HCC cells and chemically induced mouse liver cancers requires JNK1-dependent p21 downregulation. J Clin Invest **118:**3943-53.
87. **Hunot, S., M. Vila, P. Teismann, R. J. Davis, E. C. Hirsch, S. Przedborski, P. Rakic, and R. A. Flavell.** 2004. JNK-mediated induction of cyclooxygenase 2 is required for neurodegeneration in a mouse model of Parkinson's disease. Proc Natl Acad Sci U S A **101:**665-70.
88. **Jaeschke, A., M. Rincon, B. Doran, J. Reilly, D. Neuberg, D. L. Greiner, L. D. Shultz, A. A. Rossini, R. A. Flavell, and R. J. Davis.** 2005. Disruption of the Jnk2 (Mapk9) gene reduces destructive insulitis and diabetes in a mouse model of type I diabetes. Proc Natl Acad Sci U S A **102:**6931-5.
89. **Johnson, G. L., and K. Nakamura.** 2007. The c-jun kinase/stress-activated pathway: regulation, function and role in human disease. Biochim Biophys Acta **1773:**1341-8.
90. **Jung, E. J., and D. R. Kim.** 2010. Control of TrkA-induced cell death by JNK activation and differential expression of TrkA upon DNA damage. Mol Cells **30:**121-5.
91. **Kallunki, T., B. Su, I. Tsigelny, H. K. Sluss, B. Derijard, G. Moore, R. Davis, and M. Karin.** 1994. JNK2 contains a specificity-determining region responsible for efficient c-Jun binding and phosphorylation. Genes Dev **8:**2996-3007.
92. **Kaplan, D. R., B. L. Hempstead, D. Martin-Zanca, M. V. Chao, and L. F. Parada.** 1991. The trk proto-oncogene product: a signal transducing receptor for nerve growth factor. Science **252:**554-8.
93. **Kaplan, D. R., and R. M. Stephens.** 1994. Neurotrophin signal transduction by the Trk receptor. J Neurobiol **25:**1404-17.
94. **Kelkar, N., S. Gupta, M. Dickens, and R. J. Davis.** 2000. Interaction of a mitogen-activated protein kinase signaling module with the neuronal protein JIP3. Mol Cell Biol **20:**1030-43.
95. **Keramaris, E., J. L. Vanderluit, M. Bahadori, K. Mousavi, R. J. Davis, R. Flavell, R. S. Slack, and D. S. Park.** 2005. c-Jun N-terminal kinase 3 deficiency protects neurons from axotomy-induced death in vivo through mechanisms independent of c-Jun phosphorylation. J Biol Chem **280:**1132-41.
96. **Kharbanda, S., S. Saxena, K. Yoshida, P. Pandey, M. Kaneki, Q. Wang, K. Cheng, Y. N. Chen, A. Campbell, T. Sudha, Z. M. Yuan, J. Narula, R. Weichselbaum, C. Nalin, and D. Kufe.** 2000. Translocation of SAPK/JNK to mitochondria and interaction with Bcl-x(L) in response to DNA damage. J Biol Chem **275:**322-7.
97. **Kieran, M. W., S. Katz, B. Vail, L. I. Zon, and B. J. Mayer.** 1999. Concentration-dependent positive and negative regulation of a MAP kinase by a MAP kinase kinase. Oncogene **18:**6647-57.

98. **Kim, G. Y., S. E. Mercer, D. Z. Ewton, Z. Yan, K. Jin, and E. Friedman.** 2002. The stress-activated protein kinases p38 alpha and JNK1 stabilize p21(Cip1) by phosphorylation. J Biol Chem **277:**29792-802.

99. **Kim, H. L., D. J. Vander Griend, X. Yang, D. A. Benson, Z. Dubauskas, B. A. Yoshida, M. A. Chekmareva, Y. Ichikawa, M. H. Sokoloff, P. Zhan, T. Karrison, A. Lin, W. M. Stadler, T. Ichikawa, M. A. Rubin, and C. W. Rinker-Schaeffer.** 2001. Mitogen-activated protein kinase kinase 4 metastasis suppressor gene expression is inversely related to histological pattern in advancing human prostatic cancers. Cancer Res **61:**2833-7.

100. **Kishimoto, H., K. Nakagawa, T. Watanabe, D. Kitagawa, H. Momose, J. Seo, G. Nishitai, N. Shimizu, S. Ohata, S. Tanemura, S. Asaka, T. Goto, H. Fukushi, H. Yoshida, A. Suzuki, T. Sasaki, T. Wada, J. M. Penninger, H. Nishina, and T. Katada.** 2003. Different properties of SEK1 and MKK7 in dual phosphorylation of stress-induced activated protein kinase SAPK/JNK in embryonic stem cells. J Biol Chem **278:**16595-601.

101. **Kita, Y., K. D. Kimura, M. Kobayashi, S. Ihara, K. Kaibuchi, S. Kuroda, M. Ui, H. Iba, H. Konishi, U. Kikkawa, S. Nagata, and Y. Fukui.** 1998. Microinjection of activated phosphatidylinositol-3 kinase induces process outgrowth in rat PC12 cells through the Rac-JNK signal transduction pathway. J Cell Sci **111 (Pt 7):**907-15.

102. **Klein, R., S. Q. Jing, V. Nanduri, E. O'Rourke, and M. Barbacid.** 1991. The trk proto-oncogene encodes a receptor for nerve growth factor. Cell **65:**189-97.

103. **Komarov, P. G., E. A. Komarova, R. V. Kondratov, K. Christov-Tselkov, J. S. Coon, M. V. Chernov, and A. V. Gudkov.** 1999. A chemical inhibitor of p53 that protects mice from the side effects of cancer therapy. Science **285:**1733-7.

104. **Kuan, C. Y., D. D. Yang, D. R. Samanta Roy, R. J. Davis, P. Rakic, and R. A. Flavell.** 1999. The Jnk1 and Jnk2 protein kinases are required for regional specific apoptosis during early brain development. Neuron **22:**667-76.

105. **Kukekov, N. V., Z. Xu, and L. A. Greene.** 2006. Direct interaction of the molecular scaffolds POSH and JIP is required for apoptotic activation of JNKs. J Biol Chem **281:**15517-24.

106. **Kyriakis, J. M., and J. Avruch.** 2001. Mammalian mitogen-activated protein kinase signal transduction pathways activated by stress and inflammation. Physiol Rev **81:**807-69.

107. **Kyriakis, J. M., P. Banerjee, E. Nikolakaki, T. Dai, E. A. Rubie, M. F. Ahmad, J. Avruch, and J. R. Woodgett.** 1994. The stress-activated protein kinase subfamily of c-Jun kinases. Nature **369:**156-60.

108. **Lawlor, M. A., and D. R. Alessi.** 2001. PKB/Akt: a key mediator of cell proliferation, survival and insulin responses? J Cell Sci **114:**2903-10.

109. **Lee, C. M., D. Onesime, C. D. Reddy, N. Dhanasekaran, and E. P. Reddy.** 2002. JLP: A scaffolding protein that tethers JNK/p38MAPK signaling modules and transcription factors. Proc Natl Acad Sci U S A **99:**14189-94.

110. **Lee, J. K., W. S. Hwang, Y. D. Lee, and P. L. Han.** 1999. Dynamic expression of SEK1 suggests multiple roles of the gene during embryogenesis and in adult brain of mice. Brain Res Mol Brain Res **66:**133-40.

111. **Lee, T. L., Y. C. Shyu, P. H. Hsu, C. W. Chang, S. C. Wen, W. Y. Hsiao, M. D. Tsai, and C. K. Shen.** JNK-mediated turnover and stabilization of the transcription factor p45/NF-E2 during differentiation of murine erythroleukemia cells. Proc Natl Acad Sci U S A **107:**52-7.

112. **Lee, Y. M., and P. Sicinski.** 2006. Targeting cyclins and cyclin-dependent kinases in cancer: lessons from mice, hopes for therapeutic applications in human. Cell Cycle **5:**2110-4.
113. **Lei, K., and R. J. Davis.** 2003. JNK phosphorylation of Bim-related members of the Bcl2 family induces Bax-dependent apoptosis. Proc Natl Acad Sci U S A **100:**2432-7.
114. **Leppa, S., R. Saffrich, W. Ansorge, and D. Bohmann.** 1998. Differential regulation of c-Jun by ERK and JNK during PC12 cell differentiation. Embo J **17:**4404-13.
115. **Lin, A., A. Minden, H. Martinetto, F. X. Claret, C. Lange-Carter, F. Mercurio, G. L. Johnson, and M. Karin.** 1995. Identification of a dual specificity kinase that activates the Jun kinases and p38-Mpk2. Science **268:**286-90.
116. **Lin, J., C. Reichner, X. Wu, and A. J. Levine.** 1996. Analysis of wild-type and mutant p21WAF-1 gene activities. Mol Cell Biol **16:**1786-93.
117. **Lindenboim, L., R. Haviv, and R. Stein.** 1998. Bcl-xL inhibits different apoptotic pathways in rat PC12 cells. Neurosci Lett **253:**37-40.
118. **Long, B. H., and C. R. Fairchild.** 1994. Paclitaxel inhibits progression of mitotic cells to G1 phase by interference with spindle formation without affecting other microtubule functions during anaphase and telephase. Cancer Res **54:**4355-61.
119. **Madhavan, S., A. K. Singh, and R. K. Maheshawari.** 2000. Tunicamycin enhances the anticellular activity of interferon by inhibiting G1/S phase progression in 3T3 cells. J Interferon Cytokine Res **20:**281-90.
120. **Manning, B. D., and L. C. Cantley.** 2007. AKT/PKB signaling: navigating downstream. Cell **129:**1261-74.
121. **Matsuura, H., H. Nishitoh, K. Takeda, A. Matsuzawa, T. Amagasa, M. Ito, K. Yoshioka, and H. Ichijo.** 2002. Phosphorylation-dependent scaffolding role of JSAP1/JIP3 in the ASK1-JNK signaling pathway. A new mode of regulation of the MAP kinase cascade. J Biol Chem **277:**40703-9.
122. **Medrano, E. E., S. Im, F. Yang, and Z. A. Abdel-Malek.** 1995. Ultraviolet B light induces G1 arrest in human melanocytes by prolonged inhibition of retinoblastoma protein phosphorylation associated with long-term expression of the p21Waf-1/SDI-1/Cip-1 protein. Cancer Res **55:**4047-52.
123. **Michael, L., J. Swantek, and M. J. Robinson.** 2006. Cloning and expression of human mitogen-activated protein kinase kinase 7gamma1. Biochem Biophys Res Commun **341:**679-83.
124. **Mielke, K., A. Damm, D. D. Yang, and T. Herdegen.** 2000. Selective expression of JNK isoforms and stress-specific JNK activity in different neural cell lines. Brain Res Mol Brain Res **75:**128-37.
125. **Milne, D. M., L. E. Campbell, D. G. Campbell, and D. W. Meek.** 1995. p53 is phosphorylated in vitro and in vivo by an ultraviolet radiation-induced protein kinase characteristic of the c-Jun kinase, JNK1. J Biol Chem **270:**5511-8.
126. **Molton, S. A., D. E. Todd, and S. J. Cook.** 2003. Selective activation of the c-Jun N-terminal kinase (JNK) pathway fails to elicit Bax activation or apoptosis unless the phosphoinositide 3'-kinase (PI3K) pathway is inhibited. Oncogene **22:**4690-701.
127. **Mooney, L. M., and A. J. Whitmarsh.** 2004. Docking interactions in the c-Jun N-terminal kinase pathway. J Biol Chem **279:**11843-52.
128. **Moriguchi, T., H. Kawasaki, S. Matsuda, Y. Gotoh, and E. Nishida.** 1995. Evidence for multiple activators for stress-activated protein kinase/c-Jun amino-terminal kinases. Existence of novel activators. J Biol Chem **270:**12969-72.
129. **Moriguchi, T., F. Toyoshima, N. Masuyama, H. Hanafusa, Y. Gotoh, and E. Nishida.** 1997. A novel SAPK/JNK kinase, MKK7, stimulated by TNFalpha and cellular stresses. Embo J **16:**7045-53.

130. **Nakayama, K., N. Nakayama, B. Davidson, H. Katabuchi, R. J. Kurman, V. E. Velculescu, M. Shih Ie, and T. L. Wang.** 2006. Homozygous deletion of MKK4 in ovarian serous carcinoma. Cancer Biol Ther **5:**630-4.
131. **Namikawa, K., M. Honma, K. Abe, M. Takeda, K. Mansur, T. Obata, A. Miwa, H. Okado, and H. Kiyama.** 2000. Akt/protein kinase B prevents injury-induced motoneuron death and accelerates axonal regeneration. J Neurosci **20:**2875-86.
132. **Newbern, J., A. Taylor, M. Robinson, M. O. Lively, and C. E. Milligan.** 2007. c-Jun N-terminal kinase signaling regulates events associated with both health and degeneration in motoneurons. Neuroscience **147:**680-92.
133. **Nishina, H., K. D. Fischer, L. Radvanyi, A. Shahinian, R. Hakem, E. A. Rubie, A. Bernstein, T. W. Mak, J. R. Woodgett, and J. M. Penninger.** 1997. Stress-signalling kinase Sek1 protects thymocytes from apoptosis mediated by CD95 and CD3. Nature **385:**350-3.
134. **Nishitai, G., and M. Matsuoka.** 2008. Differential regulation of HSP70 expression by the JNK kinases SEK1 and MKK7 in mouse embryonic stem cells treated with cadmium. J Cell Biochem **104:**1771-80.
135. **Noguchi, K., C. Kitanaka, H. Yamana, A. Kokubu, T. Mochizuki, and Y. Kuchino.** 1999. Regulation of c-Myc through phosphorylation at Ser-62 and Ser-71 by c-Jun N-terminal kinase. J Biol Chem **274:**32580-7.
136. **Oleinik, N. V., N. I. Krupenko, and S. A. Krupenko.** 2007. Cooperation between JNK1 and JNK2 in activation of p53 apoptotic pathway. Oncogene **26:**7222-30.
137. **Patel, R., B. Bartosch, and J. L. Blank.** 1998. p21WAF1 is dynamically associated with JNK in human T-lymphocytes during cell cycle progression. J Cell Sci **111 (Pt 15):**2247-55.
138. **Perfettini, J. L., M. Castedo, R. Nardacci, F. Ciccosanti, P. Boya, T. Roumier, N. Larochette, M. Piacentini, and G. Kroemer.** 2005. Essential role of p53 phosphorylation by p38 MAPK in apoptosis induction by the HIV-1 envelope. J Exp Med **201:**279-89.
139. **Pina, B., and P. Suau.** 1987. Changes in histones H2A and H3 variant composition in differentiating and mature rat brain cortical neurons. Dev Biol **123:**51-8.
140. **Poluha, W., C. M. Schonhoff, K. S. Harrington, M. B. Lachyankar, N. E. Crosbie, D. A. Bulseco, and A. H. Ross.** 1997. A novel, nerve growth factor-activated pathway involving nitric oxide, p53, and p21WAF1 regulates neuronal differentiation of PC12 cells. J Biol Chem **272:**24002-7.
141. **Potapova, O., M. Gorospe, R. H. Dougherty, N. M. Dean, W. A. Gaarde, and N. J. Holbrook.** 2000. Inhibition of c-Jun N-terminal kinase 2 expression suppresses growth and induces apoptosis of human tumor cells in a p53-dependent manner. Mol Cell Biol **20:**1713-22.
142. **Putcha, G. V., S. Le, S. Frank, C. G. Besirli, K. Clark, B. Chu, S. Alix, R. J. Youle, A. LaMarche, A. C. Maroney, and E. M. Johnson, Jr.** 2003. JNK-mediated BIM phosphorylation potentiates BAX-dependent apoptosis. Neuron **38:**899-914.
143. **Putcha, G. V., K. L. Moulder, J. P. Golden, P. Bouillet, J. A. Adams, A. Strasser, and E. M. Johnson.** 2001. Induction of BIM, a proapoptotic BH3-only BCL-2 family member, is critical for neuronal apoptosis. Neuron **29:**615-28.
144. **Qui, M. S., and S. H. Green.** 1992. PC12 cell neuronal differentiation is associated with prolonged p21ras activity and consequent prolonged ERK activity. Neuron **9:**705-17.
145. **Raman, M., W. Chen, and M. H. Cobb.** 2007. Differential regulation and properties of MAPKs. Oncogene **26:**3100-12.

146. **Rankin, S. L., C. S. Guy, and K. M. Mearow.** 2005. TrkA NGF receptor plays a role in the modulation of p75NTR expression. Neurosci Lett **383:**305-10.
147. **Reynolds, C. H., M. A. Utton, G. M. Gibb, A. Yates, and B. H. Anderton.** 1997. Stress-activated protein kinase/c-jun N-terminal kinase phosphorylates tau protein. J Neurochem **68:**1736-44.
148. **Robbins, D. J., M. Cheng, E. Zhen, C. A. Vanderbilt, L. A. Feig, and M. H. Cobb.** 1992. Evidence for a Ras-dependent extracellular signal-regulated protein kinase (ERK) cascade. Proc Natl Acad Sci U S A **89:**6924-8.
149. **Rubenstein, R., C. L. Scalici, M. C. Papini, S. M. Callahan, and R. I. Carp.** 1990. Further characterization of scrapie replication in PC12 cells. J Gen Virol **71 (Pt 4):**825-31.
150. **Rudkin, B. B., P. Lazarovici, B. Z. Levi, Y. Abe, K. Fujita, and G. Guroff.** 1989. Cell cycle-specific action of nerve growth factor in PC12 cells: differentiation without proliferation. Embo J **8:**3319-25.
151. **Sabapathy, K., K. Hochedlinger, S. Y. Nam, A. Bauer, M. Karin, and E. F. Wagner.** 2004. Distinct roles for JNK1 and JNK2 in regulating JNK activity and c-Jun-dependent cell proliferation. Mol Cell **15:**713-25.
152. **Sabapathy, K., W. Jochum, K. Hochedlinger, L. Chang, M. Karin, and E. F. Wagner.** 1999. Defective neural tube morphogenesis and altered apoptosis in the absence of both JNK1 and JNK2. Mech Dev **89:**115-24.
153. **Sakurai, T., S. Maeda, L. Chang, and M. Karin.** 2006. Loss of hepatic NF-kappa B activity enhances chemical hepatocarcinogenesis through sustained c-Jun N-terminal kinase 1 activation. Proc Natl Acad Sci U S A **103:**10544-51.
154. **Sanchez, I., R. T. Hughes, B. J. Mayer, K. Yee, J. R. Woodgett, J. Avruch, J. M. Kyriakis, and L. I. Zon.** 1994. Role of SAPK/ERK kinase-1 in the stress-activated pathway regulating transcription factor c-Jun. Nature **372:**794-8.
155. **Sasaki, T., T. Wada, H. Kishimoto, J. Irie-Sasaki, G. Matsumoto, T. Goto, Z. Yao, A. Wakeham, T. W. Mak, A. Suzuki, S. K. Cho, J. C. Zuniga-Pflucker, A. J. Oliveira-dos-Santos, T. Katada, H. Nishina, and J. M. Penninger.** 2001. The stress kinase mitogen-activated protein kinase kinase (MKK)7 is a negative regulator of antigen receptor and growth factor receptor-induced proliferation in hematopoietic cells. J Exp Med **194:**757-68.
156. **Schroeter, H., C. S. Boyd, R. Ahmed, J. P. Spencer, R. F. Duncan, C. Rice-Evans, and E. Cadenas.** 2003. c-Jun N-terminal kinase (JNK)-mediated modulation of brain mitochondria function: new target proteins for JNK signalling in mitochondrion-dependent apoptosis. Biochem J **372:**359-69.
157. **Seger, R., and E. G. Krebs.** 1995. The MAPK signaling cascade. Faseb J **9:**726-35.
158. **Servant, G., D. T. Dudley, E. Escher, and G. Guillemette.** 1996. Analysis of the role of N-glycosylation in cell-surface expression and binding properties of angiotensin II type-2 receptor of rat pheochromocytoma cells. Biochem J **313 (Pt 1):**297-304.
159. **Shaulian, E.** 2010. AP-1--The Jun proteins: Oncogenes or tumor suppressors in disguise? Cell Signal **22:**894-9.
160. **Shi, R., Q. Huang, X. Zhu, Y. B. Ong, B. Zhao, J. Lu, C. N. Ong, and H. M. Shen.** 2007. Luteolin sensitizes the anticancer effect of cisplatin via c-Jun NH2-terminal kinase-mediated p53 phosphorylation and stabilization. Mol Cancer Ther **6:**1338-47.
161. **Shim, J., H. Lee, J. Park, H. Kim, and E. J. Choi.** 1996. A non-enzymatic p21 protein inhibitor of stress-activated protein kinases. Nature **381:**804-6.

162. **Shimoke, K., H. Amano, S. Kishi, H. Uchida, M. Kudo, and T. Ikeuchi.** 2004. Nerve growth factor attenuates endoplasmic reticulum stress-mediated apoptosis via suppression of caspase-12 activity. J Biochem **135:**439-46.
163. **Sluss, H. K., Z. Han, T. Barrett, D. C. Goberdhan, C. Wilson, R. J. Davis, and Y. T. Ip.** 1996. A JNK signal transduction pathway that mediates morphogenesis and an immune response in Drosophila. Genes Dev **10:**2745-58.
164. **Song, J. J., and Y. J. Lee.** 2005. Cross-talk between JIP3 and JIP1 during glucose deprivation: SEK1-JNK2 and Akt1 act as mediators. J Biol Chem **280:**26845-55.
165. **Steinman, R. A., B. Hoffman, A. Iro, C. Guillouf, D. A. Liebermann, and M. E. el-Houseini.** 1994. Induction of p21 (WAF-1/CIP1) during differentiation. Oncogene **9:**3389-96.
166. **Stepniak, E., R. Ricci, R. Eferl, G. Sumara, I. Sumara, M. Rath, L. Hui, and E. F. Wagner.** 2006. c-Jun/AP-1 controls liver regeneration by repressing p53/p21 and p38 MAPK activity. Genes Dev **20:**2306-14.
167. **Su, G. H., J. J. Song, E. A. Repasky, M. Schutte, and S. E. Kern.** 2002. Mutation rate of MAP2K4/MKK4 in breast carcinoma. Hum Mutat **19:**81.
168. **Su, Q. J., X. W. Chen, Z. B. Chen, and S. G. Sun.** 2008. Involvement of ERK1/2 and p38 MAPK in up-regulation of 14-3-3 protein induced by hydrogen peroxide preconditioning in PC12 cells. Neurosci Bull **24:**244-50.
169. **Swat, W., K. Fujikawa, S. Ganiatsas, D. Yang, R. J. Xavier, N. L. Harris, L. Davidson, R. Ferrini, R. J. Davis, M. A. Labow, R. A. Flavell, L. I. Zon, and F. W. Alt.** 1998. SEK1/MKK4 is required for maintenance of a normal peripheral lymphoid compartment but not for lymphocyte development. Immunity **8:**625-34.
170. **Tabakman, R., H. Jiang, I. Shahar, H. Arien-Zakay, R. A. Levine, and P. Lazarovici.** 2005. Neuroprotection by NGF in the PC12 in vitro OGD model: involvement of mitogen-activated protein kinases and gene expression. Ann N Y Acad Sci **1053:**84-96.
171. **Tafolla, E., S. Wang, B. Wong, J. Leong, and Y. L. Kapila.** 2005. JNK1 and JNK2 oppositely regulate p53 in signaling linked to apoptosis triggered by an altered fibronectin matrix: JNK links FAK and p53. J Biol Chem **280:**19992-9.
172. **Takadera, T., R. Yoshikawa, and T. Ohyashiki.** 2006. Thapsigargin-induced apoptosis was prevented by glycogen synthase kinase-3 inhibitors in PC12 cells. Neurosci Lett **408:**124-8.
173. **Takekawa, M., K. Tatebayashi, and H. Saito.** 2005. Conserved docking site is essential for activation of mammalian MAP kinase kinases by specific MAP kinase kinase kinases. Mol Cell **18:**295-306.
174. **Tararuk, T., N. Ostman, W. Li, B. Bjorkblom, A. Padzik, J. Zdrojewska, V. Hongisto, T. Herdegen, W. Konopka, M. J. Courtney, and E. T. Coffey.** 2006. JNK1 phosphorylation of SCG10 determines microtubule dynamics and axodendritic length. J Cell Biol **173:**265-77.
175. **Teng, D. H., W. L. Perry, 3rd, J. K. Hogan, M. Baumgard, R. Bell, S. Berry, T. Davis, D. Frank, C. Frye, T. Hattier, R. Hu, S. Jammulapati, T. Janecki, A. Leavitt, J. T. Mitchell, R. Pero, D. Sexton, M. Schroeder, P. H. Su, B. Swedlund, J. M. Kyriakis, J. Avruch, P. Bartel, A. K. Wong, S. V. Tavtigian, and et al.** 1997. Human mitogen-activated protein kinase kinase 4 as a candidate tumor suppressor. Cancer Res **57:**4177-82.
176. **Tischler, A. S., L. A. Greene, P. W. Kwan, and V. W. Slayton.** 1983. Ultrastructural effects of nerve growth factor on PC 12 pheochromocytoma cells in spinner culture. Cell Tissue Res **228:**641-8.

177. **Tomaselli, B., S. Z. Nedden, V. Podhraski, and G. Baier-Bitterlich.** 2008. p42/44 MAPK is an essential effector for purine nucleoside-mediated neuroprotection of hypoxic PC12 cells and primary cerebellar granule neurons. Mol Cell Neurosci **38:**559-68.
178. **Tournier, C., C. Dong, T. K. Turner, S. N. Jones, R. A. Flavell, and R. J. Davis.** 2001. MKK7 is an essential component of the JNK signal transduction pathway activated by proinflammatory cytokines. Genes Dev **15:**1419-26.
179. **Tournier, C., P. Hess, D. D. Yang, J. Xu, T. K. Turner, A. Nimnual, D. Bar-Sagi, S. N. Jones, R. A. Flavell, and R. J. Davis.** 2000. Requirement of JNK for stress-induced activation of the cytochrome c-mediated death pathway. Science **288:**870-4.
180. **Tournier, C., A. J. Whitmarsh, J. Cavanagh, T. Barrett, and R. J. Davis.** 1997. Mitogen-activated protein kinase kinase 7 is an activator of the c-Jun NH2-terminal kinase. Proc Natl Acad Sci U S A **94:**7337-42.
181. **Tournier, C., A. J. Whitmarsh, J. Cavanagh, T. Barrett, and R. J. Davis.** 1999. The MKK7 gene encodes a group of c-Jun NH2-terminal kinase kinases. Mol Cell Biol **19:**1569-81.
182. **Tsuiki, H., M. Tnani, I. Okamoto, L. C. Kenyon, D. R. Emlet, M. Holgado-Madruga, I. S. Lanham, C. J. Joynes, K. T. Vo, and A. J. Wong.** 2003. Constitutively active forms of c-Jun NH2-terminal kinase are expressed in primary glial tumors. Cancer Res **63:**250-5.
183. **Tsukada, T., Y. Tomooka, S. Takai, Y. Ueda, S. Nishikawa, T. Yagi, T. Tokunaga, N. Takeda, Y. Suda, S. Abe, and et al.** 1993. Enhanced proliferative potential in culture of cells from p53-deficient mice. Oncogene **8:**3313-22.
184. **Vaghefi, H., A. L. Hughes, and K. E. Neet.** 2004. Nerve growth factor withdrawal-mediated apoptosis in naive and differentiated PC12 cells through p53/caspase-3-dependent and -independent pathways. J Biol Chem **279:**15604-14.
185. **Vaghefi, H., and K. E. Neet.** 2004. Deacetylation of p53 after nerve growth factor treatment in PC12 cells as a post-translational modification mechanism of neurotrophin-induced tumor suppressor activation. Oncogene **23:**8078-87.
186. **Vaque, J. P., B. Fernandez-Garcia, P. Garcia-Sanz, N. Ferrandiz, G. Bretones, F. Calvo, P. Crespo, M. C. Marin, and J. Leon.** 2008. c-Myc inhibits Ras-mediated differentiation of pheochromocytoma cells by blocking c-Jun up-regulation. Mol Cancer Res **6:**325-39.
187. **Wada, T., N. Joza, H. Y. Cheng, T. Sasaki, I. Kozieradzki, K. Bachmaier, T. Katada, M. Schreiber, E. F. Wagner, H. Nishina, and J. M. Penninger.** 2004. MKK7 couples stress signalling to G2/M cell-cycle progression and cellular senescence. Nat Cell Biol **6:**215-26.
188. **Wada, T., K. Nakagawa, T. Watanabe, G. Nishitai, J. Seo, H. Kishimoto, D. Kitagawa, T. Sasaki, J. M. Penninger, H. Nishina, and T. Katada.** 2001. Impaired synergistic activation of stress-activated protein kinase SAPK/JNK in mouse embryonic stem cells lacking SEK1/MKK4: different contribution of SEK2/MKK7 isoforms to the synergistic activation. J Biol Chem **276:**30892-7.
189. **Waetzig, V., and T. Herdegen.** 2003. The concerted signaling of ERK1/2 and JNKs is essential for PC12 cell neuritogenesis and converges at the level of target proteins. Mol Cell Neurosci **24:**238-49.
190. **Waetzig, V., and T. Herdegen.** 2005. MEKK1 controls neurite regrowth after experimental injury by balancing ERK1/2 and JNK2 signaling. Mol Cell Neurosci **30:**67-78.

191. **Waetzig, V., and T. Herdegen.** 2003. A single c-Jun N-terminal kinase isoform (JNK3-p54) is an effector in both neuronal differentiation and cell death. J Biol Chem **278:**567-72.
192. **Waetzig, V., K. Loose, W. Haeusgen, and T. Herdegen.** 2008. c-Jun N-terminal kinases mediate Fas-induced neurite regeneration in PC12 cells. Biochem Pharmacol **76:**1476-84.
193. **Waetzig, V., U. Wacker, W. Haeusgen, B. Bjorkblom, M. J. Courtney, E. T. Coffey, and T. Herdegen.** 2009. Concurrent protective and destructive signaling of JNK2 in neuroblastoma cells. Cell Signal **21:**873-80.
194. **Wang, L., Y. Pan, and J. L. Dai.** 2004. Evidence of MKK4 pro-oncogenic activity in breast and pancreatic tumors. Oncogene **23:**5978-85.
195. **Welsh, C. F., K. Roovers, J. Villanueva, Y. Liu, M. A. Schwartz, and R. K. Assoian.** 2001. Timing of cyclin D1 expression within G1 phase is controlled by Rho. Nat Cell Biol **3:**950-7.
196. **Weston, C. R., A. Wong, J. P. Hall, M. E. Goad, R. A. Flavell, and R. J. Davis.** 2004. The c-Jun NH2-terminal kinase is essential for epidermal growth factor expression during epidermal morphogenesis. Proc Natl Acad Sci U S A **101:**14114-9.
197. **Whitfield, J., S. J. Neame, L. Paquet, O. Bernard, and J. Ham.** 2001. Dominant-negative c-Jun promotes neuronal survival by reducing BIM expression and inhibiting mitochondrial cytochrome c release. Neuron **29:**629-43.
198. **Whitmarsh, A. J., J. Cavanagh, C. Tournier, J. Yasuda, and R. J. Davis.** 1998. A mammalian scaffold complex that selectively mediates MAP kinase activation. Science **281:**1671-4.
199. **Widmann, C., S. Gibson, M. B. Jarpe, and G. L. Johnson.** 1999. Mitogen-activated protein kinase: conservation of a three-kinase module from yeast to human. Physiol Rev **79:**143-80.
200. **Wolter, S., J. F. Mushinski, A. M. Saboori, K. Resch, and M. Kracht.** 2002. Inducible expression of a constitutively active mutant of mitogen-activated protein kinase kinase 7 specifically activates c-JUN NH2-terminal protein kinase, alters expression of at least nine genes, and inhibits cell proliferation. J Biol Chem **277:**3576-84.
201. **Wu, B. Y., E. J. Fodor, R. H. Edwards, and W. J. Rutter.** 1989. Nerve growth factor induces the proto-oncogene c-jun in PC12 cells. J Biol Chem **264:**9000-3.
202. **Wu, G. S.** 2004. The functional interactions between the p53 and MAPK signaling pathways. Cancer Biol Ther **3:**156-61.
203. **Wu, H., M. Wade, L. Krall, J. Grisham, Y. Xiong, and T. Van Dyke.** 1996. Targeted in vivo expression of the cyclin-dependent kinase inhibitor p21 halts hepatocyte cell-cycle progression, postnatal liver development and regeneration. Genes Dev **10:**245-60.
204. **Xia, Y., Z. Wu, B. Su, B. Murray, and M. Karin.** 1998. JNKK1 organizes a MAP kinase module through specific and sequential interactions with upstream and downstream components mediated by its amino-terminal extension. Genes Dev **12:**3369-81.
205. **Xin, W., K. J. Yun, F. Ricci, M. Zahurak, W. Qiu, G. H. Su, C. J. Yeo, R. H. Hruban, S. E. Kern, and C. A. Iacobuzio-Donahue.** 2004. MAP2K4/MKK4 expression in pancreatic cancer: genetic validation of immunohistochemistry and relationship to disease course. Clin Cancer Res **10:**8516-20.
206. **Yamada, S. D., J. A. Hickson, Y. Hrobowski, D. J. Vander Griend, D. Benson, A. Montag, T. Karrison, D. Huo, J. Rutgers, S. Adams, and C. W. Rinker-Schaeffer.**

2002. Mitogen-activated protein kinase kinase 4 (MKK4) acts as a metastasis suppressor gene in human ovarian carcinoma. Cancer Res **62:**6717-23.

207. **Yan, G. Z., and E. B. Ziff.** 1997. Nerve growth factor induces transcription of the p21 WAF1/CIP1 and cyclin D1 genes in PC12 cells by activating the Sp1 transcription factor. J Neurosci **17:**6122-32.
208. **Yang, D. D., C. Y. Kuan, A. J. Whitmarsh, M. Rincon, T. S. Zheng, R. J. Davis, P. Rakic, and R. A. Flavell.** 1997. Absence of excitotoxicity-induced apoptosis in the hippocampus of mice lacking the Jnk3 gene. Nature **389:**865-70.
209. **Yang, J., L. New, Y. Jiang, J. Han, and B. Su.** 1998. Molecular cloning and characterization of a human protein kinase that specifically activates c-Jun N-terminal kinase. Gene **212:**95-102.
210. **Yao, Z., K. Diener, X. S. Wang, M. Zukowski, G. Matsumoto, G. Zhou, R. Mo, T. Sasaki, H. Nishina, C. C. Hui, T. H. Tan, J. P. Woodgett, and J. M. Penninger.** 1997. Activation of stress-activated protein kinases/c-Jun N-terminal protein kinases (SAPKs/JNKs) by a novel mitogen-activated protein kinase kinase. J Biol Chem **272:**32378-83.
211. **Yashar, B. M., C. Kelley, K. Yee, B. Errede, and L. I. Zon.** 1993. Novel members of the mitogen-activated protein kinase activator family in Xenopus laevis. Mol Cell Biol **13:**5738-48.
212. **Yasuda, J., A. J. Whitmarsh, J. Cavanagh, M. Sharma, and R. J. Davis.** 1999. The JIP group of mitogen-activated protein kinase scaffold proteins. Mol Cell Biol **19:**7245-54.
213. **Yoneda, T., K. Imaizumi, K. Oono, D. Yui, F. Gomi, T. Katayama, and M. Tohyama.** 2001. Activation of caspase-12, an endoplastic reticulum (ER) resident caspase, through tumor necrosis factor receptor-associated factor 2-dependent mechanism in response to the ER stress. J Biol Chem **276:**13935-40.
214. **Yoshida, B. A., Z. Dubauskas, M. A. Chekmareva, T. R. Christiano, W. M. Stadler, and C. W. Rinker-Schaeffer.** 1999. Mitogen-activated protein kinase kinase 4/stress-activated protein/Erk kinase 1 (MKK4/SEK1), a prostate cancer metastasis suppressor gene encoded by human chromosome 17. Cancer Res **59:**5483-7.
215. **Zentrich, E., S. Y. Han, L. Pessoa-Brandao, L. Butterfield, and L. E. Heasley.** 2002. Collaboration of JNKs and ERKs in nerve growth factor regulation of the neurofilament light chain promoter in PC12 cells. J Biol Chem **277:**4110-8.
216. **Zhao, Y., and T. Herdegen.** 2009. Cerebral ischemia provokes a profound exchange of activated JNK isoforms in brain mitochondria. Mol Cell Neurosci **41:**186-95.
217. **Zou, H., Q. Li, S. C. Lin, Z. Wu, J. Han, and Z. Ye.** 2007. Differential requirement of MKK4 and MKK7 in JNK activation by distinct scaffold proteins. FEBS Lett **581:**196-202.

8 Appendix

8.1 Abbreviations and symbols

A_{260}, A_{280}, A_{595}	absorbance at 260, 280 or 595 nm, respectively
Ala	alanine (A)
aa	amino acid(s)
AKT	protein kinase B
AP-1	activator protein 1
APS	ammonium persulphate
ASK	apoptosis signal-regulating kinase
ATF-2	activating transcription factor 2
ATP	adenosine triphosphate
Bad	Bcl-2-associated death promoter
Bax	Bcl-2-associated X protein
Bcl-2	B cell lymphoma 2
Bim	Bcl-2-interacting mediator of cell death
bp	base pairs
BrdU	5-bromo-2-deoxyuridine
BS	blocking solution
BSA	bovine serum albumin
bsk	basket
CD	common docking domain
Cdk	cyclin-dependent kinase
cDNA	complementary DNA
CHAPS	3-[(3-cholamindopropyl)dimethyl-ammonio]-1-propanesulfonate
ChIP	chromatin immunoprecipitation
cm	centimeter
CNS	central nervous system
CT	cycle threshold
d	day(s)
D	docking domain
DDW	double-destilled water
DEPC	diethyl pyrocarbonate

DLK	dual leucine zipper kinase
DMSO	dimethylsulfoxide
DNA	deoxyribonucleic acid
dNTP	2'-deoxynucleoside-5'-triphosphate
dsDNA	double-stranded deoxyribonucleic acid
gDNA	genomic deoxyribonucleic acid
DTT	dithiothreitol
DUSP	dual specificity phosphatase
DVD	domain of versatile docking
E	embryonic day(s)
E. coli	*Escherichia coli*
e.g.	*exempli gratia*
ECL	enhanced chemiluminescence
ED	glutamate/aspartate domain
EDTA	ethylenediaminetetraacetic acis
EGFP	enhanced green fluorescent protein
EGTA	ethylene glycol-bis(2-aminomethyl)-N,N,N',N'-tetraacetic acid
ELISA	enzyme-linked immunosorbent assay
ER	endoplasmatic reticulum
ERK	extracellular signal-regulated kinase
Fas-l	Fas-ligand
FCS	fetal calf serum
Fig.	figure
g	gram(s)
GAPDH	glycerinaldehyde-3-phosphate-dehydrogenase
GFP	green fluorescent protein
GTP	guanidine triphosphate
h	hour(s)
H2A.z	histone 2A variant z
hep	hemipterous
HEPES	N-2-Hydroxyethylpiperazine-N'-2-ethanesulfonic acid
HRP	horseradish peroxidase
Ile	isoleucine (I)

ID	immunodepletion
i.e.	*id est*
Ig	immunglobulin
IL	interleukin
IP	immunoprecipitation
JIP	c-Jun N-terminal kinase-interacting protein
JNK	c-Jun N-terminal kinase
JNKK	c-Jun N-terminal kinase kinase
kb	kilobase
kDa	kilodalton
l	liter(s)
LB	Luria-Bertani medium
LFU	laminar flow unit
Lys	lysine (K)
LZK	leucine zipper-bearing kinase
M	molar (mol/l)
MAP2K	mitogen-activated protein kinase kinase
MAP3K	mitogen-activated protein kinase kinase kinase
MAPK	mitogen-activated protein kinase
MEF	mouse embryonic fibroblasts
MEK	mitogen-activated protein/extracellular signal-regulated kinase kinase
MEKK	mitogen-activated protein/extracellular signal-regulated kinase kinase
mg	milligram(s)
min	minute(s)
MKK	mitogen-activated protein kinase kinase
MKKK	mitogen.activated protein kinase kinase kinase
MKP	mitogen-activated protein kinase phosphatase
ml	milliliter(s)
MLK	mixed-lineage kinase
mm	millimeter(s)
mM	millimolar (mmol/l)
MOPS	4-morpholino-propane-sulfonic acid
mRNA	messenger RNA

mV	millivolt(s)
ng	nanogram(s)
NGF	nerve growth factor
nm	nanometer(s)
OD_{600}	optical density at 600 nm
p	*probability*
p.a.	*pro analysis*
p21	$p21^{WAF1/CIP1}$
p75	p75 neutrophin receptor
Pro	proline (P)
pAB	primary antibody
PAGE	polyacrylamide gel electrophoresis
PBS	phosphate-buffered saline
PCR	polymerase chain reaction
pH	potentia hydrogenii
PI3K	phosphatidyl-inositol-2-kinase
PIPES	piperazine-N,N'-bis(2-ethanesulfonic acid)
PMSF	phenyl-methyl sulfonyl fluoride
POSH	plenty of SH3
PVDF	polyvinylidene dufluoride
QRT-PCR	quantitative real time polymerase chain reaction
r.t.	room temperature
rag	recombination activating gene
Ras	rat sacroma viral oncogene homologue
RCF	relative centrifugal force
r_{max}	maximum radius
RNA	ribonucleic acid
RNase	ribonuclease
rpm	rotations per minute
RPMI	Roswell Park Memorial Institute
rRNA	ribosomal ribonucleic acid
RT	reverse transcriptase; reverse transcription
s	second(s)

S	Svedberg unit(s)
sAB	secondary antibody
SAPK	stress-activated protein kinase
SCG10	super cervical ganglion 10
SDS	sodium dodecyl sulfate
SEK	stress-activated protein kinase/extracellular signal-regulated kinase kinase
Ser	serine (S)
siRNA	small interfering ribonucleic acid
T_A	annealing/melting temperature of primers
Tab.	table
TAK	transforming growth factor β activated kinase
TAO	thousand-and-one amino acid protein kinase
Taq	*Thermus aquaticus*
TAX	taxol
TBE	Tris-boric acid-EDTA buffer
TBS	Tris-buffered saline
TBST	Tris-buffered saline with Tween-20
TEMED	N,N,N',N'-tetramethylethylenediamine
Thr	threonine (T)
TM	tunicamycin
TNF-α	tumour necrosis factor α
Tris	tris-(hydroxymethyl)-aminomethane
TrkA	tyrosine receptor kinase A
Tyr	tyrosine (Y)
U	unit(s)
UV	ultraviolet light
vs	versus
v/v	volume per volume
w/v	weight per volume
ZAK	sterile alpha motif and leucine zipper-containing kinase
µg	microgram(s)
µl	microliter(s)
µm	micrometer(s)

8.2 Index of figures and tables

8.2.1 Figures

Fig. 1: Simplified model of the JNK signalling cascade. 2
Fig. 2: Schematic illustration of the MKK4, MKK7 and JNK structures. 4
Fig. 3: Schematic illustrastion of the six murine MKK7 splice variants. 6
Fig. 4: Cloning of *mkk4* and *mkk7* into the expression vector pEGFP-C3. 48
Fig. 5: Sequence alignment of MKK4. 50
Fig. 6: Sequence alignment of MKK7. 51
Fig. 7: Protein levels of the transfected pEGFP constructs in PC12 cells. 52
Fig. 8: Cell morphology of vector- and MKK7γ1-transfected PC12 cells. 53
Fig. 9: Viability of vector- and MKK7γ1-transfected PC12 cells. 54
Fig. 10: Protein levels and phosphorylation of JNK1/2, their direct upstream kinases MKK4 and MKK7 and some of their direct downstream targets. 56
Fig. 11: Proliferation of vector- and MKK7γ1-transfected cells. 57
Fig. 12: Protein levels of the cell cycle regulators p21 and CyclinD1. 58
Fig. 13: Protein levels of JNK targets involved in apoptosis. 59
Fig. 14: Relative mRNA levels of JNK targets. 60
Fig. 15: Viability of vector-, MKK7γ1- and MKK7β1-transfected cells following stimulation with different stressors. 63
Fig. 16: Protein levels and phosphorylation of JNKs, upstream kinases and targets after stimulation with tunicamycin. 65
Fig. 17: Protein levels of pro- and anti-apoptotic proteins under stress conditions. 67
Fig. 18: Protein level and cleavage of Caspase-3 after tunicamycin stimulation. 68
Fig. 19: Proliferation of vector-, MKK7γ1- and MKK7β1-transfected PC12 cells under stress conditions. 69
Fig. 20: Protein and mRNA levels of p21 and CyclinD1 after tunicamycin stimulation. 70
Fig. 21: p53 binding to the p21 promotor. 71
Fig. 22: JNK-dependent protein levels and phosphorylation of JNK targets in vector- and MKK7γ1-transfected PC12 cells. 72
Fig. 23: Cell cycle distribution of vector- and MKK7γ1-transfected PC12 cells 74
Fig. 24: Changes in protein levels, phosphorylation and localization of JNK isoforms after tunicamycin stimulation in MKK7γ1-transfected PC12 cells. 75
Fig. 25: JNK1 and JNK2 mRNA levels after tunicamycin stimulation. 76

Fig. 26: MKK7γ1-mediated changes in phosphorylation of single JNK isoforms after tunicamycin stimulation. 77
Fig. 27: MKK7γ1-mediated changes in protein-protein interactions. 79
Fig. 28: Viability of NGF-treated vector- and MKK7γ1-transfected differentiated PC12 cells. 82
Fig. 29: Cell numbers of vector- and MKK7γ1-transfected PC12 cells during differentiation. 83
Fig. 30: Cell morphology of NGF-treated vector- and MKK7γ1-transfected PC12 cells..... 84
Fig. 31: Sprouting of NGF-treated vector- and MKK7γ1-transfected PC12 cells. 85
Fig. 32: Protein and phosphorylation levels of NGF receptors and downstream pathways..... 87
Fig. 33: Changes in amount, phosphorylation and localization of JNK isoforms after NGF treatment in MKK7γ1-transfected PC12 cells..... 88
Fig. 34: Protein amounts and phosphorylation of JNK targets in vector- and MKK7γ1-transfected PC12 cells following NGF treatment..... 90
Fig. 35: JNK-dependent protein levels and phosphorylation of transcription factors and cell cycle regulators in NGF-treated vector- and MKK7γ1-transfected PC12 cells..... 91
Fig. 36: Influence of MKK7γ1 on p53 actions in NGF-treated PC12 cells. 92
Fig. 37: Viability of NGF-treated vector- and MKK7γ1-transfected cells following stimulation with taxol..... 94
Fig. 38: Cleavage and protein levels of Caspase-3 in NGF-treated vector- and MKK7γ1-transfected PC12 cells following stimulation with taxol and SP600125. 95
Fig. 39: Viability of NGF-treated vector- and MKK7γ1-transfected cells following stimulation with tunicamycin. 96
Fig. 40: Cleavage and protein levels of Caspase-3 in NGF-treated vector- and MKK7γ1-transfected PC12 cells following stimulation with tunicamycin and SP600125..... 97
Fig. 41: Protein levels and phosphorylation of JNKs and their targets after taxol stimulation in NGF-treated PC12 cells..... 98
Fig. 42: Electronic cell counts of vector-, MKK4- and MKK4Δ-transfected PC12 cells..... 100
Fig. 43: Protein levels and phosphorylation of JNKs, upstream kinases and targets..... 102
Fig. 44: Viability of vector-, MKK4- and MKK4Δ-transfected PC12 cells following stimulation with taxol..... 103
Fig. 45: Schematic model of MKK7γ1-mediated protein interactions..... 116

8.2.2 Tables

Tab. 1: Materials. 12
Tab. 2: PC12 cell numbers on cell culture plates. 19
Tab. 3: Composition of the RT-PCR master mix. 25
Tab. 4: Composition of the PCR master mix. 26
Tab. 5: Primer pairs and reaction conditions for PCR amplification. 27
Tab. 6: Cloning primers. 31
Tab. 7: Restriction enzymes. 31
Tab. 8: Composition of a general digestion reaction. 32
Tab. 9: Composition of resolving gels for SDS-PAGE. 40
Tab. 10: Composition of 3% stacking gels for SDS-PAGE. 41
Tab. 11: Primary and secondary antibodies for Western blots. 43
Tab. 12: MKK7γ1-mediated changes under normal cell growth conditions. 61
Tab. 13: MKK7γ1-mediated changes following tunicamycin stimulation. 80
Tab. 14: MKK7γ1-mediated changes following NGF treatment. 99
Tab. 15: MKK4- and MKK4Δ-mediated changes in naïve PC12 cells. 104

9 Curriculum vitae

Personal Information

Name	Wiebke Häusgen
Date of birth	07.03.1980
Place of birth	Essen, Germany
Citizenship	German

Education

1986 - 1990	Graf-Spee-Schule, Essen, Germany
1990 - 1995	Goetheschule, Essen, Germany
1995 - 2000	Klaus-Groth-Schule, Neumünster, Germany Graduation: Abitur
2001 - 2005	Study of biology Christian-Albrechts University, Kiel, Germany
2006	Diploma in biology (cell biology, botany, biochemistry)
2006 - present	Ph.D. student at the Institute of Experimental and Clinical Pharmacology (Neuropharmacology Group; Prof. Dr. Thomas Herdegen), University Hospital Schleswig-Holstein, Campus Kiel, Germany "The functional relevance of MKK4 and MKK7 splice variants in neural cells".

Research experience

April 2004 – July 2005	Research assistant of the GRK820 "Natürliche Antioxidantien-Ihr Wirkungsspektrum in Pflanzen, Lebensmitteln, Tier und Mensch". Christian-Albrechts-University, Kiel, Germany.
April 2005 – July 2005	Teaching assistant at the Institute of Botany, Christian-Albrechts University, Kiel, Germany. Course: "Cytologie und Physiologie der Pflanze".
October 2005 – February 2006	Teaching assistant at the Institute of Botany, Christian-Albrechts University, Kiel, Germany. Course: "Zellbiologie"
October 2005 – August 2006	Diploma thesis: "Untersuchung zur Bedeutung der Tocopherole bei Kühlestress an der Modellpflanze *Arabidopsis thaliana*". Plant Cell Biology Group (Prof. Dr. Karin Krupinska; Institute of Botany; Christian-Albrechts University, Kiel, Germany
September 2006 - November 2006	Service contract at the Institute of Botany (Plant Cell Biology Group; Prof. Dr. Karin Krupinska), Christian-Albrechts University, Kiel, Germany. "HPLC-Analyse von Tocochromanolextrakten aus Gerstenkörnern".

10 Declaration (Erklärung)

Apart from the advice of my supervisors, this thesis is wholly the result of my own work. The work has been done follwing the rules of good scientific practice of the Deutsche Forschungsgemeinschaft. No part of it has been submitted to any other board for another qualification. Part of the results have already been published in peer reviewed journals and abstract form (see below).

Hiermit erkläre ich, dass diese Dissertation – abgesehen von der Beratung durch meine akademischen Lehrer – nach Inhalt und Form meine eigene Arbeit ist. Die Arbeit ist unter Einhaltung der Regeln guter wissenschaftlicher Praxis der Deutschen Forschungsgemeinschaft entstanden. Sie hat weder im Ganzen noch zum Teil an anderer Stelle im Rahmen eines Promotionsverfahrens vorgelegen. Ein Teil der Ergebnisse dieser Arbeit wurde bereits in Form von Veröffentlichungen oder Kongressbeiträgen publiziert (siehe unten).

Kiel, ... (Wiebke Häusgen)

11 Publications

Paper

Waetzig V, Loose K, **Haeusgen W**, Herdegen T.
c-Jun N-terminal kinases mediate Fas-induced neurite regeneration in PC12 cells.
Biochemical Pharmacology 76 (2008): 1476 - 1484

Waetzig V, Wacker U, **Haeusgen W**, Bjoerkblom B, Courtney MJ, Coffey ET, Herdegen T.
Concurrent protective and destructive signaling of JNK2 in neuroblastoma cells.
Cellular Signalling 21 (2008): 873 - 880.

Haeusgen W, Boehm R, Herdegen T, Waetzig V.
Specific activities of c-Jun N-terminal kinases in the brain.
Neuroscience 161 (2009): 951 - 959.

Haeusgen W, Herdegen T, Waetzig V.
Specific regulation of JNK signalling by the novel rat MKK7γ1 isoform.
Cellular Signalling 22 (2010): 1161 - 1172.

Haeusgen W, Herdegen T, Waetzig V.
The bottleneck of JNK signalling: Molecular and functional characteristics of MKK4 and MKK7.
Submitted.

Haeusgen W, Herdegen T, Waetzig V.
The power of MKK splice variants: MKK7γ1 reverses PC12 cell programs of differentiation and stress.
Submitted.

Website

Haeusgen W, Herdegen T, Waetzig V.
UCSD-Nature Signaling Gateway Molecule Page for JNK2.
Molecule Page ID A001297.
Accepted for publication.

Sequence data

Haeusgen W, Herdegen T, Waetzig V.

Rattus norvegicus strain NEDH MKK7gamma1 mRNA, complete cds

Accession number: GU264001

GenBank

Congress abstracts

Zhao Y, **Haeusgen W**, Waetzig V, Herdegen T.

Regulation of JNK isoforms at brain mitochondria.

4th Annual Meeting of the global college of neuroprotection and neurodegeneration.

Garmisch-Partenkirchen, March 2007.

Haeusgen W, Wacker U, Herdegen T, Waetzig V.

Simultaneous protective and destructive signaling of JNK2.

Apoptosis World 2008. Luxembourg, January 2008.

Haeusgen W, Wacker U, Herdegen T, Waetzig V.

Simultaneous protective and destructive signaling of JNK2.

6th FENS. Geneva, July 2008.

Haeusgen W, Wacker U, Herdegen T, Waetzig V.

A single JNK isoform controls both cell cycle progression and cell death.

EJCB. 88; 59, (75), 2009.

Danksagung

An erster Stelle möchte ich mich bei Prof. Dr. Thomas Herdegen für die Bereitstellung des interessanten Themas und die Möglichkeit, meine Doktorarbeit in seiner Arbeitsgruppe durchführen zu können, bedanken. Ich bin Ihnen sehr dankbar für die vielen Diskussionen über meine Arbeit, Ihre interessanten Ideen für weitere Projekte und dafür, dass Sie mir die Freiheit gegeben haben meine eigenen Ideen zu verfolgen.

Ganz besonders möchte ich mich bei Frau Prof. Dr. Manuela Dittmar vom Zoologischen Institut der Christian-Albrechts-Universität zu Kiel für die Übernahme des Korreferates und die damit verbundenen Mühen bedanken. Vielen Dank für Ihr Interesse an meiner Arbeit und Ihr stets offenes Ohr.

Zu großem Dank bin ich Dr. Vicki Wätzig für die praktische und fachliche Betreuung meiner Arbeit verpflichtet. Deine unermüdliche Hilfs- und Diskussionsbereitschaft in und außerhalb des Labors haben maßgeblich zum Gelingen dieser Arbeit beigetragen.

Bei Angela Schulz, Elke Schröder, Irina Naujoks und Annika Mütze möchte ich mich für die gute Zusammenarbeit im Labor bedanken. Danke Mädels, für die tolle Arbeitsatmosphäre und die zahlreichen leckeren Kuchen, die mir die Zeit sehr versüßt haben.

Herzlichen Dank an Prof. Dr. Martin Gramatzki und Dr. Matthias Peipp aus der Sektion für Stammzelltherapie und Immuntherapie am Universitätsklinikum Schleswig-Holstein Campus Kiel für die Einweisung und Möglichkeit der Nutzung des FACS-Gerätes.

Vielen Dank an Prof. Dr. Stefan Schreiber, Dr. Robert Häsler und Dorina Ölsner vom Institut für Klinische Molekularbiologie des Universitätsklinikums Schleswig-Holstein Campus Kiel für die Unterstützung bei der quantitativen *real time* PCR.

Mein herzlicher Dank gilt allen ehemaligen und aktuellen Mitarbeitern und Gastwissenschaftlern des Institutes für Experimentelle und Klinische Pharmakologie der Christian-Albrechts-Universität zu Kiel für die gute Zusammenarbeit.

Danke, an meinem „Büromitbewohner“ Dr. Ruwen Böhm, insbesondere für seine Hilfe bei Computerproblemen.

Ein besonderer Dank gilt auch Dr. Ursula Hoffmann. Mit Ihrem ausgezeichneten Unterricht haben Sie in mir das Interesse an der Biologie und der Wissenschaft geweckt.

Sandra und Katrin danke ich für die legendären Mittwochabende und das Korrekturlesen der Arbeit.

Für ihr stets offenes Ohr, die kraftgebenden Gespräche und die schönen Wochenende möchte ich mich bei Goentje ganz herzlich bedanken.
Mein tiefster Dank gilt Sönke, für seine immerwährende Unterstützung und den Halt, den er mir während der gesamten Zeit gegeben hat. Auch seiner Familie sei für die wunderbaren gemeinsamen Tage gedankt.
Schließlich möchte ich ganz herzlich meinen Eltern danken. Ohne Eure Unterstützung wäre vieles nicht möglich gewesen.